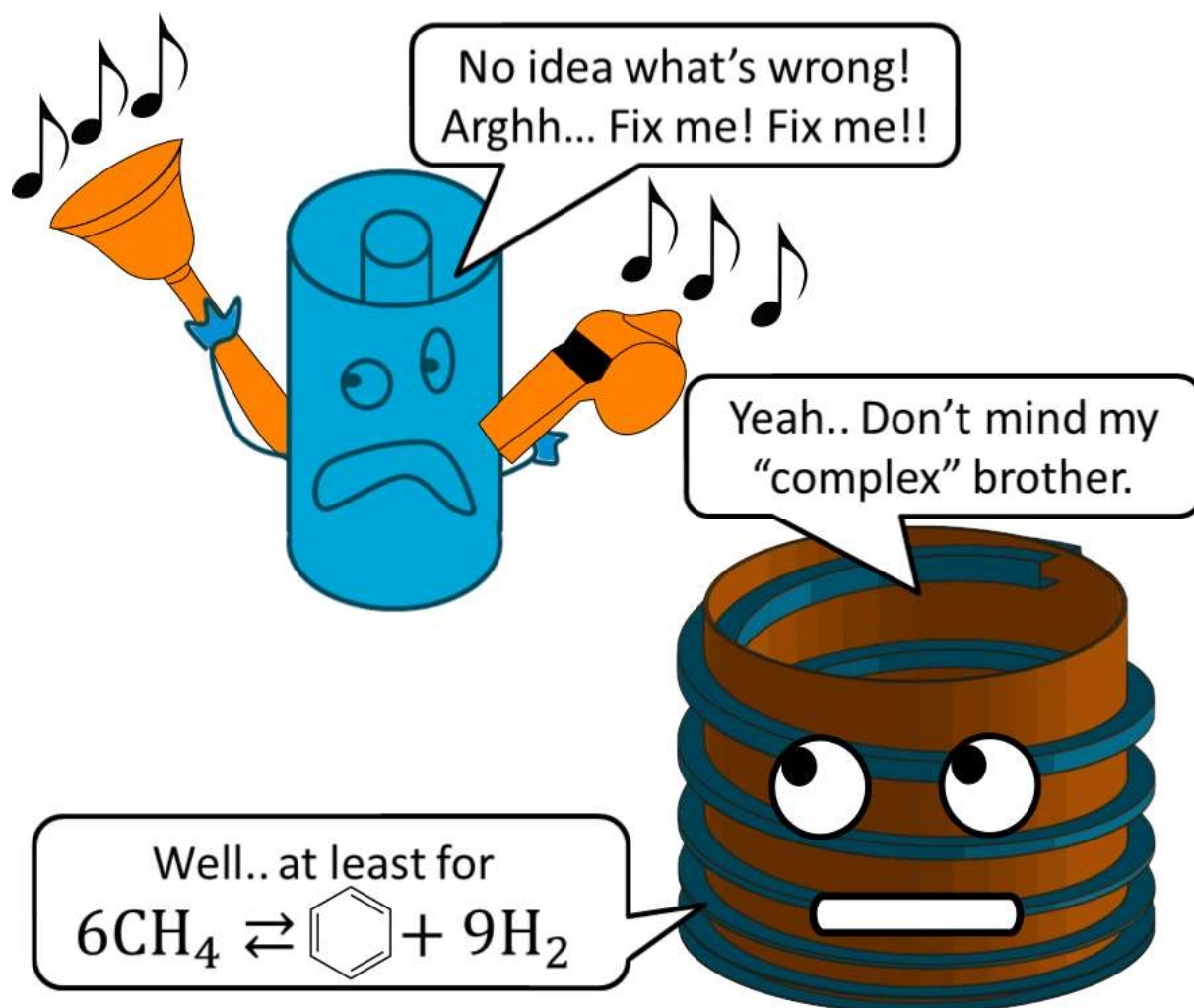


Travelling microwave reactor design

Master of science thesis

T. van der Schans




TU Delft

Report number: P&E-2767

Travelling microwave reactor design

by

T. van der Schans

in partial fulfilment of the requirements for the degree of

Master of Science

in

Mechanical engineering

at Delft University of Technology,

to be defended on Wednesday December 13th, 2017 at 14:00 PM.

Daily supervisor: F. Eghbal Sarabi

Supervisor: Dr. Ir. G.S.J. Sturm

Chairman: Prof. Dr. Ir. A.I. Stankiewicz

Second reviewer: Prof. Dr. Ir. M. Makkee

Section: Intensified reaction and separation systems

Department: Process & Energy

Faculty: Mechanical, Maritime and Materials engineering



Contents

Preface	ix
Abstract	xi
1 Introduction	1
2 Design	5
2.1 The requirements	5
2.2 Challenges	5
2.3 Four steps to solve the challenges	7
3 Discussion	17
3.1 Evaluating the designed reactor	17
3.2 Improving the designed reactor	17
3.3 Evaluating and improving the methods	21
3.4 Giving attention to ignored opportunities	22
4 Conclusion and recommendations	25
Bibliography	29
A Finding challenges	37
A.1 Material check-list	37
A.2 Process check-list	37
A.3 Reactor check-list	37
A.4 Microwave check-list	37
A.4.1 Unknown challenges	38
A.5 Block diagram	38
B Finding solutions	41
B.1 Essence of creative designing	41
B.2 Abstracted solutions	42
B.3 Sub-solutions evaluation	45
C Derivations	47
C.1 Travelling microwave reactor topology	47
C.2 Accelerated deactivation spots	49
C.3 Stable heat dissipating permittivity	49
C.3.1 Diffusion temperature gradient	51
C.3.2 Shielding electromagnetic field	52
C.4 Limited conventional heat transfer	53

C.5 Catalyst thickness	54
C.6 Channel width	55
C.7 Asymmetric annular monolith	57
C.8 Attenuation constant	57
C.9 Expansion limit	58
C.10 Dielectric loss factor	58
C.11 Heating limit	60
C.12 Reflection porous media	60
C.13 Reflectionless slab	61
C.14 Economic potential	61
D Process design	63
E Materials	65
F Pathfinder	67

List of Symbols

c_0	Speed of light in vacuum	m/s
c_{in}	Electric strength derivative of power at inlet	V/m
c_{out}	Electric strength derivative of power at outlet	V/m
c_p	Molar heat capacity	J/(mol K)
C	Price	\$/kg
C_{vol}	Price per volume	\$/m ³
$C_{benzene}$	Price benzene	0.126 \$/kg
d	Channel diameter	m
D_{12}	Diffusivity in channels	$1 \times 10^{-4} \text{m}^2/\text{s}$
E	Electric field intensities	V/m
E	Elastic modulus	MPa
E_i	Electric field strength at inner conductor	V/m
E_o	Electric field strength at outer conductor	V/m
f	Operating frequency	Hz
GHSV	Gas-hourly space velocity	1.5L/(g _{cat} h)
h_{cat}	Catalyst height	m
K_{IC}	Fracture toughness	Pa m ^{0.5}
L	Length channel	1.5 m
MW_{CH_4}	Molecular weight methane	16 g/mol
MW_{H_2}	Molecular weight hydrogen	2 g/mol
N_C	Number of channels	#
N_R	Number of channel rows	#
n	refractive index	
p	Pressure	50 atm
P	Electrical power	W
Q	Heat needed by reaction	W
r	Radius	m
r_i	Inner conductor radius	m
r_m	Inner monolith radius	m
r_o	Outer conductor radius	m
r_{cat}	Catalyst radius caused by liquid tension	m
r_{geom}	Channel fillet radius	m
R_T	Thermal shock resistance	
t	Time	s
t_w	Minimal wall thickness	0.125 mm
t_l	Channel row width	1.25 mm
T_{creep}	Creep temperature	K
T_{in}	Temperature reactant at inlet	K

T_r	Temperature of reaction	K
T_m	Melting temperature	K
T_{max}	Maximum service temperature	K
u	Velocity	m/s
V_b	Dielectric breakdown methane	3×10^6 V/m
V	Volume	m^3
V_{cat}	Catalyst volume	m^3
x	Length	m
X_{conv}	Conversion	12 %
Z_c	Characteristic impedance	Ω
α	Thermal expansion coefficient	m/K
α_f	Attenuation constant	
ϵ	Electric permittivity $\epsilon = \epsilon_0 \epsilon_r$	F/m
ϵ_e	Electric permittivity of environment	F/m
ϵ_0	Electric permittivity of vacuum	8.85×10^{-12} F/m
ϵ_r	Relative electric permittivity $\epsilon = \epsilon'_r - \epsilon''_r$	
ϵ'_r	Dielectric constant	
ϵ''_r	Dielectric loss factor	
$\epsilon_{r,gas}$	ϵ_r of the gas	1
$\epsilon'_{r,cat}$	ϵ'_r of the catalyst	5
$\epsilon_{r,sup}$	ϵ_r of the support	
$\epsilon_{r,mon}$	ϵ_r of the monolith	
ρ_{cat}	Catalyst density	680 kg/m^3
ρ	Methane density at 1atm	656 g/m^3
μ	Methane viscosity	3.5×10^{-5} Pa s
σ	Electric resistivity	Ωm
λ	Thermal conductivity	W/(m K)
ω	Angular frequency	rads/s
Δh_f	Enthalpy of formation	523 kJ/mol
ν	Poisson ratio	
ϕ	Generalized Thiele modulus	
η		
σ_f	Ultimate tensile strength	Pa
σ_y	Yield strength	Pa
τ_{year}	Seconds in a year	31557600 s

Glossary

Attenuation	Loss of electromagnetic intensity through absorption and reflection.
Dielectric breakdown	current flow through an electrical insulator. An example of dielectric breakdown is lightning.
Grid search	Optimization in which first a subset of values are manually specified for each parameter. Then all possible combination are tried and finally the most optimal combination is chosen.
Higher order modes	Any electromagnetic propagation mode with more nodes and bellies than the lowest mode for that specific cavity
Manufacturable	whether a part is able to be manufactured at acceptable cost
Rectifier	A device that converts alternating current to direct current.

Preface

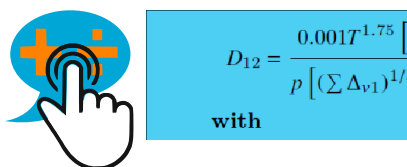
For my master of science thesis, I came across the assignment to design a travelling microwave reactor. This assignment was perfect to test my acquired capabilities and knowledge as a mechanical engineering student. Especially, to test my capabilities to a life-long learning. Simply, because I have never designed a chemical reactor before nor have I done any engineering with microwaves.

Eventually, my work resulted in this report, known as report 5 in my administration. The only purpose of report 5 is to pass my master of science examination. For example, report 1 was written to transfer the methods to design a microwave reactor while report 3 was written to transfer the understanding to design a microwave reactor. Neither of these were accepted by G.S.J. Sturm nor A.I. Stankiewicz. So, after 9 months of engineering and 13 months of disagreeing report 5 came into existence. I can see that report 5 looks like a master thesis report. However, a lot of information has been removed. Some of the removed information can be found on [my LinkedIn](#) and [Dropbox](#). Furthermore, the digital report is also available in the TU Delft repository [1].

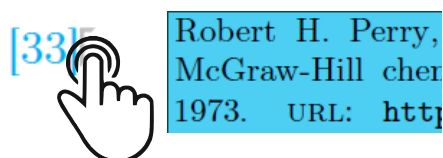
Reading tips

Why do we still print? Because, the benefits of digital reports are not exploited. Therefore, extra information is directly available in the digital version of this report by clicking on balloons and images. Furthermore, reference information is shown when clicking behind a reference. It is important to click behind the references unless you want to use the link, because all cyan coloured texts are active links. Moreover, videos and interactive models are shown when the play button is clicked. These benefits can be found in the digital version of this report [1].

Click on balloons



Click behind references



Click on play



Abstract

In this work, the work of G.S.J. Sturm on microwave reactors was continued [2]. Microwave reactors are developed, because they have potential to increase safety and economically reduce waste. This work focused on microwaves and chemical processes, instead of just heating water, by designing a travelling microwave reactor for non-oxidative methane dehydroaromatization.

The travelling microwave reactor was designed using a structured approach. First, the objective was set to an economical conversion to aromatics of otherwise flared methane. Therefore, a successfully designed reactor is able to reduce the CO₂ emissions and make many other reactions economical. Secondly, twenty-one challenges for microwave reactors were found using check-lists and a self-developed phenomena exploration method. This method was used to find unknown challenges on the intersection of established engineering fields. Then sub-solutions solving these challenges were extracted from existing reactors and reactor concepts. Finally, a few sub-solutions were selected and forced to work together to obtain the designed reactor.

The designed reactor consists of a high performance coated asymmetric annular monolith in an inert container with narrowing conductors in axial direction and an anisotropic porous media (Figure 1). The achieved production volume is three orders of magnitude larger than of a mono-mode microwave reactor at same operation frequency. The designed reactor is capable of obtaining another five orders of magnitude by increasing the temperature up to 1500 K, pressure up to 50 atm, catalyst activity with at least two orders of magnitude and lowering the operating frequency. However, only four orders of magnitude were reached, because the designed reactor hit a flow limit.

The designed reactor with the three plus four order of magnitude improvement is not yet economical feasible. More advanced designs such as the spiralling narrowing rectangular microwave reactor might be. Furthermore, the designed reactor could become economically feasible in case of a more valuable product. Eventually, this work revealed some unsolved problems and opportunities of microwave reactors as well as information gaps. Moreover, it brought microwave reactors closer to industrial application.

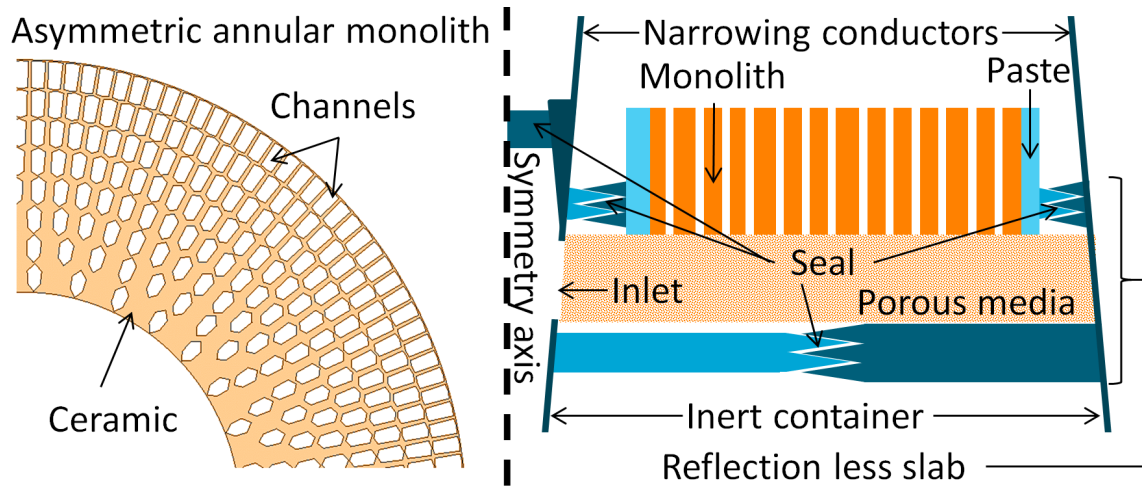


FIGURE 1: Asymmetric annular monolith top view and axis symmetric view designed reactor.

1 | Introduction

Current status and challenges of microwave reactors

In the 1980s, the first experiments with chemical microwave reactors were performed [3][4][5][6]. Some experiments [4] showed that the high selective power input of microwave reactors is able to reduce reaction times and increase yields causing the reactor to be safer [7] and generate less waste [8]. However, the used mono-mode (Figure 1.1) and multi-mode (Figure 1.2) microwave cavities are too small and too unpredictable for industrial use.

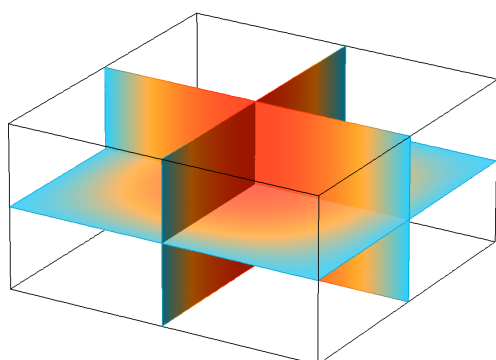


FIGURE 1.1: The mono-mode cavity has only one fluctuating electromagnetic intensity belly. (Animation [1])

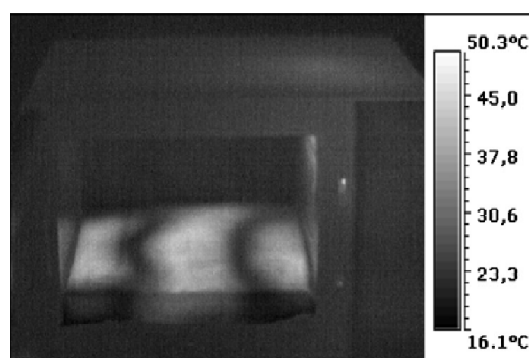


FIGURE 1.2: Thermal image of non-uniform temperatures in multi-mode cavity. Image by G.S.J. Sturm [9].

The travelling microwave reactor concept [9]

In 2013, the travelling microwave reactor was suggested to increase the size and predictability. The travelling microwaves have no intensity peaks averaged in time and thus eliminate the size constraint in 1 direction (Figure 1.3). Furthermore, the coaxial waveguide has no lower cut-off frequency for the used transverse electromagnetic mode that together with the travelling microwaves makes the reactor more predictable than multi-mode microwave cavities. Moreover, a microwave recycle would reduce the wasted microwave energy (Figure 1.4), the channel shape interaction with microwaves would create uniform heating (Figure 1.5), a large area to volume ratio can be used for exchanging heat and/or mass and an expanding inner conductor would correct the attenuation (Figure 1.5). However, to the best of our knowledge, this concept and other microwave reactor work have not yet lead to an industrial microwave reactor.

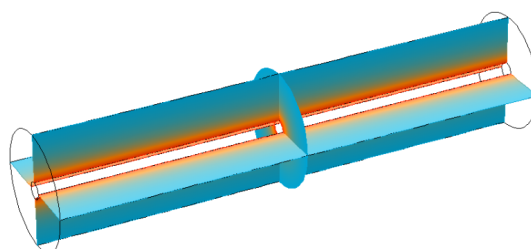


FIGURE 1.3: In the image, the travelling wave averaged over time shows a flat intensity (same colour) in axial direction. In the animation ([1]), the coaxial waveguide with a travelling microwave.

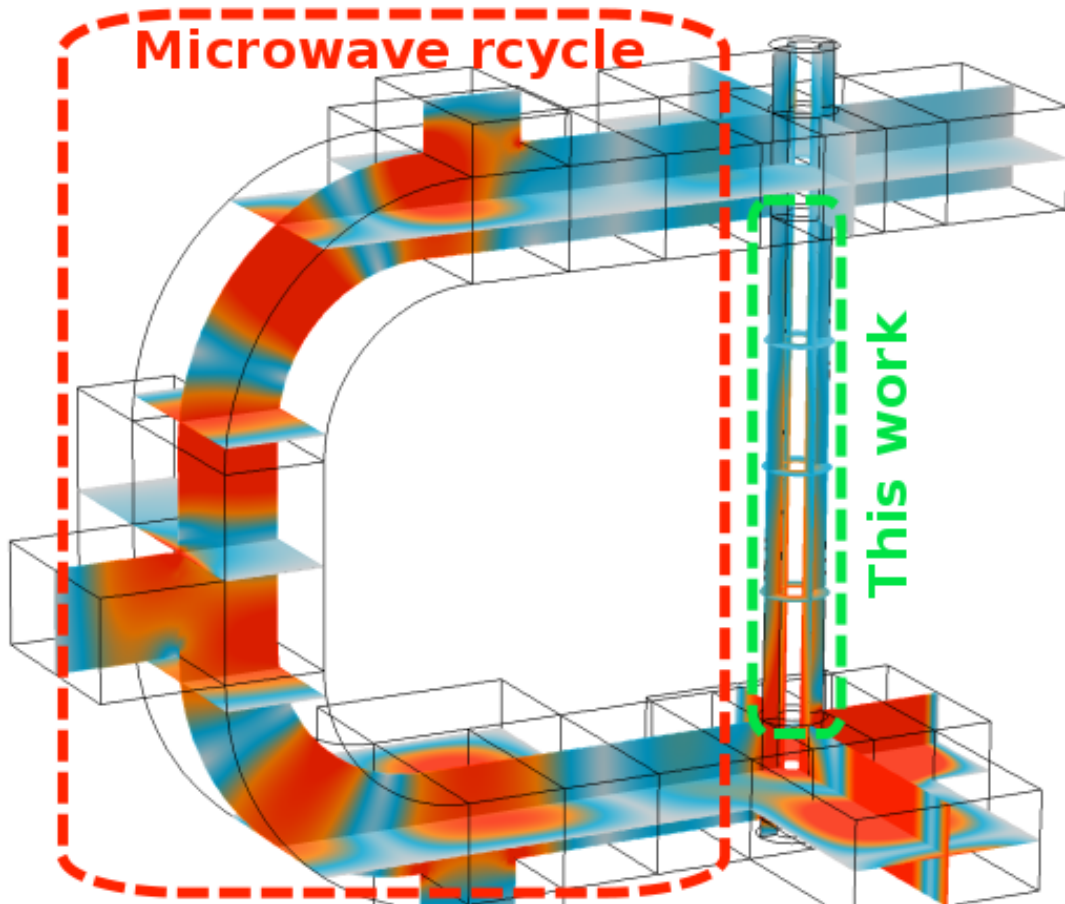


FIGURE 1.4: The travelling microwave reactor uses a microwave recycle to return unused microwave energy to the start. In this work, the coaxial waveguide in which reactant and microwaves interact is developed. In the image, the electric field is averaged over time and shows in the coaxial waveguide an exponential decaying intensity (orange to grey) in axial direction. In the animation [1], the orange spots travel upwards in the coaxial waveguide while in the recycle the orange spots stand still.

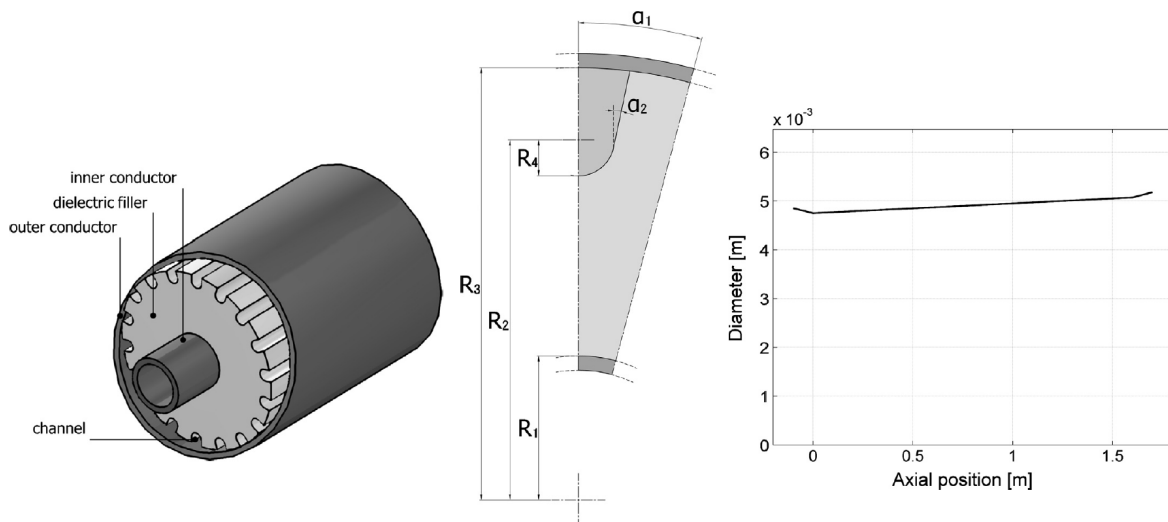


FIGURE 1.5: The design proposed by G.S.J. Sturm (left image). It consisted of specific channel shapes to obtain uniform heating (middle image) and an expanding inner conductor (right image). Images reprinted from [9].

Literature review, research question and answering method

Most published microwave reactor work [4][10][11] involved studying the yields of chemical reaction. However, incorrect measuring of the temperature often leads to false results. Therefore, measurements in microwave reactors have been improved [12][13][14][15]. Finally, some microwave reactors were developed to solve challenges ahead [16][17][18][19]. This work will also continue to solve the challenges of a (travelling) microwave reactor ahead. In this work, the part of the travelling microwave reactor where reactant and microwaves interact was further developed using conservation equations [20], Maxwell's equations [21] and material properties. Eventually, the following research questions are answered:

- What is needed to know to build a working travelling microwave reactor?
- What are the operation ranges of the travelling microwave reactor?

These two research questions were simultaneously answered by designing a travelling microwave reactor following the design loop (Figure 1.6). In this report, the many design iterations have been presented as three single loop iterations. First in Chapter 2, the requirements, the challenges and the first design are obtained. Then in Chapter 3, the design is evaluated and improved twice. Furthermore in Chapter 3, some used methods are evaluated and ignored opportunities are given attention. Finally in Chapter 4, the research questions are answered.

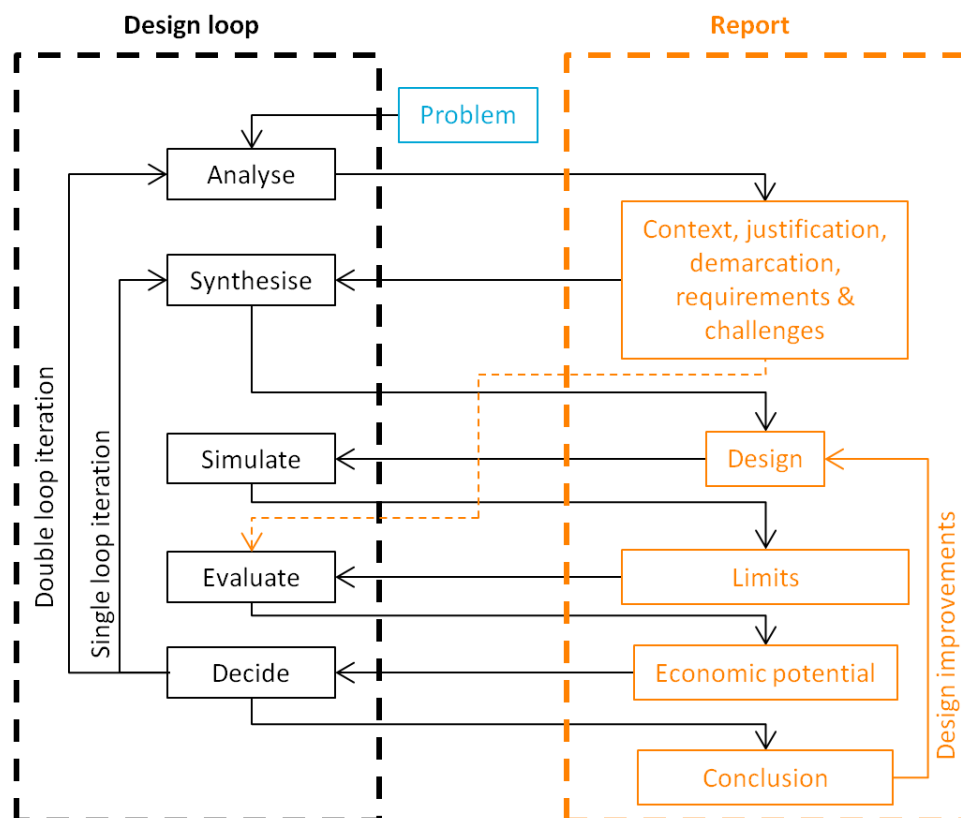


FIGURE 1.6: Any design goes through the design loop (left) [22]. Therefore, the report is structured in these steps (right).

Demarcation through case and single part design

This work is made more tangible through a case and by constraining it to a part of the reactor. The chosen case is non-oxidative methane dehydroaromatization supplied by ADREM, because this case is social relevant and widely applicable. Firstly, it is social relevant, because the design might economically convert the currently 139 billion cubic meters of flared gas contributing to CO₂-pollution into products [23]. Secondly, the lessons learned, tools developed and solutions found for this case can be widely applied. Especially, because non-oxidative methane dehydroaromatization is a troublesome conversion. It has high temperature (973 K or higher), cheap products (0.126\$/kg), flammable reactants, toxic products, catalyst deactivation, a low gas-hourly space velocity (1.5L/(g_{cat}h)) and, in some cases, fluctuating operation [24][25][26]. Finally, the travelling microwave reactor in this work is constrained to the space where microwaves, catalyst and reactants interact with each other. Auxiliary elements, such as the magnetron or pumps are beyond the scope of this study.

Main challenge in designing a microwave reactor

Designing a reactor is a challenge, because proper trade-offs need to be made between concentration, temperature and velocity to obtain a profitable reactor. In a microwave reactor, these phenomena are enriched by the electromagnetic field (Figure 1.7). The electromagnetic field is also influenced directly by any design geometry decision and coupled to the temperature. Thus, decisions on reactor geometry and materials need to account all four at once.

However, decisions on all four are not common, because Maxwell's equations are not part of the chemical engineering curricula neither is physical transport phenomena for electrical engineers [27]. Therefore, in microwave reactor design decisions need to be made on the intersection of these engineering fields. Furthermore, both fields are matured and have established solutions to obtain goals within the field. In general, engineering mostly consists of obtaining the required information and following procedures to rightly connect or adjust established solutions. For example, thermodynamic properties are obtained and heuristics are followed to obtain a separation train [28]. However, this study focus on obtaining a new solution by pinpointing the information needed and defining the procedure to rightly connect or adjust the new solution. Therefore, the more abstract structured design methodology is used as a guide.

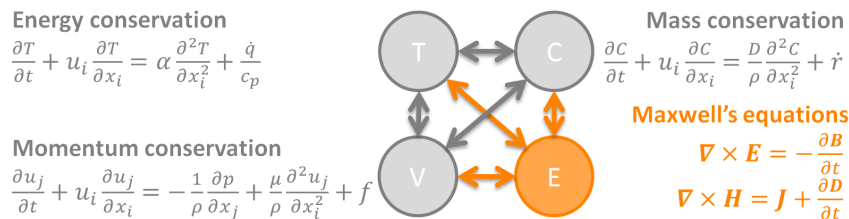


FIGURE 1.7: The conventional reactor phenomena, temperature, concentration and velocity are enriched with the electromagnetic field, and thus the design trade-offs shown by the arrows are doubled in microwave reactors.

2 | Design

In [Chapter 1](#), it has been explained that a travelling microwave reactor was designed to answer the research questions. In this chapter, the designing of the travelling microwave reactor is explained. First, how the requirements and the challenges were obtained. Then, how the challenges were solved by selecting and sizing the specific materials and shapes of the travelling microwave reactor.

2.1 The requirements

The requirements are used to evaluate the designed reactor. The following requirements were codetermined by the industry and academic groups participating in the [ADREM project](#). As mentioned in [chapter 1](#) the case chosen for developing the travelling microwave reactor was taken from ADREM. Therefore, the same requirements apply. For example, the container sized and adaptable product distribution (from ethylene to aromatics) makes the reactor moveable and employable at different types of locations. [\[26\]](#)

- Travelling microwave reactor for methane aromatization [\[26\]](#)
- Equipment size smaller than 2 x 2 x 2 m container [\[26\]](#)
- Adaptable product distribution (from ethylene to aromatics) [\[26\]](#)
- Overall costs lower than 0.126 \$/kg benzene [\[25\]](#)
- Safe operation

2.2 Challenges

There are numerous challenges in the design of a TMR, which, when unsolved, can lead to serious consequences such as unpredictable reactor behaviour or an explosion due to a leakage. Therefore, the design should address all challenges to obtain a safe and working reactor, and to address challenges they need to be known. Most of the challenges were found using check-lists and functions derived from the process flow diagram. However, on the intersection between engineering fields there are no check-lists. Therefore, a self-developed phenomena exploration method was used to find unknown challenges on intersecting engineering fields. In this variation on the force-to-fit creativity method (Y. Ruiter, [creative thinking workshop](#), February 2017), words from a travelling microwave reactor topology (derived in [section C.1](#)), HAZOP [\[29\]](#) and life cycle assessment (LCA) [\[30\]](#) were combined and thought up on. The essence of the phenomena exploration method is answering a question using the *italic* words in [Table 2.1](#) to find new phenomena on the intersection of the chemical and electrical engineering field. For example, "*How would [no] [catalyst] in [operation] influence the [reaction rate]?*"

TABLE 2.1: The phenomena exploration methods created approximately $7^4 \times 6 = 14406$ combinations, because the guide words can be applied to both topology as parameters. However, only $1 \times 7 \times 4 \times 2 = 56$ combinations gained attention, because the words were limited to the *italic* filled cells and the guide words were only applied to the catalyst. These remaining combinations gained attention, because they were expected to bring the most important insights.

HAZOP guide words	TMR topology	LCA	HAZOP parameters
<i>as well as</i>	Reactant	material processing	flow
<i>no</i>	<i>Catalyst</i>	<i>manufacturing</i>	pressure
<i>more</i>	Filler 1	assembly	<i>temperature</i>
<i>less</i>	Filler 2	packaging	<i>electric field strength</i>
<i>part of</i>	Conductor	transportation	<i>reaction rate</i>
<i>instead</i>	Insulation	construction	<i>equilibrium</i>
<i>fluctuations</i>	Environment	<i>operation</i>	

TABLE 2.2: The 21 challenges that were addressed in the designed reactor. These challenges could cause to 3 problems inefficiency (profit loss), reactant mixture leakage (hazards) and non-homogeneous temperature (inefficiency and/or leakage).

Mechanics-related	This challenge could cause
(inverse-)corrosion	All
Polymorphism	Non-homogeneous temperatures
Thermal shock	Reactant mixture leakage
Material creep	Reactant mixture leakage
Temperature influence on gaps needed for assembly and adaptability	Reactant mixture leakage
Pressure influence on gaps needed for assembly and adaptability	Reactant mixture leakage
Pressurized rupture	Reactant mixture leakage
Volume utilisation	Inefficient
Manufacturability	Inefficient
Hydrodynamics-related	This challenge could cause
Preferential flow	Non-homogeneous temperature
Pressure drop	Inefficient
Reactants bypassing	Inefficient
Microwave-related	This challenge could cause
Dielectric breakdown	Non-homogeneous temperatures
Escaping microwaves	Inefficient
Higher order modes	Non-homogeneous temperatures
Attenuation	Non-homogeneous temperatures
Reflection	Non-homogeneous temperatures
Radial decaying field	Non-homogeneous temperatures
Electrical field at material interfaces	Non-homogeneous temperatures
Unstable permittivity	Non-homogeneous temperatures
Accelerated deactivation spots	Non-homogeneous temperatures

Eventually, 21 challenges were addressed in the designed reactor (Table 2.2). All used methods to find these challenges have been further explained in Appendix A. The previously described phenomena exploration method added two newly found challenges which are unstable permittivity and accelerated deactivation spots to the table above. Therefore, both newly found challenges will be explained.

The newly found challenge **unstable permittivity** answered the phenomena exploration method question, "*How would* [impurities in the (as well as rephrased)] [catalyst] *influence the* [temperature] *during* [operation]?" Unstable permittivity revolves around the fact that a material is never perfect causing small perturbations in the dielectric heating. These perturbations combined with specific dielectric properties may cause thermal runaways. Unstable permittivity formulas (Equation 2.1) were derived in section C.3 using Ohmic loss equation differentiated to temperature, because permittivity is temperature dependent [31][32] and then combined with differential Gauss's law. The formula shows that unstable permittivity only occurs when the dielectric loss factor ϵ'' increases or the dielectric constant ϵ' decreases.

$$\frac{\partial \epsilon''}{\partial T} + 2\epsilon''\epsilon' \frac{\partial 1\epsilon'}{\partial T} < 0 \quad \& \quad \frac{\partial \epsilon''}{\partial T} + 2\epsilon''(\epsilon' + 2\epsilon_e) \frac{\partial 1(\epsilon' + 2\epsilon_e)}{\partial T} < 0 \quad (2.1)$$

The newly found challenge **accelerated deactivation spot** answered the phenomena exploration method question, "*How would* [more] [catalyst] *caused by* [manufacturing] *influence the* [reaction rate]?" Accelerated deactivation revolves around the fact that manufacturing is often not perfect causing differences called spots. These spots may cause a self-enhancing deactivation phenomenon of a self-poisoning catalyst in a microwave reactor, because the deactivated catalyst converts less heat into endothermic products while still absorbing microwave power causing the temperature to rise even further and thus accelerating the deactivation rate. Thus, an accelerated deactivation spot is prevented by giving catalyst sites the same history. This is a variation on the process intensification principle of giving each molecule the same history [33].

Summary finding challenges

In this section, the 21 challenges were found using check-lists, functions derived from the process flow diagram and the self-developed phenomena exploration method. The phenomena exploration uses a question filled in with words from a HAZOP, life cycle assessment and topology to stimulate thought and find new challenges. Finally, two newly found challenges, unstable permittivity and accelerated deactivation spot, were found and explained.

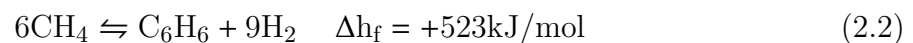
2.3 Four steps to solve the challenges

The methods to solve challenges included challenge definition, extracting and then abstracting solutions from existing reactors and extrapolating those solutions. These methods

to find solutions have been explained in more detail in [Appendix B](#). Eventually, the 21 challenges were addressed in four steps. The four steps consisted of obtaining process information, matching shapes and materials, sizing calculations and choosing more specific solutions.

1) Obtaining information to get the process right

Before the reactor can be sized information is needed. First, information on the methane aromatization process was obtained [24]. Among other things, the travelling microwave reactor should convert methane into benzene at the remote locations where it is currently being flared. The optimal process conditions were obtained by following a methane volume through the process and assigning elementary process functions to it in time [34](section A.5). A methane volume starts by entering the reactor. In the reactor, the methane is heated to temperatures above 973 K to obtain sufficient conversion, because the conversion stops at thermodynamic equilibrium [35]. During conversion, heat needs to be continuously added to keep the reaction going. The often used catalyst, Mo/HZSM-5 [36], deactivates quickly through self-poisoning [37]. The deactivation mechanism is dominated by ethylene cracking to coke in which hydrogen addition reduces coke formation [38][39]. Thus, the dominant deactivation path makes in-situ removal of hydrogen undesirable. On the other hand, the in-situ removal of aromatics is unnecessary, as it does not prevent deactivation. Thus, the products will be separated from the mixture exiting the reactor and the unreacted methane can be recycled. 🗨️



After setting the process conditions, the values needed to size the reactor were obtained. All values needed in the sizing calculation scheme can be found in [Table 2.3](#). Furthermore, the values of the variables were assumed or estimated as follows:

Details about the needed values

- The process conditions of experiments were at 973 K and 1 atm. However, to future proof the reactor, process conditions of 1500 K and 50 bar were assumed during material selection.
- The diffusion coefficients in the channels at high temperatures were approximated with Fuller-Schettler-Giddings 🗨️ [40].
- The dynamic viscosity of the gas was calculated using the method of Bromley and Wilke 🗨️ [41] combined with fitted polynomials [42][43].
- The density was assumed to be defined by the ideal gas law.
- Selectivity to benzene is assumed to be 100% for simplicity.
- The catalyst dielectric constant is assumed to be 5. (L.S. Gangurda, personal communication, August 2016)

TABLE 2.3: Only the following listed values are needed to size the designed reactor when the sizing calculation scheme is used.

Symbol	Property	Value	Reference
c_0	Speed of light in vacuum	3×10^8 m/s	constant
c_p	Molar heat capacity	35.69 J/(mol K)	[41]
$C_{V,benzene}$	Price benzene	0.126 \$/kg	[25]
$D_{12,c}$	Diffusivity in channels	1×10^{-4} m ² /s	[40]
f	Operating frequency	2.45 GHz	chosen
GHSV	Gas-hourly space velocity	1.5 L/(g _{cat} h)	[44]
L	Length channel	1.5 m	requirement
MW_{CH_4}	Molecular weight methane	16 g/mol	
$MW_{C_6H_6}$	Molecular weight hydrogen	78 g/mol	
p	Pressure	50 atm	chosen
t_w	Minimal wall thickness	0.125 mm	[45]
t_1	Channel row width	1.25 mm	assumed
V_b	Dielectric breakdown methane	3×10^6 V/m	[46]
X_{conv}	Conversion	12 %	[44]
ρ_{cat}	Catalyst density	680 kg/m ³	[47]
ρ	Methane density at 1 atm	0.656 kg/m ³	
Δh_f	Enthalpy of formation	523 kJ/mol	[24]
τ_{year}	Time	31 557 600 s	constant
ϵ_0	Electric permittivity of vacuum	8.85×10^{-12} F/m	constant
$\epsilon_{r,gas}$	ϵ_r of the gas	1	assumed
$\epsilon'_{r,cat}$	ϵ'_r of the catalyst	5	assumed

	Electrical engineering, waveguide				Chemical engineering, catalyst contacting			
	rectangular	microstrip line	coaxial	cylindrical	random packed bed	monolith	fluidised bed	static mixer
Predictability	✗	✗	✗	✗	✗	✗	✗	✗
Volume utilisation	✗		✗		✗	✗	✗	✗
Manufacturability			✗	✗	✗	✗	✗	

FIGURE 2.1: Combining existing waveguide [21][48] and reactor [49][50] mechanisms to maximise the predictability, volume utilisation and producibility using elimination method.

2) Finding the best shape and material match

There are many possible shapes and materials that could be considered in the design of a TMR. A quick shape and material match was made to prevent the tedious task of trying them all. The shape match was obtained by combining familiar electrical and chemical engineering shapes. These shapes need to be compatible, because reacting and heating are happening within the same volume. In this study, the coaxial waveguide was combined with a monolith, because this combination was expected to maximise the predictability, volume utilisation and economic manufacturability (Figure 2.1). Other, rectangular travelling wave microwave reactor [11], and similar, coaxial wideband microwave reactor [19], combinations

had been proposed before. Then, the volume utilisation of the coaxial waveguide/monolith combination was further maximised by preventing the radial decay described by Gauss's law through the use of an asymmetric annular monolith which is a new geometry (Figure 2.2).

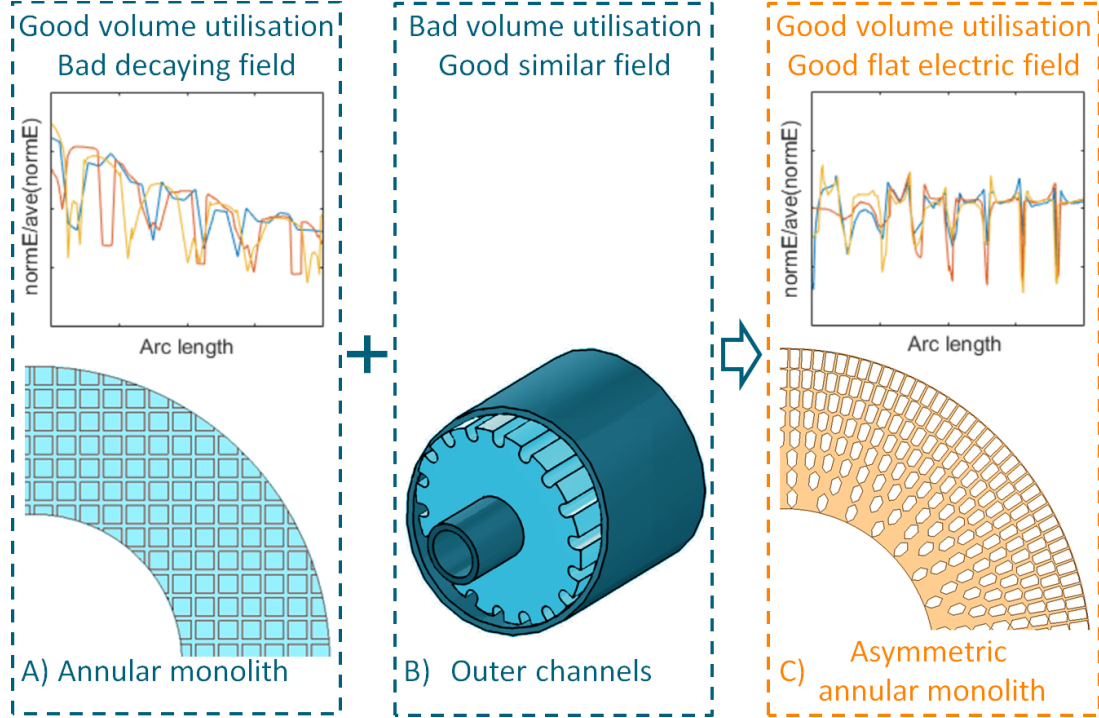


FIGURE 2.2: A) A bad decaying electric field is obtained when using an annular monolith. B) A bad volume utilisation is obtained when only using outer channels [9]. C) An axial annular asymmetric monolith keeps a flat profile while obtaining a better volume utilisation

TABLE 2.4: Selecting conductor and monolith materials. (Extended tables Appendix E)

Property		Conductor	Monolith
Maximum service temperature	T_{\max}	≥ 1500 K	≥ 1500 K
Thermal shock resistance	R_T	maximise	high
Leak-before-break criterion	LBB	$\geq 0.25p\pi r$	$\geq 0.25p\pi r$
Oxidation rate		low	low
De-oxidation rate		low	low
Dielectric strength	V_b	-	$\geq 3 \times 10^6$ V/m
Thermal expansion coefficients	α	minimise	minimise
Elastic modulus	E	maximise	maximise
Creep temperature	T_{creep}	maximise	maximise
Dielectric constant	ϵ'	-	minimise
Permittivity stability		-	?
Flammability		low	low
Costs	C_V	minimise	minimise
Electrical resistivity	ρ_e	minimise	-
Selected material		Ta-10W alloy	Alumina 85

The *material match* has quite more possibilities, because there are more than 160,000 readily available engineering materials to choose from [51]. Thus, CES edupack [52] was used to filter 3,900 materials through Ashby's method [53] with the constraints defined in Table 2.4. The filter showed that refractory metals for the conductor can be replaced by a semi-conductor materials at low pressures (Appendix E). Eventually, Alumina 85 was chosen for the monolith and Tantalum-Tungsten alloy Ta-10W for the conductor, because these materials are capable of coping with the process conditions.

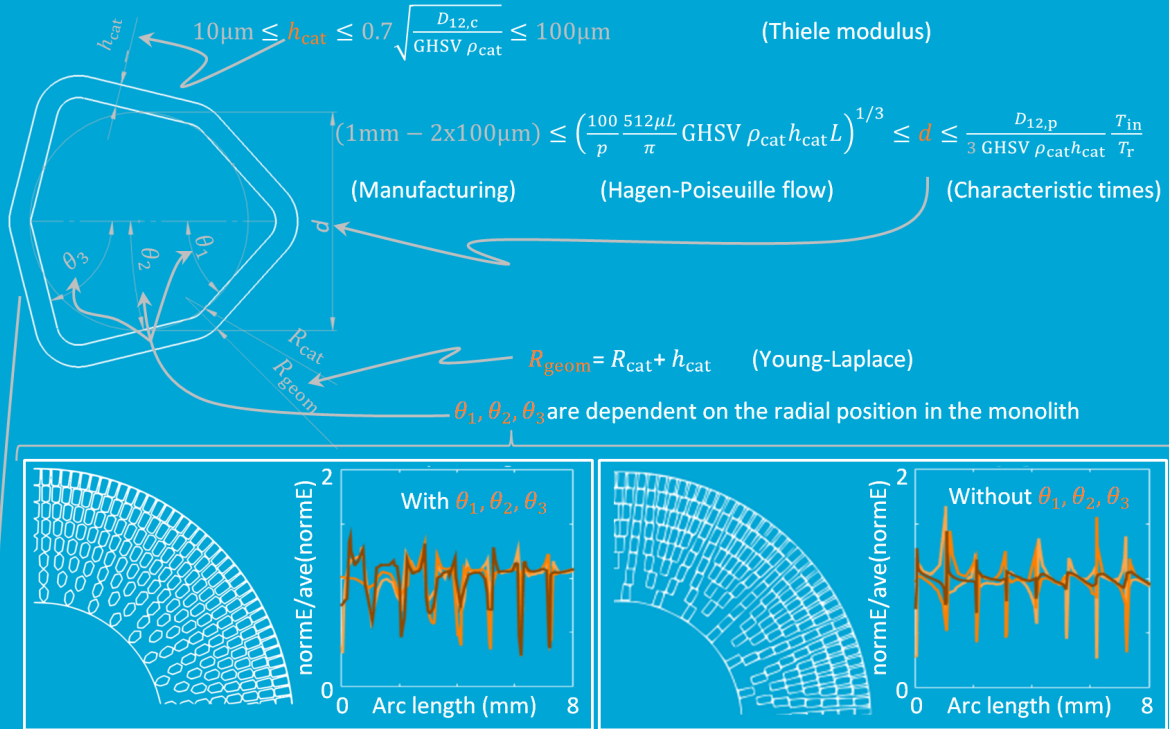
3) Sizing calculations

The channel was the first part to size using earlier obtained information (Figure 2.3). The channel geometry needs to maximise the catalyst deposition while staying manufacturable and avoiding accelerated deactivation spots, reactants bypassing and too high pressure drop. The maximum economic and manufacturable catalyst deposition was calculated using derivations from the mass and momentum conservation laws. Furthermore, some rule of thumb-based engineering numbers (< 0.7 for generalised Thiele modulus [54], 10-100 μm for catalyst thickness [45], 1 mm for minimum channel width [10], 3 for convective characteristic time divided by diffusive characteristic time (G. Stefanidis, personal communication, September 2016) and 0.01 for pressure drop divided by operation pressure) were put in place to address these challenges.

The monolith was the next part to size (Figure 2.3). The monolith geometry needs to fit as many earlier sized channels as possible without higher order modes propagating. The maximum number of channels was obtained using a MatLab [55] optimisation grid search script in combination with the RF-module of COMSOL [56]. The grid search optimisation maximises the number of channel rows for a pre-set inner conductor radius, inner monolith radius and outer conductor radius while keeping propagation of higher order modes sufficiently low. These channel rows were simplified using electrical circuit analysis to accelerate the simulation. Moreover, the grid search was done for an outer conductor touching the monolith to decrease the degrees of freedom. Furthermore, the algorithm assumes a minimal producible wall thickness of 0.125 mm which is similar to 400 CPSI monolith. Finally, a halving of the higher order modes electric power on every 1 percent of the reactor length was assumed to be necessary.

The created grid search data need to be compared with each other. Thus, the number of rows was translated into a number of channels through reversing the parallel circuit formula (Figure 2.4). The optimal cross section derived from the data has an outer diameter of 26 mm and a relative permittivity of 8 for the monolith material.

A) Channel sizing



B) Monolith sizing

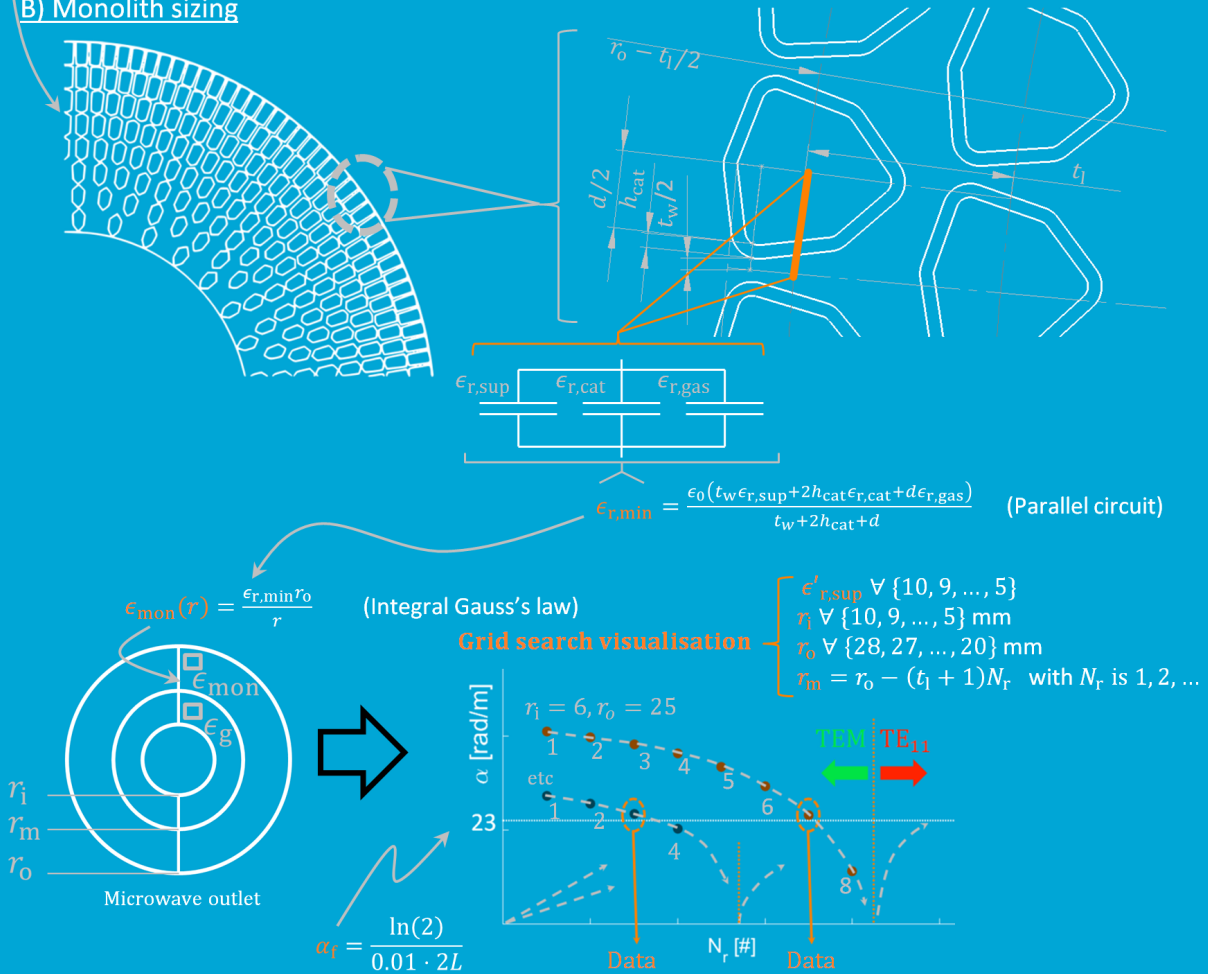


FIGURE 2.3: Sizing calculation scheme of the channel and monolith. A rectangular within the model stands for a mapped domain mesh of that domain.

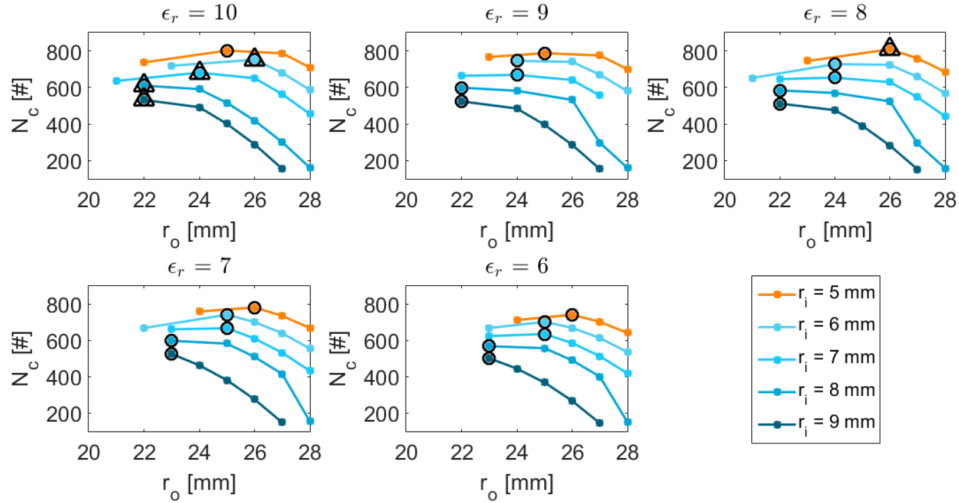


FIGURE 2.4: The highest number of channels per dielectric constant per inner diameter is circled. The highest number of channels per inner diameter of all dielectric constants is triangled. The data shows the inner conductor diameter should be minimised and that a specific dielectric constant for the asymmetric annular monolith is needed.

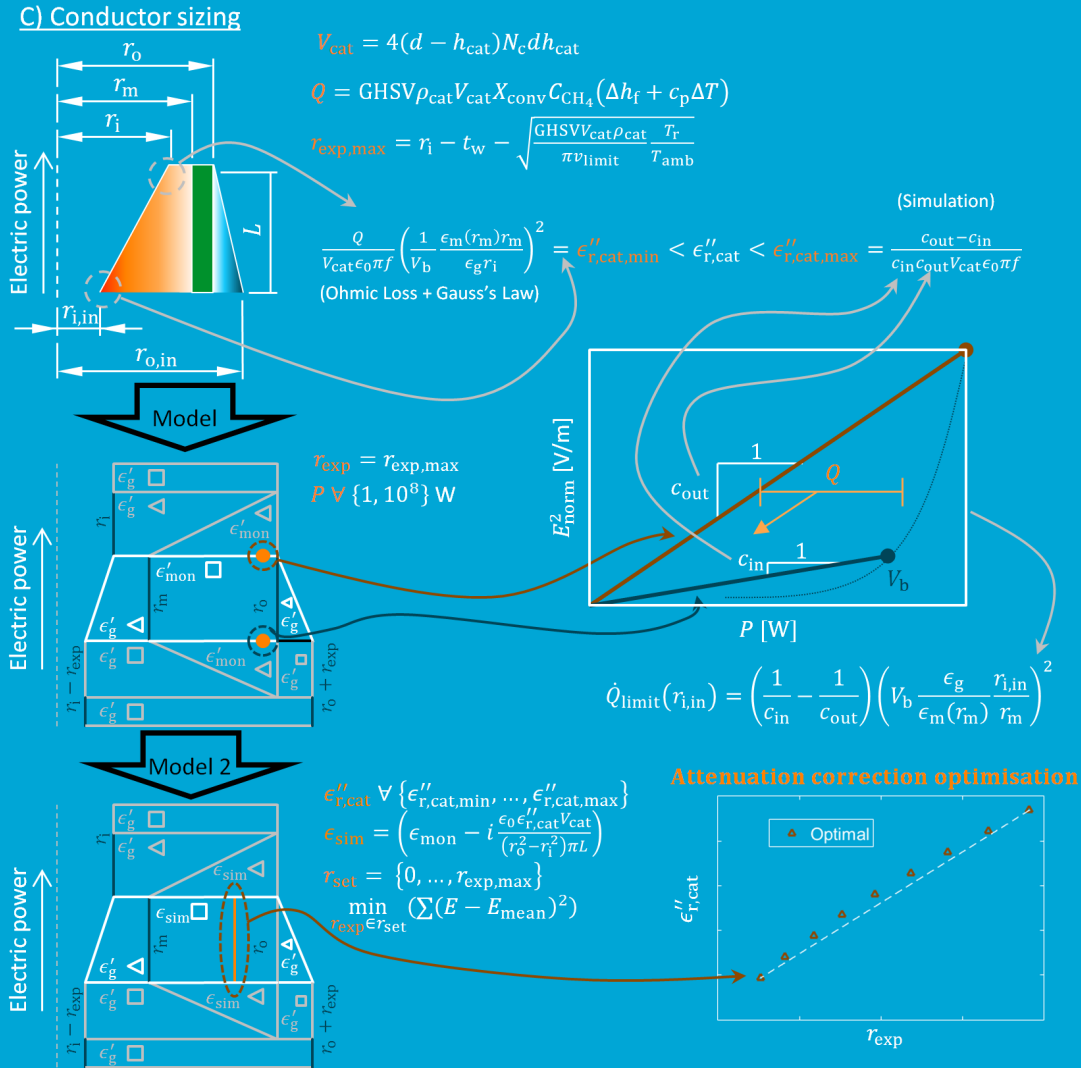


FIGURE 2.5: Sizing calculation scheme of the conductors based on dielectric loss factor limits. Rectangles and triangles within the model stands for a mapped and free triangular domain mesh.

Finally, the conductors were sized (Figure 2.5). The conductor's geometries need to maximise volume utilisation while preventing dielectric breakdown, attenuation and higher order modes. Longer conductors will contain more catalyst. Thus, the length of the conductors was maximised to 1.5 m to leave room for the inlet, outlet and the rectangular to coaxial waveguide parts in the requested 2x2x2 m container. Furthermore, the fixed length sets a minimum and maximum for the dielectric loss factor due to dielectric breakdown and attenuation. The minimal and maximal dielectric loss factor were derived (section C.10) using Ohmic loss equation, Gauss's law and the RF-module of COMSOL while avoiding higher order modes. A derivation of the cut-off frequency formula is used to avoid higher order modes. Finally, the minimal and maximal dielectric loss factors were used together with the heating need of the reaction to optimise which amount of linear narrowing is needed. The attenuation correction optimisation graph is used to decide how much narrowing of both conductors is needed based on the dielectric loss factor of the catalyst to solve attenuation. Narrowing both conductors has not been suggested before for microwave reactors and is used to increase the heating limit.

4) *Choosing more specific solutions*

The designed reactor (Figure 2.6 and Figure 2.7) was obtained after solving the remaining challenges through choosing more specific solutions. These solutions sacrificed reactor length to assure the microwaves and the gas mixture to enter and leave correctly. First of all, the flow direction of the gas is from wide to small such that the seals are pressed in the conductors to prevent leakage. Moreover, the seals need to be stretched and compressed during assembly to assure no gaps are formed at operation temperature and pressure. Furthermore, the number of seals and the length of the seals is minimised by using the inner conductor as inlet which is a new idea. However, this forces the reactant through some bends which cause preferential flow. Preferential flow is prevented using the newly defined geometry of an anisotropic porous media with higher pressure drop in axial direction than the other directions. An additional simulation showed that the anisotropic media does not cause reflection at thin enough layers (section C.12). Finally, the seals combined with the porous media at inlet and outlet needs to be multiples of half-wavelengths to prevent reflection [21] which is a new idea.

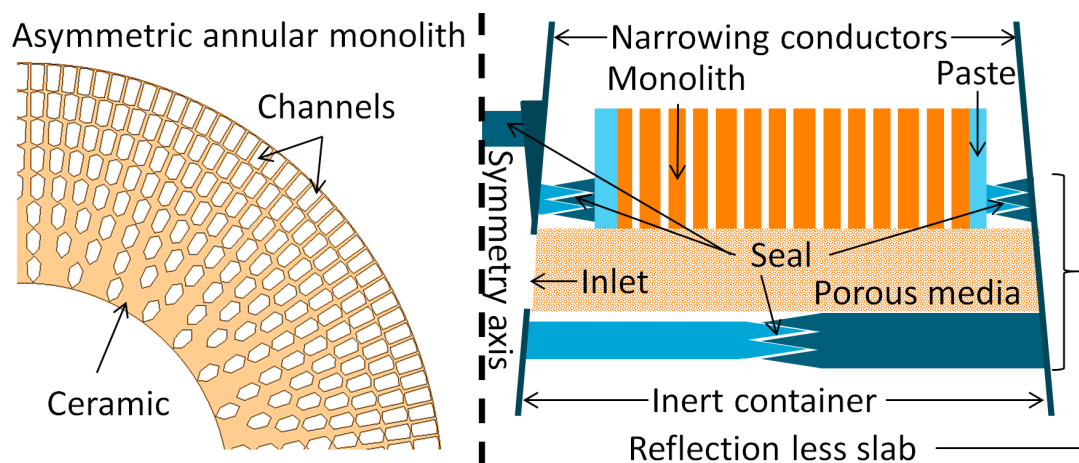


FIGURE 2.6: Asymmetric annular monolith and overview travelling microwave reactor applicator.

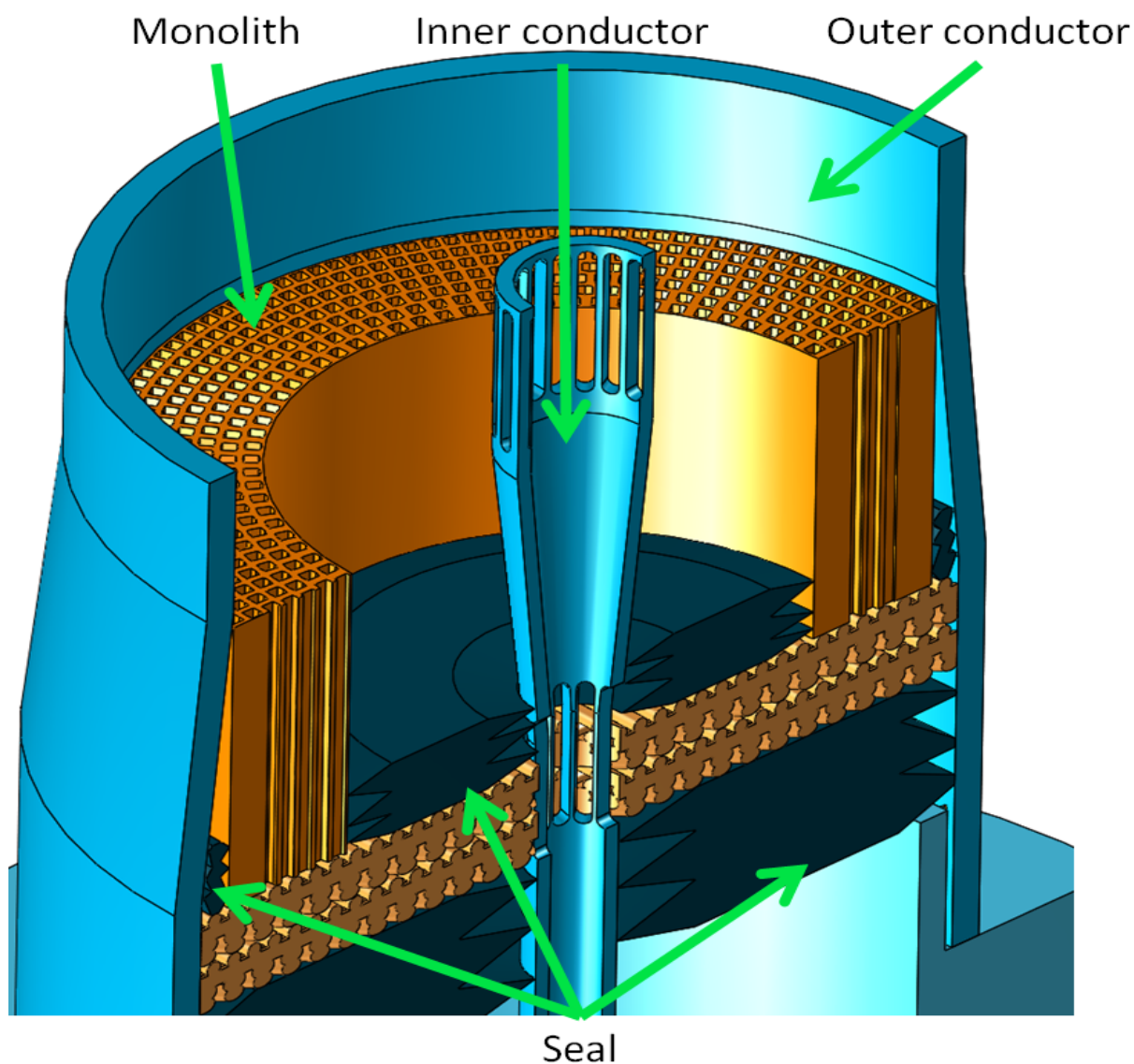


FIGURE 2.7: The designed reactor is represented with the 1.5 m monolith replaced by a 2 cm monolith to make the model manageable in the report.

3 | Discussion

In [Chapter 2](#), the travelling microwave reactor has been designed. In this chapter, the designed reactor and the used methods are evaluated. First, the designed reactor is evaluated on the set requirements followed by a discussion of possible improvements. Then, the intrinsic flaws of the methods are discussed. Finally, some ignored opportunities that could further improve the reactor performance are presented.

3.1 Evaluating the designed reactor

The designed reactor was evaluated on the requirements ([section 2.1](#)). The only requirement that has not been addressed so far is economic feasibility. The economic feasibility is accessed by calculating the economic potential ([Equation 3.1](#) derived in [section C.14](#)). The economic potential [57] of the designed reactor is defined as the price difference product minus feed in a full-year of operation while keeping the GHSV the same as in experiments (A.I. Stankiewicz, personal communication, September 2016). The feed cost is assumed to be zero, because in the chosen case the methane would be flared otherwise.

$$EP = V_{\text{cat}} \rho_{\text{cat}} \text{GHSV} (T) \rho (p) X_{\text{conv}} \left(\frac{\text{MW}_{\text{C}_6\text{H}_6}}{6\text{MW}_{\text{CH}_4}} \right) \tau_{\text{year}} C_{\text{benzene}} \quad (3.1)$$

TABLE 3.1: Economic potential of different microwave reactors. The catalyst thickness of monoliths is set to 100 μm .

	Length [mm]	Cross flow area [mm ²]	Catalyst weight [g]	Economic potential [\$/y]	Reference
Conventional packed bed	7.5	113	0.4	0.04	[58]
Mono-mode monolith	15	81	0.3	0.03	[10]
TMR Pathfinder	300	778	2.8	0.29	Appendix F
TMR Designed	1500	830	304.8	32.30	section 2.3

3.2 Improving the designed reactor

The evaluation shows that the \$32.3 a year economic potential of the designed reactor is at least 4 orders of magnitude too low and needs to be improved, because the equipment cost is assumed to be in the order of \$100,000 which is based on the expected insufficient budget for the pathfinder (current prototype concept [Appendix F](#)) (G.S.J. Sturm, personal communication, June 2016). There are 6 ways to increase the economic potential of the TMR given in [Table 3.2](#). The first four which are changing the catalyst, increasing the temperature, increasing the pressure and lowering the frequency, have an accumulated improvement factor of 70000. This improvement factor is obtained through extrapolation of

data [59][35][60][61]. However, it is expected that these improvements will also increase the costs with at least an order of magnitude, because microwave generators are not capable of delivering sufficient power yet [62][63], with the higher operation pressure a compressor is needed and the costs of downstream processing should also be taken into account. Thus, the \$415,000 a year economic potential of the improved reactor will give a payback time for a \$1,000,00 device of at least 2.5 years. However, a theoretical limit at \$415,000 a year for a \$1,000,000 device that still needs many experiments and prototypes makes the travelling microwave reactor not economically feasible yet. Furthermore, catalyst regeneration will reduce production time and catalyst stability is another challenge.

TABLE 3.2: Six ways to increase economic feasibility. The factors are extrapolated using data from the given references.

How?	What?	Factor	Reference
1) <i>Change catalyst</i> Mo/HZSM-5 → Fe@SiO ₂	reduce coking	-	[59]
	accelerate reaction rate	↓	[59]
2) <i>Increase temperature</i> 973 K → 1500 K	accelerate reaction rate	25	[59] 🗨️
	favours equilibrium	8	[35] 🗨️
3) <i>Increasing pressure</i> 1 atm → 50 atm	accelerate reaction rate	50	[60]
	worsens equilibrium	1	[61] 🗨️
4) <i>Lower frequency</i> 2.45 GHz → 915 MHz	increase size	7	
Combine (1-4)	improvement	70000	=7×25×50×8/1
5) <i>Change the design</i>	solve limits		
6) <i>Change the reaction</i>	valuable products		

TABLE 3.3: Economic potential of the designed travelling microwave reactor and improved travelling microwave reactor.

	Length [mm]	Cross flow area [mm ²]	Catalyst weight [g]	Economic potential [\$/y]	Reference
Improved	1500	1025	376.4	415 × 10 ³	section 3.2
Designed	1500	830	304.8	32.30	section 2.3
Improvement				415 × 10 ³ /32.30 = 12850	

Change the design to achieve economic feasibility

The production rate improvement of 70000 (Table 3.2) was checked on feasibility using the calculation scheme in section 2.3. This improvement cannot be achieved in the designed reactor (Table 3.3), because the higher reaction rate causes the reactants bypassing the catalyst (convection divided by diffusion characteristic time ratio drops below 1), too high pressure drop (increases to 0.01 P_r) and too high flow velocity at the inlet (increases to 15 m/s, section C.6). Thus, a different design concept such as the more difficult to manufacture radial design (Figure 3.1) can solve reactants bypassing (Dean vortex),

pressure drop (shorter reactor length) and preferential flow (larger cross flow area of the monolith, inlet and outlet, [section C.6](#)). Additionally, a new idea of breakdown protection (a material around the inner conductor with a higher breakdown voltage than air and a relative permittivity of 1) can be used to increase the heating limitation. Additionally, multiple half-wave slab outer conductor inlets can be added to decrease the flow velocity, because the flow velocity caused the 915 MHz not to obtain the 70000 increase. However, multiple outer conductor inlets need a higher attenuation constant and thus decreases catalyst loading per meter, because the interrupted reactor length is more likely to create higher order modes. Cross flow area can also be increased by a (stacked) rectangular waveguide ([Figure 3.2](#)). A quick calculation on the stacked rectangular waveguide ([Figure 3.2](#)) also showed that a rectangular waveguide is currently more beneficial. Finally, a spiralling narrowing rectangular waveguide with reactant cross-flow is the most promising design ([Figure 3.3](#)). The spiralling reactor was not earlier implemented, because it was disregarded by the assumptions made in the shape match ([Figure 2.1](#)). In this spiralling reactor, the microwaves are completely absorbed. Therefore, there is no need for a microwave recycle. Furthermore, the space within the spiralling reactor can be filled with a smaller radius spiralling reactor to roughly double the catalyst loading. A quick calculation shows that the spiralling reactor have a sufficient economic potential ([Table 3.4](#)). However, microwave leakage between revolutions needs to be checked to assure uniform heating will take place.

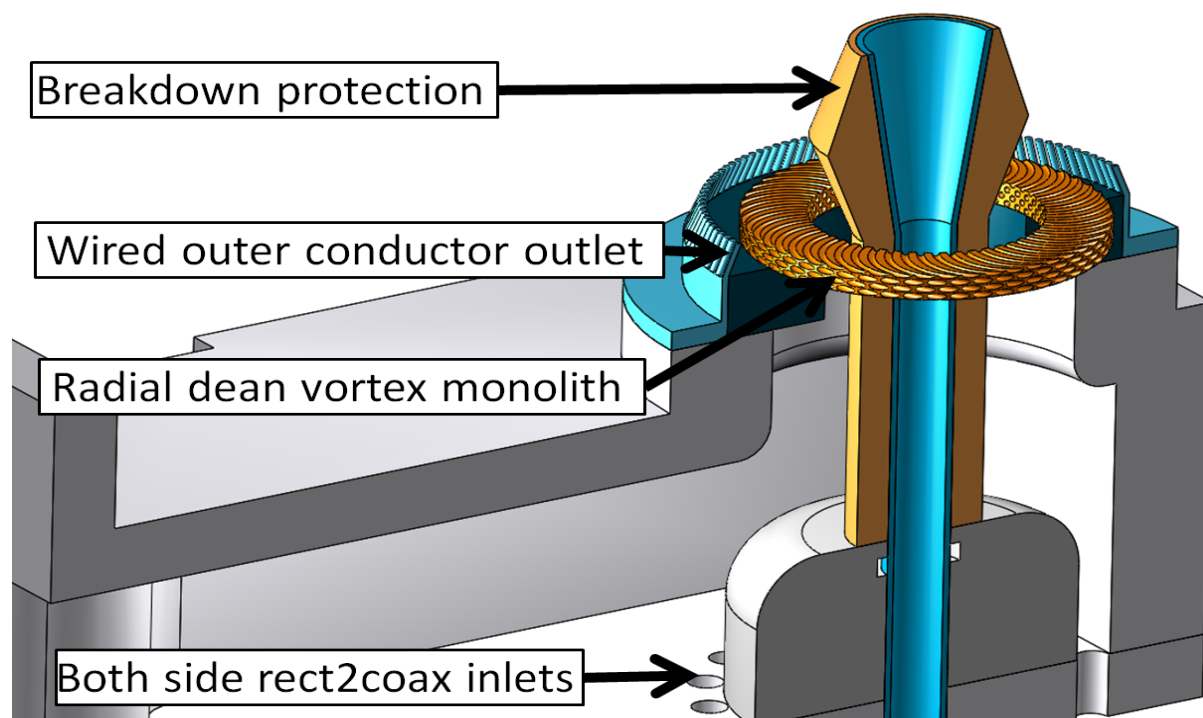


FIGURE 3.1: The advanced radial design uses radially outwards curved channels to induce a dean vortex for mixing. Furthermore, the space between inner and outer conductor is used as inlet and a wired outer conductor is used to let the product out.

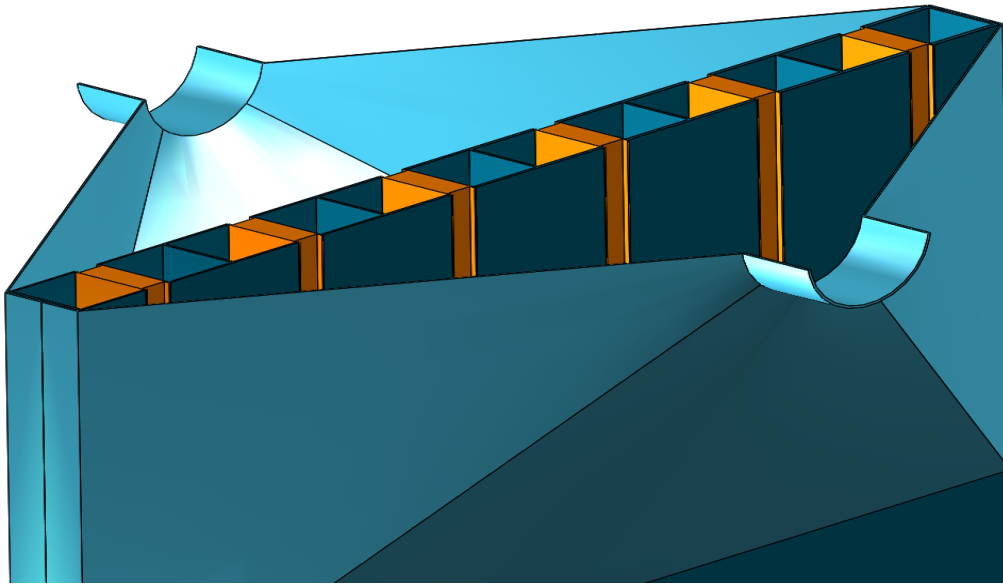


FIGURE 3.2: The stacked rectangular waveguide reactor which consist of 6 rectangular waveguides. This reactor is calculated while assuming the monolith and catalyst dielectric constants are 1, the catalyst dielectric loss factor is exactly what is needed and the reaction area has atleast 95% heating of maximum heating. The slabbed has $EP=3.6 \times 10^6$ $\$/y$, $Q=6 \times 10^6$ W and $m_{cat}=3.26$ kg while the extruded monolith catalyst has $EP=8.27 \times 10^6$ $\$/y$, $Q=14 \times 10^6$ W and $m_{cat}=7.49$ kg. However, the maximum heating is limited to 7×10^6 W. The calculations of the stacked rectangular waveguide reactor also reveal that a single rectangular waveguide (divide the results by 6) will outperform the asymmetric annular monolith.

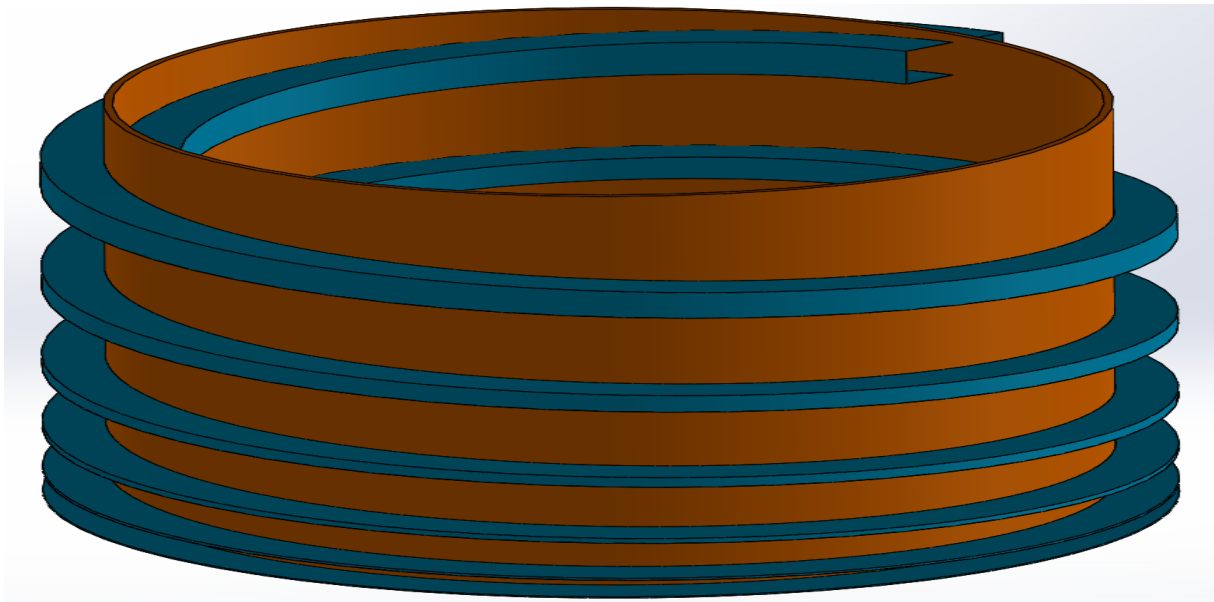


FIGURE 3.3: The waveguide of the spiralling narrowing rectangular reactor is stretched to better show the spiralling waveguide. However, the waveguide should keep contact after each revolution. This reactor is calculated while assuming the catalyst dielectric constant is 5, the catalyst dielectric loss factor is exactly what is needed and the reaction area has atleast 95% heating of maximum heating.

Two spiral reactors within a 2x2x2m container could have a catalyst loading of 64 kg.

TABLE 3.4: Economic potential of the rectangular waveguide and spiralling narrowing rectangular waveguide microwave reactor. The spiralling reactor is calculated for methane to benzene and methane to ethylene with $C_6H_6 = 0.126$ \$/kg and $C_2H_4 = 1.4$ \$/kg [25].

	Length [mm]	Cross flow area [m ²]	Catalyst weight [g]	Economic potential [\$/y]	Reference
Rectangular design	1500	0.03	1.2×10^3	1.4×10^6	Figure 3.2
Spiralling design benzene	1500	0.11	64.7×10^3	71.4×10^6	section 3.2
Spiralling design ethylene	1500	0.11	64.7×10^3	7.9×10^8	section 3.2

Change the reaction within the designed reactor limits

The above improvements revealed the limits of the designed reactor (Table 3.5). These limits might be pushed by refining the calculation. However, these limits roughly reveal what a travelling microwave reactor is able to do. Thus, these limits can be used to check whether more valuable products will become economically feasible. For example the 7.9×10^8 \$/y economic potential of the spiralling reactor in Table 3.4 has also been calculated for methane to ethylene.

TABLE 3.5: Optimistic limits of the designed reactor

Limit	Variable	Value 2.45 GHz	Value 915 MHz	Reference
Flow volume	V_{limit}	0.46m ³ /h	14.1m ³ /h	section C.9
Catalyst volume	V_{cat}	4.5×10^{-4} m ³	5.5×10^{-4} m ³	section C.10
Energy dissipation	Q_{limit}	54 kW	20 MW	section C.11

Summarising the travelling microwave reactor designs

The previous paragraphs showed that the economic potential of the designed reactor to the improved reactor increased by 4 orders of magnitude. The designed reactor needed to be improved, because the requirement (section 2.1) to economically convert methane to benzene was not possible. However, the improved reactor faces hydrodynamic-related limits (Table 2.2). Furthermore, reaction rate at higher pressure and temperature is uncertain. The hydrodynamic-related limits can be solved with a spiralling reactor design (Figure 3.3). This spiralling reactor was not implemented earlier, because it was disregarded by the assumptions made in the shape match (Figure 2.1). Finally, microwave leakage between the waveguides of the spiralling reactor still needs to be checked.

3.3 Evaluating and improving the methods

The previous section shows that more solution and opportunities can be found by reconsidering assumptions. Furthermore, finding more solution, opportunities and challenges within the assumptions can still be done by other engineers, because the methods used (phenomena exploration method Appendix A and essence of creative design Appendix B) were limited by my subjective interpretation.

3.4 Giving attention to ignored opportunities

The designed reactor so far completely ignored the opportunity of balance shift. In this work thermodynamic equilibrium shift is renamed to thermodynamic balance shift. Balance shift can reduce energy losses due to lower mean operating temperatures than normally found at similar chemical fractions. Zhang et al. [64] stated that “[hot-spots] could create local shifts in equilibrium constant [of a chemical reaction]”, “if the residence times of the gases flowing over the catalyst are relatively long compared to the half-lives for the reaction”. In other words, equipment can be built to shift thermodynamic balances. In fact, this equipment might have been built already [65][66].

Thermodynamic balance shifting devices were developed by different groups. Altman et al. [65] showed that the dielectric loss factor influences the thermodynamic balance and Gao et al. [66] showed that the dielectric constant influences the thermodynamic balance. Neither group reported correlation with the other dielectric property. Both groups concluded that their chosen dielectric property influences the vapour-liquid balance distribution coefficient β . Furthermore, Altman et al. [65] claimed while Gao et al. [66] declaimed that the microwave power influences the distribution coefficient. Moreover, Gao et al. [66] claimed while Altman et al. [65] declaimed that difference in boiling points influences the distribution coefficient. However, both concluded that the interface needed to undergo microwave heating and that the influence on the distribution coefficient is expected to be caused by linked phenomena. Thus, a linked phenomena theory is made based on a time interval ignored by both groups. This linked phenomena theory shows that the shift in the distribution coefficient can be said to be at thermodynamic balance.

Thermodynamic balance shift terminology

Before thermodynamic balance shift can be explained, the terminology going hand-in-hand with it needs to be explained. Firstly, the term pulsated is used with balance and volume. In this work pulsated means that energy is added and removed periodically such that the net energy is zero. Secondly, a thermodynamic balance fulfils a chemical balance (no net flow of mass) and thermal balance (no net flow of energy). Thus, a volume at thermodynamic equilibrium is also at thermodynamic balance. In Figure 3.4 can be noticed that the thermodynamic equilibrium line and pulsated thermodynamic balance line are different. This difference is called thermodynamic balance shift. When a point is picked on the thermodynamic equilibrium line and moved isothermally up to the pulsated thermodynamic balance line then the temperature of the thermodynamic balance has changed. Thus, in the context of this work chemical balance shift means that the fraction of a pulsated volume in thermal balance with a volume in thermodynamic equilibrium is different. When a point is picked on the thermodynamic equilibrium line and moved “isochemically” sideways to the pulsated thermodynamic balance then the fraction of the thermodynamic balance has changed. Thus, in the context of this work thermal balance shift means that

the temperature of a pulsated volume in chemical balance with a volume in thermodynamic equilibrium at similar fraction is different. Furthermore, if you want to compare the position in which the energy of the volume is similar you will end up somewhere in between.

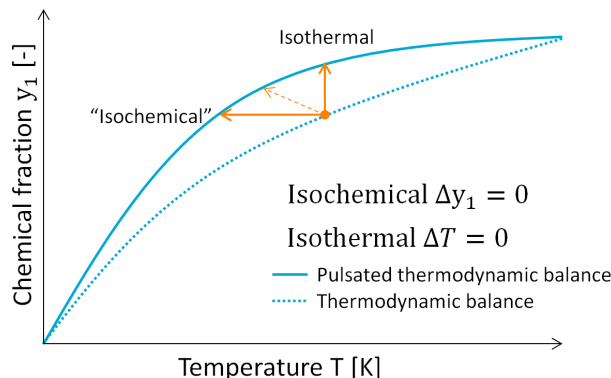


FIGURE 3.4: This figure is used in explaining the terminology of thermodynamic balance shift, chemical balance shift and thermal balance shift in microwave reactors.

Phenomena and equipment causing thermodynamic balance shift

The previously mentioned time interval is caused by cheaper half-wave rectifiers without smoothing combined with the alternating current electricity grid (Figure 3.5). These cheaper rectifiers cause a pulsing power supply which might have caused changed thermodynamic balance (G.S.J. Sturm, personal communication, October 2015). It has to be noted that an engineering decision was made to favour microwave generation in most microwave oven magnetron causing a pulsating power supply [67]. Figure 3.6 shows that pulsing microwave energy is capable of changing the chemical balance, because Arrhenius equation [40] is exponential and local selective heating causes locally raised temperatures. Arrhenius equation states that the reaction rate at higher temperature is faster. This change is exploited in periods of thermal balance. A period of thermal balance consist of a microwave energy dissipating pulse followed by convection and diffusion of the energy such that no net flow of energy in the control volume is achieved. In a period of thermal balance the backwards reaction at lower temperature cannot completely convert the forward reaction at elevated temperature back to the thermodynamic equilibrium. Thus, a shifted thermodynamic balance is obtained under pulsated power supply after sufficient periods of thermal balance, because the changed concentration accelerates the backwards reaction causing the backwards reaction to completely convert back the forward reaction. Periods of thermal balance are in practice achievable by selectively heating. Moreover, a pulsing power supply was patented in 1986 to control selectivity in a methane to ethylene process [68]. The higher selectivity is claimed to be caused by fewer side-reaction due to lower bulk temperature. Thus, this means that a shifted thermodynamic balance and a higher selectivity can be obtained with microwave power pulsing, the right rigorous mixing in higher order mode heating patterns, electric field contraction due to a material interface (such as in packed beds and at a turbulent vapour-liquid interface) or abruptly changing heating patterns.

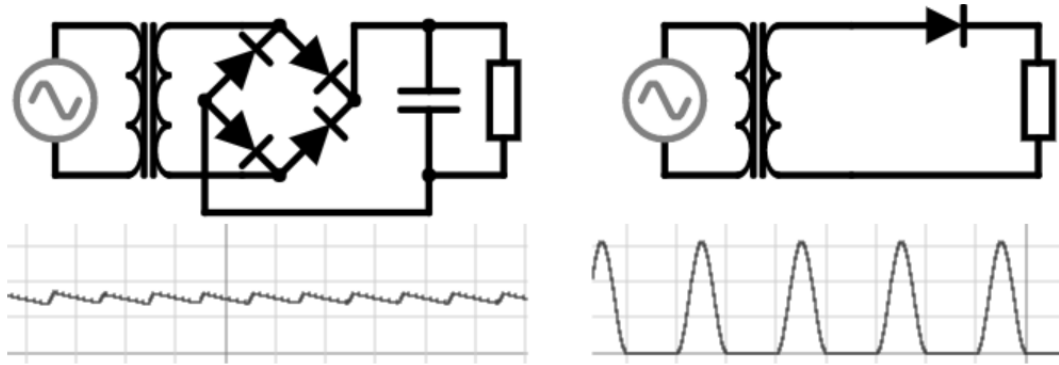


FIGURE 3.5: A simplified representation of **rectifiers**. Left) A single-phase full-wave rectifier with smoothing in which a diode bridge first changes alternating current to a fluctuating direct current. Then, a capacitor is used to smooth the peaks which result in an almost flat power supply (left below). Right) The cheapest rectifiers might only consist of a single diode which changes the alternating current to a direct current. However, only using a single diode results in a pulsating power supply (right below). Furthermore, DC-to-DC converters can also cause fluctuation.

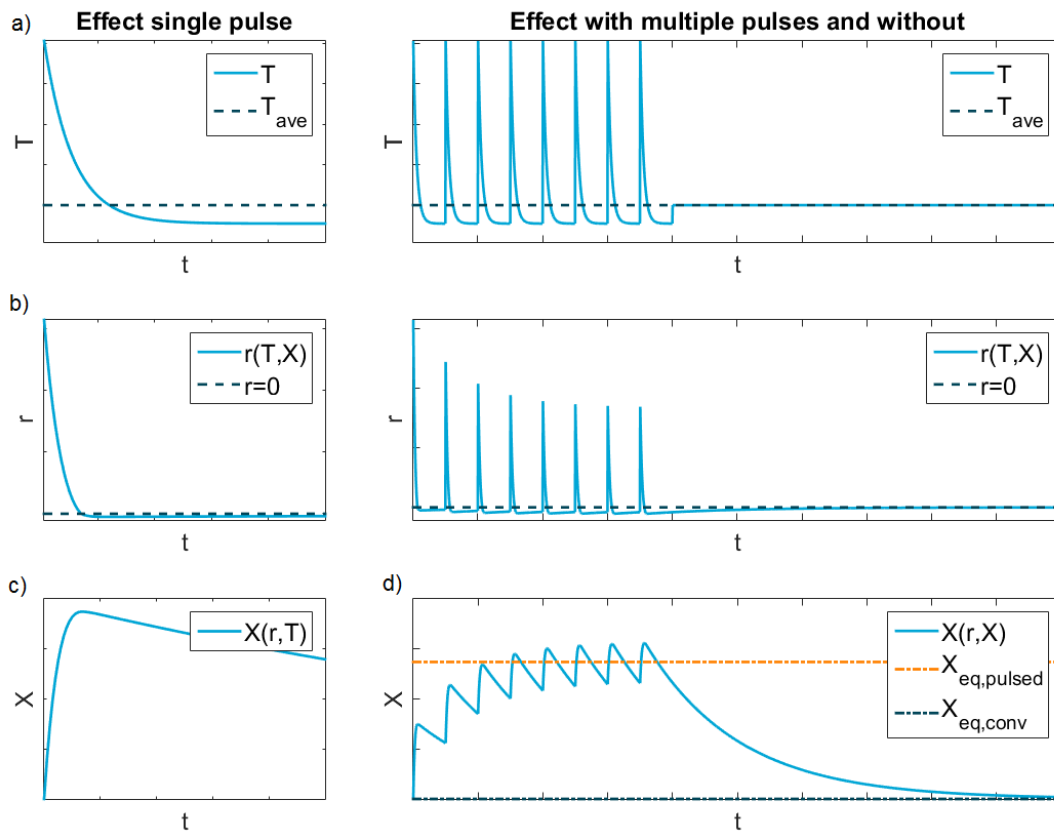


FIGURE 3.6: The influence of pulsing on thermodynamic balance without taking the heat of reaction into account. a) A pulse increases the temperature of the dissipating dielectric. The heat is then transferred to the fluid through diffusion. [69, Fig. 1.17] b) The reaction rate increases with higher temperature. (Arrhenius equation) The temperature then drops below the temperature needed for thermodynamic equilibrium and the reaction is reversed. c) Finally, the reaction has not recovered fully to thermodynamic equilibrium before the next pulse is applied. Thus, the balance constant of the reaction is slightly higher than the equilibrium constant. (accumulation) d) Eventually, after sufficient pulses, a shifted thermodynamic balance is reached due to changed concentration (reaction kinetics). Furthermore, the thermodynamic balance moves to a thermodynamic equilibrium when the pulsation is stopped.

4 | Conclusion and recommendations

In the introduction was stated that a travelling microwave reactor would be designed in this study to answer two questions. One question, "*What are the operation ranges of a travelling microwave reactor?*", can be answered by looking at the design. The designed reactor consists of a *high performance coated asymmetric annular monolith in an inert coaxial waveguide with narrowing conductors in axial direction and an anisotropic porous media for flow distribution to maximise volume utilisation* (Figure 4.1). This design was established by letting the engineer combine, extrapolate and abstract ideas of existing solutions. The obtained operation ranges are a temperature below 1500 K, a pressure below 50 atm, energy dissipation rate below 20 MW and a volume flow below 14.1 m³/h. These operation ranges are not sufficient for economically transforming methane to aromatics. Therefore, it is recommended to switch to another endothermic gas phase reaction which is economical in the calculated operation ranges or obtain another design. For example, the suggested spiralling narrowing rectangular microwave reactor design.

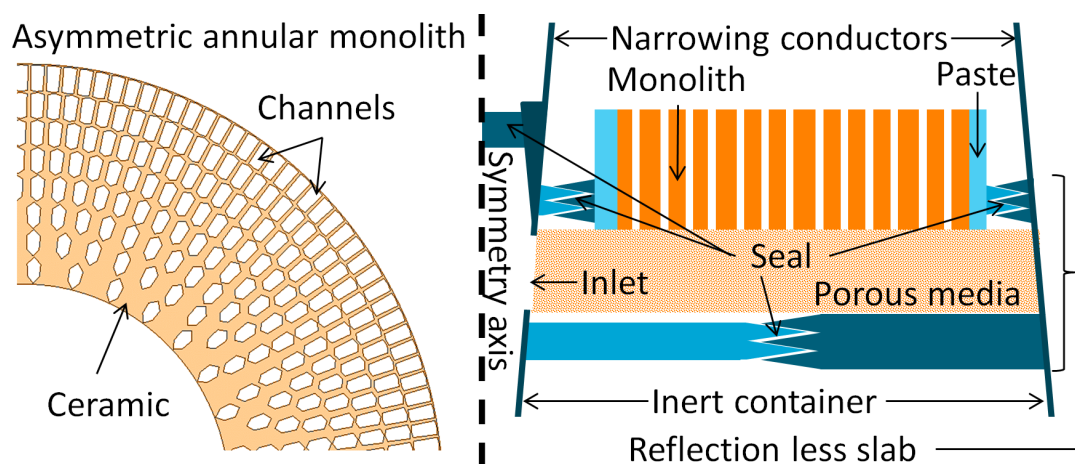


FIGURE 4.1: Asymmetric annular monolith top view and axis symmetric view of the designed reactor.

The other question, "*What do I need to know to build a working travelling microwave reactor?*", is answered by looking back on the designing. The designed reactor and its operation range resulted from solving 21 challenges (Table 4.1). The microwave reactor specific *unstable permittivity* and *accelerated deactivation spots* challenges were found using the self-developed phenomena exploration method. The phenomena exploration method is specifically developed to reveal unknown challenges on the intersection of established engineering fields by letting the engineer think further on combination of words. The used words were taken from microwave reactor topology, hazard operability study and life-cycle assessment study. Eventually, all these and unknown challenges should be taken into account in future microwave reactor designs. Thus, the (thermodynamic) material properties needed during this study to solve these challenges need to be known as well (Table 4.2).

TABLE 4.1: Overview of which sub-solution contributed solving which challenges at which step.

This sub-solution	addresses this challenge	at this step
Process design	Reaction troubles	Information
Alumina 85 and Ta-10W alloy	Material phase changes	Material matching
	Thermal cracks	Material matching
	(inverse-)corrosion	Material matching
	Thermal increasing gaps	Material matching
Ta-10W alloy	Pressurized rupture	Material matching
	Material creep	Material matching
	Pressure increasing gaps	Material matching
Alumina 85	Unstable dielectric heating	Material matching
Channel geometry	Reactants bypassing	Channel sizing
	Pressure drop	Channel sizing
	Material interface	Channel sizing
High performance coating	Accelerated deactivation spots	Channel sizing
Asymmetric annular monolith	Radial decaying field	Monolith sizing
	Higher order modes	Monolith sizing
	Volume utilisation	Shape matching
	Manufacturability	Shape matching
Coaxial waveguide	Manufacturability	Shape matching
	Volume utilisation	Shape matching
	Higher order modes	Shape matching
	Pressure increasing gaps	Specific solutions
Narrowing conductors	Attenuation	Conductor sizing
	Dielectric breakdown	Conductor sizing
	Higher order modes	Conductor sizing
Flow direction	Pressure increasing gaps	Specific solutions
Compressed seal	Pressure increasing gaps	Specific solutions
	Thermal increasing gaps	Specific solutions
Stretched seal	Thermal increasing gaps	Specific solutions
Inner conductor as in- and outlet	Material phase changes	Material matching
	Manufacturability	Specific solutions
	Thermal increasing gaps	Specific solutions
	Pressure increasing gaps	Specific solutions
	Escaping microwaves	Specific solutions
Anisotropic porous media	Preferential flow	Specific solutions
Reflectionless half-wave slab	Reflection	Specific solutions

TABLE 4.2: Overview of which (thermodynamics) material properties needed to be know in this study.

Microwave-related	Mechanics-related	Hydrodynamics-related
Molar heat capacity	Operation time	Viscosity
Enthalpy of formation	Thermal conductivities	Molecular weights
Selectivity	Elastic moduli	Diffusion volumes
Conversion	Yield strengths	Catalyst density
Catalyst liquid tension	Conductor creep temperature	Gas-hourly space velocity
Permittivity stability	Conductor fracture toughness	Methane density
Dielectric loss factors	Environmental resistance	
Dielectric constants	Price product	
Dielectric breakdown mixture	Thermal expansion coefficients	
	Maximum service temperature	
	Minimal wall thickness	

Furthermore, there are two more opportunities to push the economic potential of a microwave reactor. Firstly, thermodynamic balaance shifts in microwave reactors have gained an explanation using diffusion, selective dielectric heating and Arrhenius equation. This explanation shows that higher conversion rates can be obtained at lower outlet temperatures through energy pulsation. Secondly, reflecting on the designing process showed that combining knowledge of multiple engineers is also an opportunity for a more economical industrial microwave reactor, because the used methods are subjective and have only been used by a solitary engineer. Thus, a different travelling microwave reactor design, another reaction and/or other process intensification concepts can help achieve a sustainable future. A future in which the chemical industry converts waste into products while simultaneously storing energy.

To conclude, the following recommendations are made

- Find an endothermic heterogeneous gas-phase catalytic reaction with a more valuable product, use the sizing calculation scheme to size the designed reactor and finally check the *local* economic potential.
- Check the spiralling narrowing rectangular microwave reactor design with sufficient economic potential, or create a different microwave reactor design that is economical feasible. Do not forget to at least solve the 21 challenges. Furthermore, focus on how the reactor reacts on variation around the designed specification.

Bibliography

- [1] T. van der Schans. *Travelling microwave reactor design*. Delft university of technology, 2017. URL: <http://www.repository.tudelft.nl>.
- [2] Guido S.J. Sturm. *Microwave Field Applicator Design in Small-Scale Chemical Processing*. Institutional Repository. 2013. ISBN: 9789461919458. DOI: [10.4233/uuid:0407019d-248c-4061-b349-f9ea81085da1](https://doi.org/10.4233/uuid:0407019d-248c-4061-b349-f9ea81085da1).
- [3] Jeffrey K.S. Wan. “Method for disposal of chemical waste”. Patent US 4345983 (US). Aug. 1982. URL: <https://www.google.com/patents/US4345983>.
- [4] Richard Gedye et al. “The use of microwave ovens for rapid organic synthesis”. In: *Tetrahedron Letters* 27.3 (1986), pp. 279–282. ISSN: 0040-4039. DOI: [10.1016/S0040-4039\(00\)83996-9](https://doi.org/10.1016/S0040-4039(00)83996-9).
- [5] Raymond J Giguere et al. “Application of commercial microwave ovens to organic synthesis.” In: *Tetrahedron Letters* 27.41 (1986), pp. 4945–4948. ISSN: 0040-4039. DOI: [10.1016/S0040-4039\(00\)85103-5](https://doi.org/10.1016/S0040-4039(00)85103-5).
- [6] Heiko Will, Peter Scholz, and Bernd Ondruschka. “Microwave-Assisted Heterogeneous Gas-Phase Catalysis”. In: *Chemical Engineering & Technology* 27.2 (2004), pp. 113–122. ISSN: 1521-4125. DOI: [10.1002/ceat.200401865](https://doi.org/10.1002/ceat.200401865).
- [7] Trevor A. Kletz. “21. Inherently Safer Design”. In: *What Went Wrong? (4th Edition)*. Elsevier, 1999, Chapter 21. ISBN: 978-0-88415-920-9. URL: <http://app.knovel.com/hotlink/toc/id:kpWWWE0003/what-went-wrong-4th-edition/what-went-wrong-4th-edition>.
- [8] Christopher Roy Strauss and David W. Rooney. “Accounting for clean, fast and high yielding reactions under microwave conditions”. In: *Green Chem.* 12 (8 2010), pp. 1340–1344. DOI: [10.1039/C0GC00024H](https://doi.org/10.1039/C0GC00024H).
- [9] Guido S.J. Sturm et al. “Microwaves and microreactors: Design challenges and remedies”. In: *Chemical Engineering Journal* 243 (2014), pp. 147–158. ISSN: 1385-8947. DOI: [10.1016/j.cej.2013.12.088](https://doi.org/10.1016/j.cej.2013.12.088).
- [10] Adrián Ramírez et al. “Ethylene epoxidation in microwave heated structured reactors”. In: *Catalysis Today* 273 (2016). 5th International Conference on Structured Catalysts and Reactors, ICOSCAR-5, Donostia-San Sebastián, Spain, 22-24 June, 2016, pp. 99–105. ISSN: 0920-5861. DOI: [10.1016/j.cattod.2016.01.007](https://doi.org/10.1016/j.cattod.2016.01.007).
- [11] P.D. Muley et al. “Ex situ thermo-catalytic upgrading of biomass pyrolysis vapors using a traveling wave microwave reactor”. In: *Applied Energy* 183 (2016), pp. 995–1004. ISSN: 0306-2619. DOI: [10.1016/j.apenergy.2016.09.047](https://doi.org/10.1016/j.apenergy.2016.09.047).

- [12] Tomasz Durka et al. “On the accuracy and reproducibility of fiber optic (FO) and infrared (IR) temperature measurements of solid materials in microwave applications”. In: *Measurement Science and Technology* 21.4 (2010), p. 045108. URL: <http://stacks.iop.org/0957-0233/21/i=4/a=045108>.
- [13] Guido S.J. Sturm et al. “On the effect of resonant microwave fields on temperature distribution in time and space”. In: *International Journal of Heat and Mass Transfer* 55.13–14 (2012), pp. 3800–3811. ISSN: 0017-9310. DOI: [10.1016/j.ijheatmasstransfer.2012.02.065](https://doi.org/10.1016/j.ijheatmasstransfer.2012.02.065).
- [14] Daichi Wada et al. “Temperature distribution monitoring of a coiled flow channel in microwave heating using an optical fiber sensing technique”. In: *Sensors and Actuators B: Chemical* 232 (2016), pp. 434–441. ISSN: 0925-4005. DOI: [10.1016/j.snb.2016.03.156](https://doi.org/10.1016/j.snb.2016.03.156).
- [15] Adrian Ramirez et al. “In situ temperature measurements in microwave-heated gas-solid catalytic systems. Detection of hot spots and solid-fluid temperature gradients in the ethylene epoxidation reaction”. In: *Chemical Engineering Journal* 316 (2017), pp. 50–60. ISSN: 1385-8947. DOI: [10.1016/j.cej.2017.01.077](https://doi.org/10.1016/j.cej.2017.01.077).
- [16] Guido S.J. Sturm et al. “Exploration of rectangular waveguides as a basis for microwave enhanced continuous flow chemistries”. In: *Chemical Engineering Science* 89 (2013), pp. 196–205. ISSN: 0009-2509. DOI: [10.1016/j.ces.2012.11.039](https://doi.org/10.1016/j.ces.2012.11.039).
- [17] C. Oliver Kappe. “Unraveling the Mysteries of Microwave Chemistry Using Silicon Carbide Reactor Technology”. In: *Accounts of Chemical Research* 46.7 (2013), pp. 1579–1587. DOI: [10.1021/ar300318c](https://doi.org/10.1021/ar300318c).
- [18] Peiping Zhou et al. “Microwave-Assisted Continuous-Flow Reactor Based on a Ridged Waveguide”. In: *Chemical Engineering & Technology* 38.8 (2015), pp. 1334–1339. ISSN: 1521-4125. DOI: [10.1002/ceat.201400634](https://doi.org/10.1002/ceat.201400634).
- [19] Tomohiko Mitani et al. “Development of a wideband microwave reactor with a coaxial cable structure”. In: *Chemical Engineering Journal* 299 (2016), pp. 209–216. ISSN: 1385-8947. DOI: [10.1016/j.cej.2016.04.064](https://doi.org/10.1016/j.cej.2016.04.064).
- [20] K. Hanjalić et al. *Analysis and modelling of physical transport phenomena*. Corrected. VSSD, 2009.
- [21] Sophocles J. Orfanidis. *Electromagnetic Waves and Antennas*. 2014. URL: <http://www.ece.rutgers.edu/~orfanidi/ewa/>.
- [22] N.F.M. Roozenburg and J. Eekels. *Productontwerpen, Structuur En Methoden*. Utrecht: Lemma, 2003.
- [23] Christopher D. Elvidge et al. “A Fifteen Year Record of Global Natural Gas Flaring Derived from Satellite Data”. In: *Energies* 2.3 (2009), pp. 595–622. ISSN: 1996-1073. DOI: [10.3390/en20300595](https://doi.org/10.3390/en20300595).

- [24] Canan Karakaya and Robert J. Kee. “Progress in the direct catalytic conversion of methane to fuels and chemicals”. In: *Progress in Energy and Combustion Science* 55 (2016), pp. 60–97. ISSN: 0360-1285. DOI: [10.1016/j.pecs.2016.04.003](https://doi.org/10.1016/j.pecs.2016.04.003).
- [25] William Taifan and Jonas Baltrusaitis. “{CH₄} conversion to value added products: Potential, limitations and extensions of a single step heterogeneous catalysis”. In: *Applied Catalysis B: Environmental* 198 (2016), pp. 525–547. ISSN: 0926-3373. DOI: [10.1016/j.apcatb.2016.05.081](https://doi.org/10.1016/j.apcatb.2016.05.081).
- [26] Project description. *SPIRE-05-2015 - New adaptable catalytic reactor methodologies for Process Intensification*. Proposal No. **680777 - ADREM** – RIA, European Commission. 2015.
- [27] E. R. Peterson. “Microwave chemical processing”. In: *Research on Chemical Intermediates* 20.1 (1994), pp. 93–96. ISSN: 1568-5675. DOI: [10.1163/156856794X00108](https://doi.org/10.1163/156856794X00108).
- [28] Scott D. Barnicki and James R. Fair. “Separation system synthesis: a knowledge-based approach. 2. Gas/vapor mixtures”. In: *Industrial & Engineering Chemistry Research* 31.7 (1992), pp. 1679–1694. DOI: [10.1021/ie00007a014](https://doi.org/10.1021/ie00007a014).
- [29] Wikipedia. *Hazard and operability study*, Last checked 2016-oct-03. URL: https://en.wikipedia.org/wiki/Hazard_and_operability_study.
- [30] Wikipedia. *Life-cycle assessment*, Last checked 2017-mar-26. URL: https://en.wikipedia.org/wiki/Life-cycle_assessment.
- [31] Zoe Barber et al. *Variation of the dielectric constant in alternating fields*, Last checked 2016-oct-15. URL: <http://www.doitpoms.ac.uk/tlplib/dielectrics/index.php>.
- [32] Lambert E. Feher. *Energy Efficient Microwave Systems : Materials Processing Technologies for Avionic, Mobility and Environmental Applications*. Berlin: Springer., 2009. URL: <http://public.eblib.com/choice/publicfullrecord.aspx?p=438039>.
- [33] Tom Van Gerven and Andrzej Stankiewicz. “Structure, Energy, Synergy, Time—The Fundamentals of Process Intensification”. In: *Industrial & Engineering Chemistry Research* 48.5 (2009), pp. 2465–2474. DOI: [10.1021/ie801501y](https://doi.org/10.1021/ie801501y).
- [34] Hannsjörg Freund and Kai Sundmacher. “Towards a methodology for the systematic analysis and design of efficient chemical processes: Part 1. From unit operations to elementary process functions”. In: *Chemical Engineering and Processing: Process Intensification* 47.12 (2008), pp. 2051–2060. ISSN: 0255-2701. DOI: [10.1016/j.cep.2008.07.011](https://doi.org/10.1016/j.cep.2008.07.011).
- [35] P. Moghimpour Bijani, M. Sohrabi, and S. Sahebdehfar. “Thermodynamic Analysis of Nonoxidative Dehydroaromatization of Methane”. In: *Chemical Engineering & Technology* 35.10 (2012), pp. 1825–1832. ISSN: 1521-4125. DOI: [10.1002/ceat.201100436](https://doi.org/10.1002/ceat.201100436).

- [36] Linsheng Wang et al. “Dehydrogenation and aromatization of methane under non-oxidizing conditions”. In: *Catalysis Letters* 21.1 (1993), pp. 35–41. ISSN: 1572-879X. DOI: [10.1007/BF00767368](https://doi.org/10.1007/BF00767368).
- [37] J.A. Moulijn, A.E. van Diepen, and F. Kapteijn. “Catalyst deactivation: is it predictable?: What to do?”. In: *Applied Catalysis A: General* 212.1–2 (2001). Catalyst Deactivation, pp. 3–16. ISSN: 0926-860X. DOI: [10.1016/S0926-860X\(00\)00842-5](https://doi.org/10.1016/S0926-860X(00)00842-5).
- [38] Yang Song et al. “A clue to exploration of the pathway of coke formation on Mo/HZSM-5 catalyst in the non-oxidative methane dehydroaromatization at 1073 K”. In: *Applied Catalysis A: General* 482 (2014), pp. 387–396. ISSN: 0926-860X. DOI: [10.1016/j.apcata.2014.06.018](https://doi.org/10.1016/j.apcata.2014.06.018).
- [39] Yang Song et al. “The distribution of coke formed over a multilayer Mo/HZSM-5 fixed bed in {H₂} co-fed methane aromatization at 1073 K: Exploration of the coking pathway”. In: *Journal of Catalysis* 330 (2015), pp. 261–272. ISSN: 0021-9517. DOI: [10.1016/j.jcat.2015.07.017](https://doi.org/10.1016/j.jcat.2015.07.017).
- [40] Robert H. Perry, Cecil H. Chilton, and John Howard Perry. *Chemical Engineers’ Handbook*. McGraw-Hill chemical engineering. New York: McGraw-Hill, 1973. URL: <http://app.knovel.com/hotlink/toc/id:kpYHTPHC09/yaws-handbook-thermodynamic/yaws-handbook-thermodynamic>.
- [41] Michael Kleiber and Ralph Joh. “VDI Heat atlas, D1 Calculation Methods for Thermophysical Properties”. In: Berlin, Heidelberg: Springer Berlin Heidelberg, 2010, pp. 119–152. ISBN: 978-3-540-77877-6. DOI: [10.1007/978-3-540-77877-6_10](https://doi.org/10.1007/978-3-540-77877-6_10).
- [42] Carl L. Yaws. *Yaws’ Handbook of Thermodynamic Properties for Hydrocarbons and Chemicals*. Knovel, 2009. ISBN: N/A. URL: <http://app.knovel.com/hotlink/toc/id:kpYHTPHC09/yaws-handbook-thermodynamic/yaws-handbook-thermodynamic>.
- [43] Carl L. Yaws. *Yaws’ Handbook of Thermodynamic and Physical Properties of Chemical Compounds*. Knovel, 2003. ISBN: N/A. URL: <http://app.knovel.com/hotlink/toc/id:kpYHTPPCC4/yaws-handbook-thermodynamic/yaws-handbook-thermodynamic>.
- [44] Lingling Su et al. “Creating Mesopores in ZSM-5 Zeolite by Alkali Treatment: A New Way to Enhance the Catalytic Performance of Methane Dehydroaromatization on Mo/HZSM-5 Catalysts”. In: *Catalysis Letters* 91.3 (2003), pp. 155–167. DOI: [10.1023/B:CATL.0000007149.48132.5a](https://doi.org/10.1023/B:CATL.0000007149.48132.5a).
- [45] Jacob A. Moulijn and Freek Kapteijn. “Monolithic reactors in catalysis: excellent control”. In: *Current Opinion in Chemical Engineering* 2.3 (2013). Energy and environmental engineering / Reaction engineering and catalysis, pp. 346–353. ISSN: 2211-3398. DOI: [10.1016/j.coche.2013.05.003](https://doi.org/10.1016/j.coche.2013.05.003).
- [46] Denis Denissov et al. *Dielectric Strength of Different Gases in GIS, Last checked 2017-mar-12*. URL: http://www.uni-stuttgart.de/ieh/forschung/veroeffentlichungen/2005_ISH_Denissov.pdf.

- [47] NCCP. *Zeolite catalysts*, Last checked 2017-apr-04. URL: http://www.nccp.ru/en/products/zeolite_catalysts/?PAGEN_1=3.
- [48] D. M. Pozar. *Microwave engineering*. 4th ed. J. Wiley, 2012. URL: <http://catdir.loc.gov/catdir/toc/wiley041/2003065001.html>.
- [49] Georgios Stefanidis. *Process Intensification*, Last checked 2016-oct-12. URL: <https://ocw.tudelft.nl/courses/process-intensification/>.
- [50] W.P.M van Swaaij, A.G.J van der Ham, and A.E Kronberg. “Evolution patterns and family relations in G-S reactors”. In: *Chemical Engineering Journal* 90.1-2 (2002). Catalytic Reaction and Reactor Engineering EuropaCat V Limerick, Sept 2-7 2001, pp. 25 –45. ISSN: 1385-8947. DOI: [10.1016/S1385-8947\(02\)00066-9](https://doi.org/10.1016/S1385-8947(02)00066-9).
- [51] M. F. Ashby, Hugh. Shercliff, and David Cebon. *Materials : Engineering, Science, Processing and Design*. 2nd. Oxford: Butterworth-Heinemann., 2010.
- [52] Granta Design. CES EDUPACK®2015A. 2016.
- [53] Michael F. Ashby. *Materials Selection in Mechanical Design (4th Edition)*. Elsevier, 2011. ISBN: 978-1-85617-663-7. URL: <http://app.knovel.com/hotlink/toc/id:kpMSMDE022/materials-selection-in-2/materials-selection-in-2>.
- [54] R. Krishna and S.T. Sie. “Chemical Reaction Engineering: Science & Technology Strategies for multiphase reactor selection”. In: *Chemical Engineering Science* 49.24 (1994), pp. 4029 –4065. ISSN: 0009-2509. DOI: [10.1016/S0009-2509\(05\)80005-3](https://doi.org/10.1016/S0009-2509(05)80005-3).
- [55] MathWorks. MATLAB®2015A. 2015.
- [56] COMSOL MULTIPHYSICS®5.2 with RF-module, Heat Transfer module, Concentrated Species and Laminar flow. 2015.
- [57] Herman Kramer. “Batch vs. continuous Input - output structure Reactor systems Recycle structure”. In: (2015), p. 7.
- [58] Benzhen Yao et al. “Intrinsic kinetics of methane aromatization under non-oxidative conditions over modified Mo/HZSM-5 catalysts”. In: *Journal of Natural Gas Chemistry* 17.1 (2008), pp. 64 –68. ISSN: 1003-9953. DOI: [10.1016/S1003-9953\(08\)60027-4](https://doi.org/10.1016/S1003-9953(08)60027-4).
- [59] Xiaoguang Guo et al. “Direct, Nonoxidative Conversion of Methane to Ethylene, Aromatics, and Hydrogen”. In: *Science* 344.6184 (2014), pp. 616–619. ISSN: 0036-8075. DOI: [10.1126/science.1253150](https://doi.org/10.1126/science.1253150).
- [60] Lin Li, Richard W Borry, and Enrique Iglesia. “Design and optimization of catalysts and membrane reactors for the non-oxidative conversion of methane”. In: *Chemical Engineering Science* 57.21 (2002), pp. 4595 –4604. ISSN: 0009-2509. DOI: [10.1016/S0009-2509\(02\)00314-7](https://doi.org/10.1016/S0009-2509(02)00314-7).
- [61] ASPENPLUS ® with Gibbs equilibrium reactor. 2016.
- [62] Sairem. *100 kW, 915 MHz MICROWAVE GENERATOR*, Last checked 2017-mar-29. URL: <http://www.sairem.com/the-generators-44.html>.

- [63] Ferrite Microwave technology. *GET2024 MICROWAVE GENERATOR*, Last checked 2017-mar-29. URL: <http://ferriteinc.com/industrial-microwave-systems/products-services/products/systems/>.
- [64] Xunli Zhang, David O. Hayward, and D. Michael P. Mingos. “Apparent equilibrium shifts and hot-spot formation for catalytic reactions induced by microwave dielectric heating”. In: *Chem. Commun.* (11 1999), pp. 975–976. DOI: [10.1039/A901245A](https://doi.org/10.1039/A901245A).
- [65] Ernesto Altman et al. “Process Intensification of Reactive Distillation for the Synthesis of n-Propyl Propionate: The Effects of Microwave Radiation on Molecular Separation and Esterification Reaction”. In: *Industrial & Engineering Chemistry Research* 49.21 (2010), pp. 10287–10296. DOI: [10.1021/ie100555h](https://doi.org/10.1021/ie100555h).
- [66] Xin Gao et al. “Influence of a microwave irradiation field on vapor–liquid equilibrium”. In: *Chemical Engineering Science* 90 (2013), pp. 213–220. ISSN: 0009-2509. DOI: [10.1016/j.ces.2012.12.037](https://doi.org/10.1016/j.ces.2012.12.037).
- [67] A. S. Gilmour. *Klystrons, Traveling Wave Tubes, Magnetrons, Crossed-Field Amplifiers, and Gyrotrons*. ARTECH HOUSE, 2011, p. 534.
- [68] Jeffrey K.S. Wan. “Microwave induced catalytic conversion of methane to ethylene and hydrogen”. Patent US 4574038. Mar. 1986. URL: <https://www.google.com/patents/US4574038>.
- [69] A.F. Mills. *Basic Heat and Mass Transfer*. 2nd ed. Pearson, 1999.
- [70] J.-M. Commenge and L. Falk. “Methodological framework for choice of intensified equipment and development of innovative technologies”. In: *Chemical Engineering and Processing: Process Intensification* 84 (2014). {EPIC} 2013, pp. 109–127. ISSN: 0255-2701. DOI: [10.1016/j.cep.2014.03.001](https://doi.org/10.1016/j.cep.2014.03.001).
- [71] Paul Breedveld. *Essence of Creative Designing*, Last checked 2016-oct-12. URL: https://ocw.tudelft.nl/wp-content/uploads/BID_2011_Lecture2_Essence_of_Creative_Designing_OCW.pdf.
- [72] A. van. Beek. *Advanced Engineering Design : Lifetime Performance and Reliability*. Delft: TU Delft., 2009. URL: <http://p://www.engineering-abc.com..>
- [73] C.W.M. Hermans. *Concept development of rotating bed chemical looping combustion reactor*. 2013. URL: <http://resolver.tudelft.nl/uuid:b4c86df8-ba25-4ce0-90b9-98e65908bc00>.
- [74] S. S. Stevens. “On the Theory of Scales of Measurement”. In: *Science* 103.2684 (1946), pp. 677–680. ISSN: 0036-8075. DOI: [10.1126/science.103.2684.677](https://doi.org/10.1126/science.103.2684.677).
- [75] Ari Sihvola. *Electromagnetic mixing formulas and applications*. The Institution of Electrical Engineers, 1999.
- [76] Wikipedia. *Thermal diffusivity*, Last checked 2016-oct-03. URL: https://en.wikipedia.org/wiki/Thermal_diffusivity.

- [77] Canan Karakaya, Huayang Zhu, and Robert J. Kee. “Kinetic modeling of methane dehydroaromatization chemistry on Mo/Zeolite catalysts in packed-bed reactors”. In: *Chemical Engineering Science* 123 (2015), pp. 474–486. ISSN: 0009-2509. DOI: [10.1016/j.ces.2014.11.039](https://doi.org/10.1016/j.ces.2014.11.039).
- [78] Yanbin Cui et al. “The effect of zeolite particle size on the activity of Mo/HZSM-5 in non-oxidative methane dehydroaromatization”. In: *Applied Catalysis A: General* 393.1–2 (2011), pp. 348–358. ISSN: 0926-860X. DOI: [10.1016/j.apcata.2010.12.017](https://doi.org/10.1016/j.apcata.2010.12.017).
- [79] Dieter. Muhs, Herbert Wittel, and Vossiek Jannasch Dieter an Joachim. *Roloff/Matek Machine-onderdelen tabellenboek (4e druk)*. SDU Uitgevers bv, 2010.
- [80] Sairem. *6000 W, 2450 MHz Microwave Generator, Last checked 2017-mar-29*. URL: <http://www.sairem.com/the-generators-44.html>.
- [81] Lin Li, Richard W. Borry, and Enrique Iglesia. “Reaction-transport simulations of non-oxidative methane conversion with continuous hydrogen removal - homogeneous-heterogeneous reaction pathways”. In: *Chemical Engineering Science* 56.5 (2001), pp. 1869–1881. ISSN: 0009-2509. DOI: [10.1016/S0009-2509\(00\)00465-6](https://doi.org/10.1016/S0009-2509(00)00465-6).
- [82] Changyong Sun et al. “Methane dehydroaromatization with periodic CH₄-H₂ switch: A promising process for aromatics and hydrogen”. In: *Journal of Energy Chemistry* 24.3 (2015), pp. 257–263. ISSN: 2095-4956. DOI: [10.1016/S2095-4956\(15\)60309-6](https://doi.org/10.1016/S2095-4956(15)60309-6).
- [83] Ahmad Fauzi Ismail, Kailash Chandra Khulbe, and Takeshi Matsuura. *Gas Separation Membranes*. Vol. 1. Springer International Publishing, 2015, p. 14. ISBN: 978-3-319-01095-3. DOI: [10.1007/978-3-319-01095-3](https://doi.org/10.1007/978-3-319-01095-3).

A | Finding challenges

The challenges of the travelling microwave reactor are found using existing check-lists of existing engineering fields. However, what about the unknown challenges caused by interactions between different engineering fields? These unknown challenges have been found using a force to fit method. The check-lists and the force to fit method can be found in this appendix.

A.1 Material check-list

Density, price, elastic moduli, yield strength, ultimate strength, compressive strength, failure strength, hardness, elongation, fatigue endurance limit, fracture toughness, toughness, damping capacity, melting point, glass temperature, maximum service temperature, minimum service temperature, thermal conductivity, specific heat, thermal expansion coefficient, thermal shock resistance, electrical resistivity, dielectric constant, breakdown potential, power factor, optical, refractive index, energy to extract, oxidation rates, wear rate constant. [53]

A.2 Process check-list

Fluid-solid mass transfer, fluid-fluid mass transfer, mixing single-phase transfer, heat transfer, kinetics, thermodynamic phenomenon, residence time distribution, dynamics/inertia/transient effect, fluid or equipment volume, non-uniform properties or conditions, size distribution, difficult activation, saturation effect, safety, pressure drop/mechanical energy, energetic consumption, utilities consumption.[70]

A.3 Reactor check-list

Catalyst design, reactant and energy injection strategies, hydrodynamic flow regimes. [54]

A.4 Microwave check-list

1. Resonance will cause non-uniform heating if not dealt with properly [2, Design principle 1 and 2]. What is the length of the cavity and the length of the electromagnetic wave? How will the wave fit inside the cavity? What electromagnetic mode will the reactor have?
2. “The presence of [small differences] strongly distorts the microwave field.” [16, Fig. 2] How is the material distributed in the reactor? How does the material in the cavity influence the electromagnetic mode?

3. The magnitude of the electric field distributes differently under different electric field angles which causes non-uniform heating profiles. [16, Fig. 4] What is the angle between the sample(s) (lossy dielectrics) and the electric field vector?
4. Unstable permittivity could cause temperature runaways. (section C.3) Is the permittivity of each material in the cavity stable?
5. Deactivated catalyst becomes a only heating source. (section C.2) Will catalyst deactivation cause growing hot spots?
6. The alternating electricity net could shift the equilibrium. (section 3.4) Will the power source influence the process?

A.4.1 Unknown challenges

Some unknown challenges are found using phenomena exploration method which is a force to fit method. In the phenomena exploration method words are forced together to generate challenges. Challenges are obtained by combining words from TMR topology, HAZOP [29] and LCA [30] (Table 2.1). Combination of these words expanded the microwave check-list with growing hot spots and unstable permittivity. Growing hot spots originated from catalyst, more, reaction rate and manufacturing. Unstable permittivity originated from catalyst, as well as, temperature, operation. Furthermore, the equilibrium shift could have been found through the phenomena exploration method with catalyst, fluctuations, electric field strength and operation.

A.5 Block diagram

The designed process is collected in a block diagram (Figure A.1). The functions for the TMR can be derived from the block diagram. In Figure A.1, the dashed lines are functions and the rectangles are volumes. The volumes need to be resistant to the conditions inside the volume. The functions connect two volumes and thus needs to be resistant to the conditions in both the volumes. Furthermore, the functions should not change anything else. For example adding microwaves should not cause reactants leakage. The EPF method is used for methane, microwave and operation. The derived functions from the block diagram through EPF method can be found below.

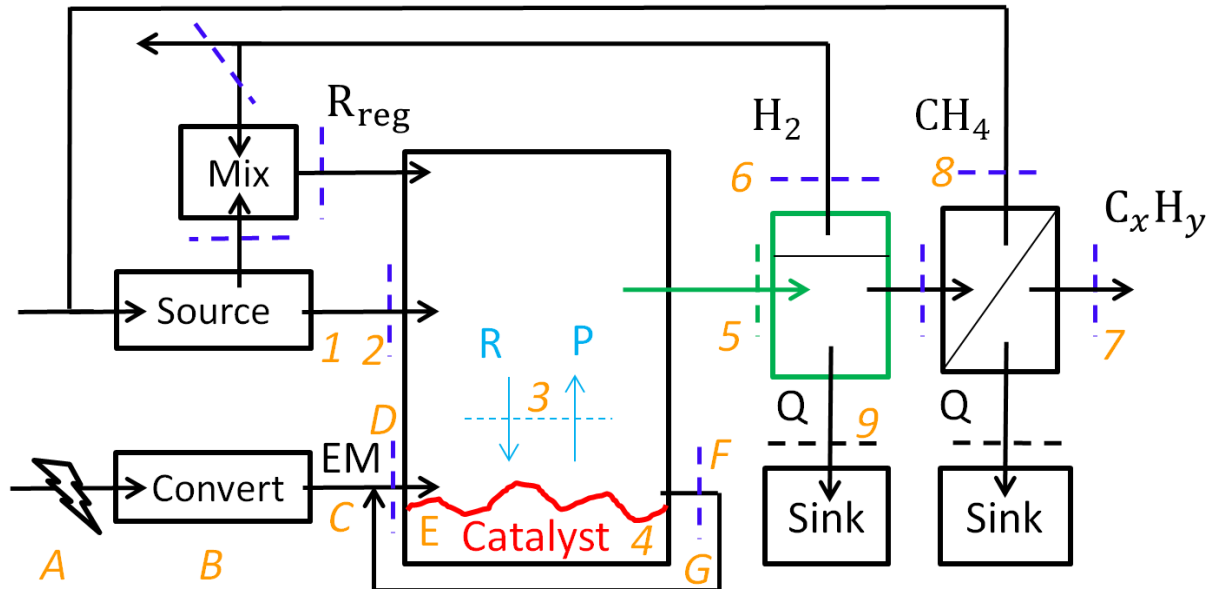


FIGURE A.1: The elementary process functions are found by following a volume element. A methane volume element (VE) is stored. From the storage, the VE enters a reaction volume. In the reaction volume, the VE diffuses towards the catalyst. The VE undergoes a reaction at the catalyst site consuming heat. The catalyst heat is supplied with a microwave which enters and exits the reaction volume. The exiting microwave is recycled. After the reaction, the VE diffuses to the bulk. The hydrogen is then removed from the VE. Then the higher hydrocarbons are removed from the VE. During the mass removal energy is also removed. The remaining VE is recycled. Sometimes hydrogen is recycled and mixed with the VE to burn off the coke.

Functions

The functions are derived from [Figure A.1](#). On the left you will find the function and on the right a solution concept.

Methane

1 Guide fluids	[Piping]
2 Add fluids	[Seal]
3 Refresh activation site	[Diffusion/convection]
4 Activate methane	[Catalyst]
5 Remove fluids	[Seal]
6 Remove hydrogen	[Membrane]
7 Remove aromatics	[VLE]
8 Recycle methane	[Piping loop]
9 Remove heat	[Transport area]

Microwave

A Guide electricity	[Power cable]
B Electricity to microwaves	[Magnetron]
C Guide electromagnetic waves	[Wave guide]
D Add electromagnetic waves	[Anti-reflection]
E Microwaves to heat	[Permittivity distribution]
F Assure one way EM propagation	[Impedance tuners]
G Recycle remaining EM	[Waveguide loop]

Operation

α	TMR needs to be self-standing during operation	[Robust]
β	Know what is going on	[Sensors]
γ	Change conditions	[Actuators]
δ	Acquire similar process history	[Mixing/distribution]
ϵ	Regenerate deactivated catalyst	[Operation]
ζ	Prevent material degradation	[Material selection/Coatings]
η	Extra safety measurements	[Safety]
θ	Adaptable applicator	[Modular]
ι	Continuous flow direction	[Flow]

The functions can be solved separately. However, other functions need to be kept in mind to assure the travelling microwave reactor parts fit together. In this thesis, only the orange functions will be solved, because all grey functions are outside the scope. Along finding sub-solutions, some function names have been changed to be more specific or general and the functions are classified in applicator core, applicator to environment and catalyst selection.

TMR for MA function renaming and classification

- Catalyst is changed to extra phase [core] and catalyst selection
- Mixing/distribution and diffusion convection are changed to component control [core] and flow distribution [environment]
- Permittivity distribution to dissipation control [core]
- Seal to leakage prevention [environment]
- Modular [environment], robust [environment], flow [core] and safety are kept the same

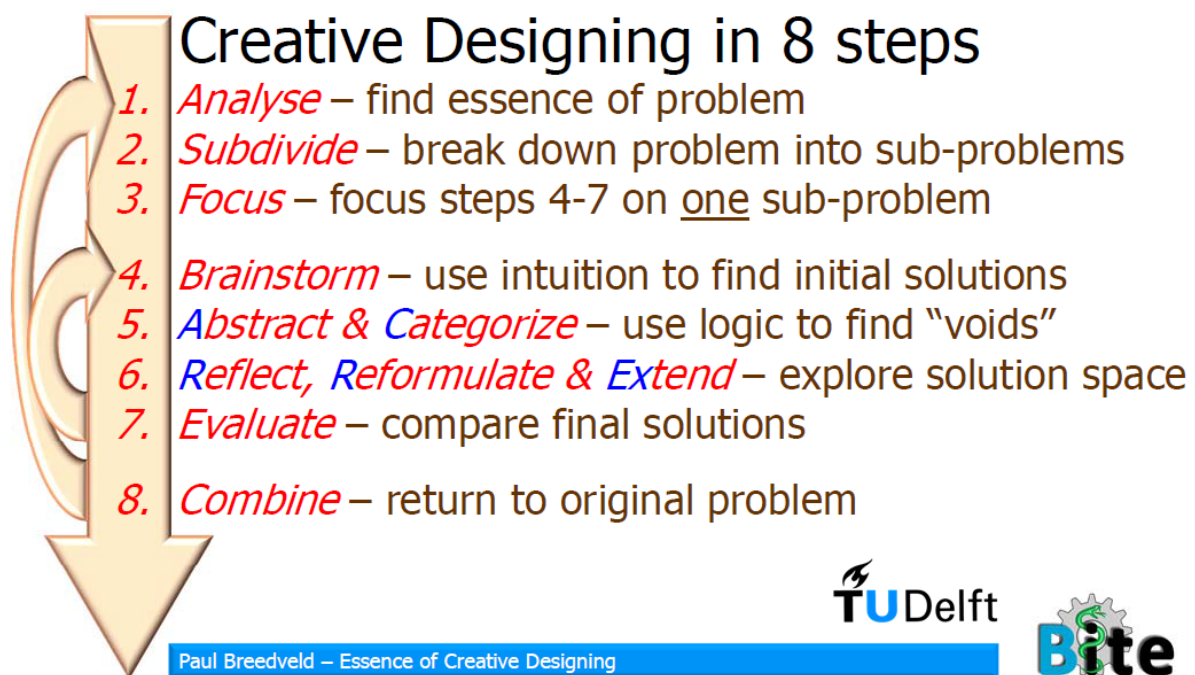
The functions are classified to prioritise which functions to solve first. The most important function group is the applicator core. When the economic potential of the combined sub-solutions of the applicator core is negative, there is no need for solution in the environment class. The combined sub-solution of the applicator is able to pinpoint how the catalyst should be improved. Then, if the economic potential is positive the environment class should be developed followed by safety. Understand that safety should also be sufficient! Yes, it is awful to kill a reactor with a positive economic potential and many man hours.

B | Finding solutions

Essence of creative designing [71] is used to find solutions by analysing similar devices. The state-of-the-art [49] and best-practice [50] reactors are used as similar devices. Catalyst papers for dehydroaromatization are used to construct the catalyst ideas. These reactors are abstracted to gain access to the essence of the sub-solution. Finally, the guide words none and infinite are used to complete the solution space. The solution space consists of all solutions that solves the complex problem. The travelling microwave reactor for dehydroaromatization solution space is presented in a mind-map.

B.1 Essence of creative designing

In this section essence of creative design is explained using the slides [71].



The often used example starts with a car and a bike. Abstract and categorize will give the number of wheels and (non)-motorized and will show voids such as 3 wheels and 1 wheel. Reflect, reformulate and extend will give the idea of no wheels and infinite wheels. Thus, guide words such as a different number as well as no and infinite are used to extrapolate.



Common ACRREx Traps..

Difficulties in finding basic principles

- Use your engineering knowledge!
- Use alternative approaches!
- Go to extremes to find the essence!

Overstructuring!

- Explore a branch until you are nearly certain that it does not lead to a well-working solution.
- It makes no sense then to go further to the leaf!

B.2 Abstracted solutions

Solution space

The ideas for the applicator are created by abstracting state-of-the-art and best-practice reactors. The abstract ideas can be combined. For instance, axial with tangential flow results in a helical tube. The ideas have been subdivided in three categories core, environment and catalyst. Each category has its own morphological web ([Figure B.1](#), [Figure B.2](#), [Figure B.3](#)).

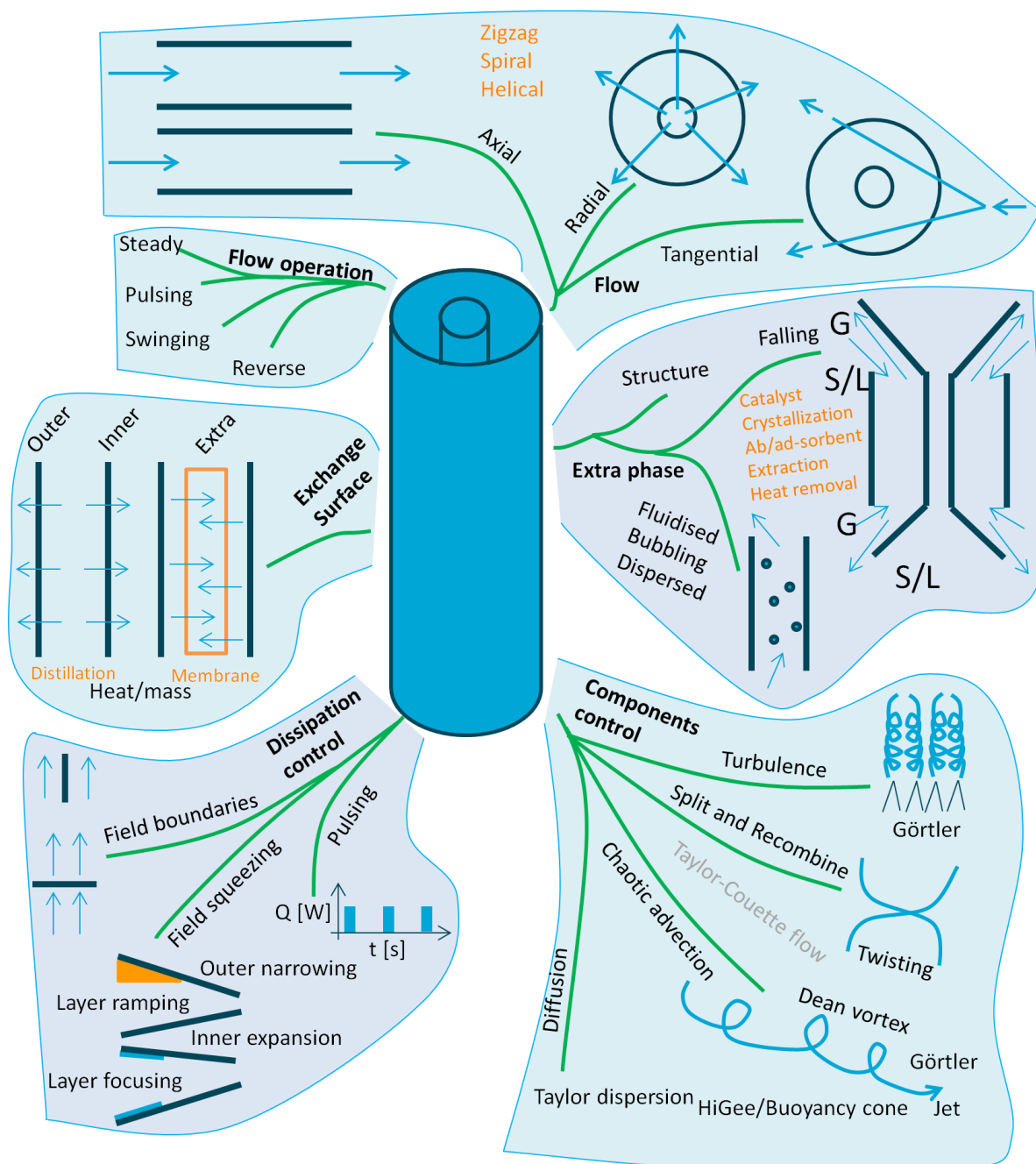


FIGURE B.1: Travelling microwave reactor applicator core ideas in evolution format. **Flow** is the direction of the flow in the coaxial tube. **Extra phase** could be the catalyst, separation phase or heat removal capacity. **Components control** are ways of controlling the concentration. **Dissipation control** are the ways of controlling dielectric heating. **Exchange surface** are ways to use the exchange surfaces of the TMR. **Flow operation** are ways of controlling the feed flow.

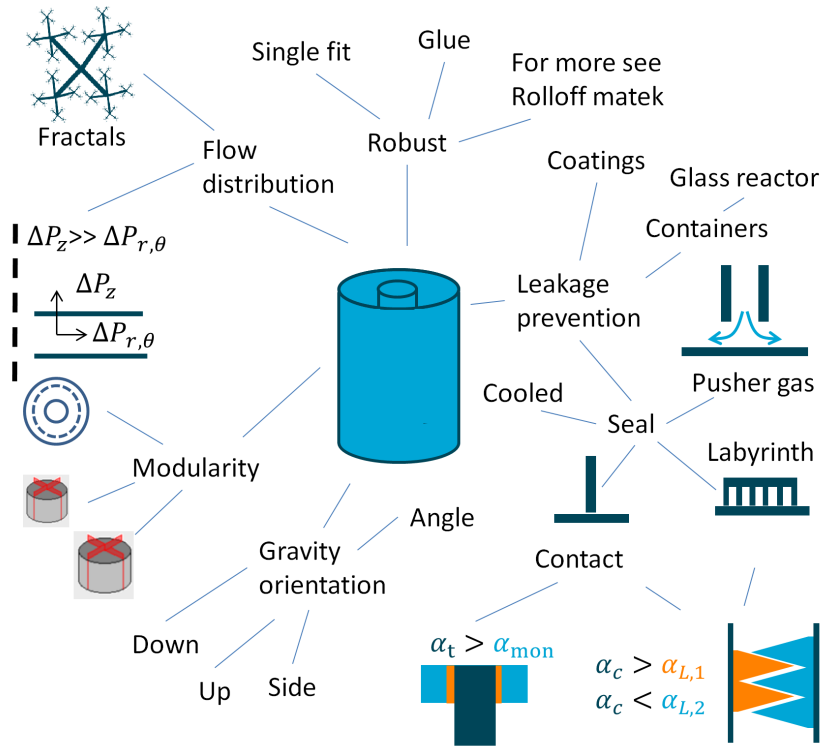


FIGURE B.2: TMR applicator to environment ideas in evolution format [72] [73]

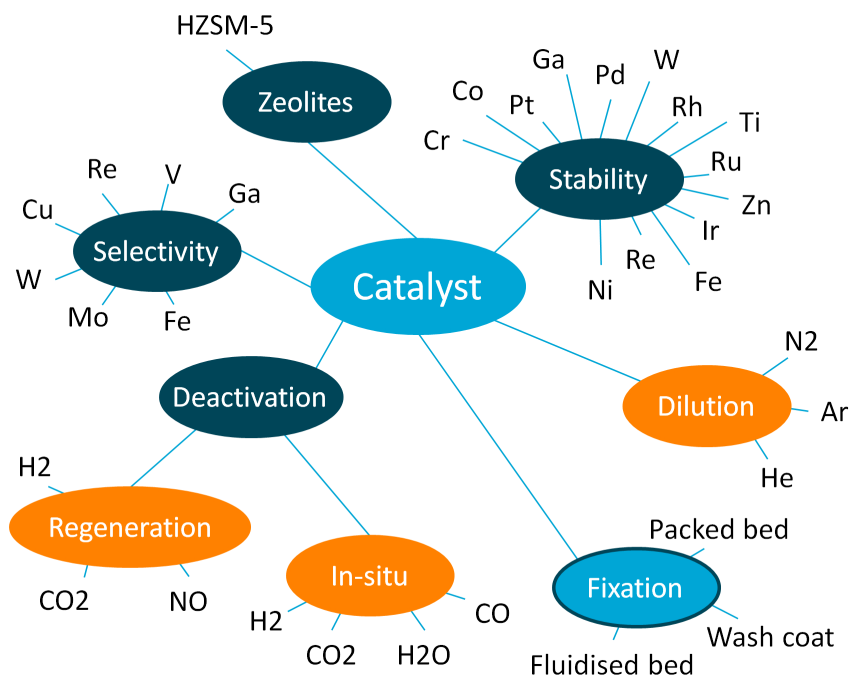


FIGURE B.3: Catalyst ideas in evolution format

B.3 Sub-solutions evaluation

Many complete solutions can be made using these sub-solutions. Therefore, ideas need to be eliminated through evaluating aspects [22] at ordinal scale [74]. In this study, the sub-solutions that are not expected to fulfil predictable, volume utilisation maximising and manufacturable aspects are scrapped. Furthermore, the chosen sub-solutions layer focusing and pressure drop distribution where extrapolated using the infinite and zero concepts.. Therefore, the new extrapolated solutions asymmetric annular monolith and anisotropic porous media are explained below.

Layer focusing extrapolation to asymmetric annular monolith

The guide word infinite is used to complete the solution space for layer focusing. Infinite layer focusing is able to maximise the cross flow area between the conductors. Layer focusing is putting a material boundary perpendicular to the electric field vector. The electric field will be pushed in the layer with a lower permittivity. This push will be called focusing. On top of that layer, another layer doing the same could be dropped which again pushes the electric field further. This method could be used to flatten the radial electric field magnitude decay from the inner to the outer conductor (Figure B.4). Thus infinite many layers are able to create a homogeneous electric field. All these layers together is a material with a decaying permittivity. A material that has a decaying permittivity is quite special. However using 2 materials the effective permittivity at any periphery is able to create any decay. Finally, the layer focusing is combined with positioning the electric field boundaries (Figure B.5).

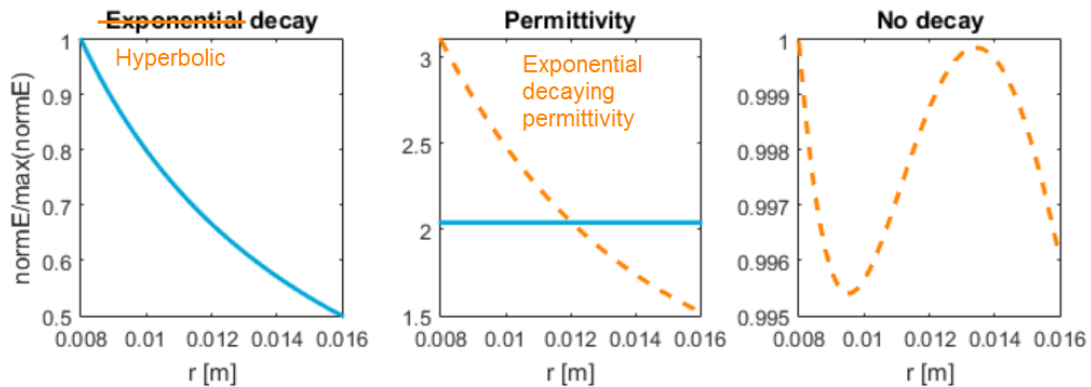


FIGURE B.4: A radial homogeneous electric field is able to be acquired using an exponential decaying permittivity. Later obtained understanding showed that a hyperbolic decaying permittivity flattens better.

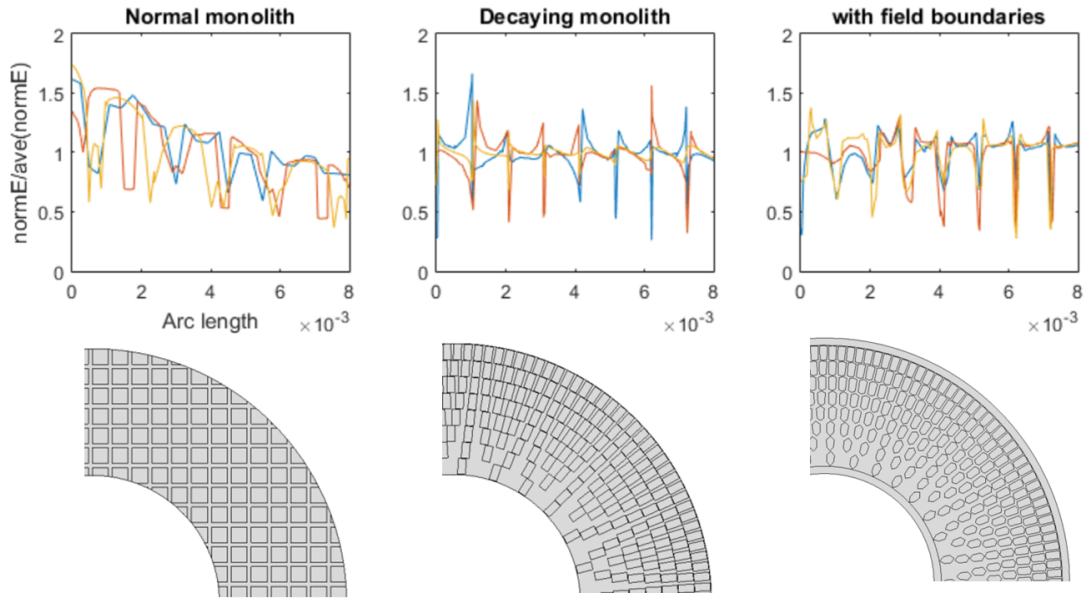


FIGURE B.5: In this figure, the normalised electric field is shown radially along 0° , 22.5° and 45° . The normal monolith shows a hyperbolic decay. The permittivity decaying monolith shows a quite homogeneous field. Finally, the permittivity decaying monolith with field boundary positioning shows an even more homogeneous field.

Pressure drop distribution extrapolation to anisotropic porous media

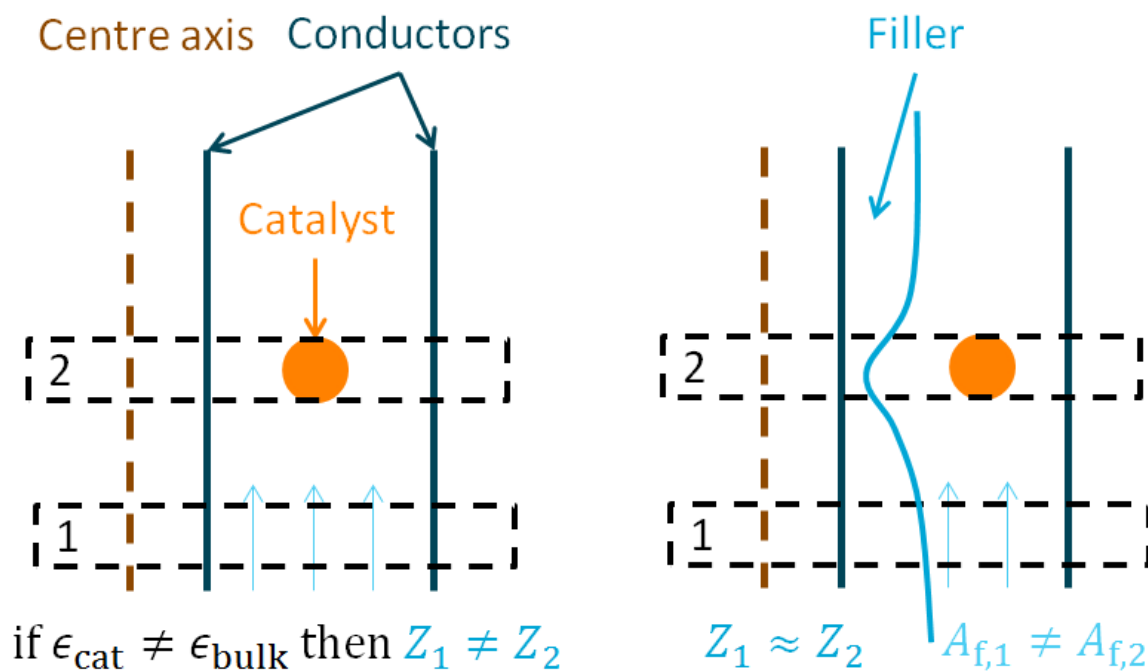
The lack of pressure drop makes a monolith susceptible for maldistribution through preferential flow. The pressure drop distribution sub-solution can be used to acquire a better distribution. The idea needs to be extrapolated. Pressure drop distribution is nothing more than changing the number of pores. Thus, an infinite number of pores becomes a porous material while zero pores result in solution-diffusion. Thus, the pressure drop distribution method could be a layer of porous material.

C | Derivations

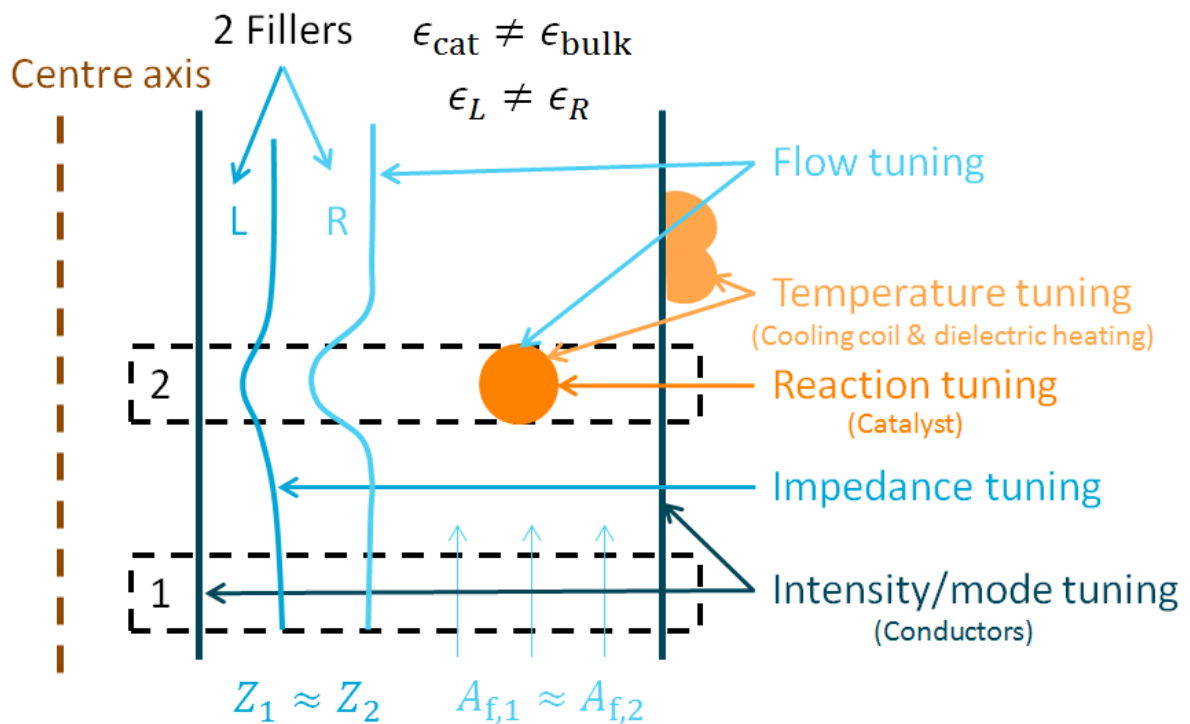
In this appendix, all derivations, mathematical and thought, can be found.

C.1 Travelling microwave reactor topology

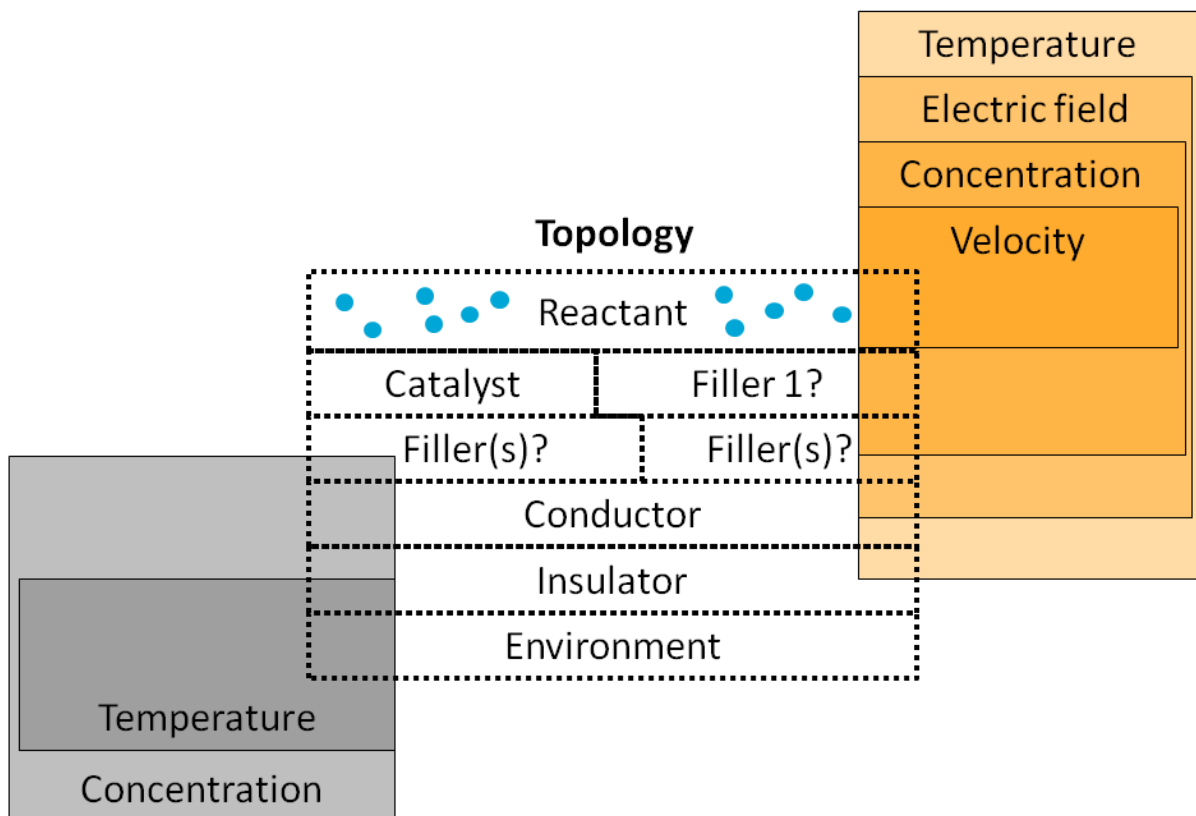
The travelling microwave reactor topology is obtained by trying to control each phenomenon separately through geometry. The geometry starts with the minimal for a travelling microwave reactor which is an inner and outer conductor, a catalyst and reactant flow. The implementation of a catalyst at a specific point between the conductors causes the impedance Z to change abruptly. An abrupt change in impedance often causes unwanted reflection. This can be prevented using a filler which changes shape where the catalyst is implemented.



Reflection is prevented with this filler. However, the flow area might not be completely optimal yet. A second filler is added to gain control of the flow area. Furthermore, heating, cooling or insulation can be added outside the conductors. Thus, with the new construct the intensity, impedance, flow and temperature can be tuned.



This geometry was eventually translated to a topology. Furthermore, it shows which layers influence which phenomena. The phenomena in grey are neglected, because it is assumed impermeable and insulating material.



C.2 Accelerated deactivation spots

Deactivation through poisoning and sintering are examples of unwanted changing material properties through usage and temperature respectively. Local deviations caused by manufacturing tolerances (Figure C.1) and deactivation could influence the heating. The temperature is most likely to increase in an endothermic reaction, because deactivated catalyst stays a heating source while losing its activity. The increased heating rate will affect the neighbours through thermal diffusion (Figure C.2) and thus the process will be affected. The deactivation and increased heat dissipation will be called accelerated deactivation spots. Thus temperature overshoots that could change reaction rate or dielectric properties need to be avoided such as melting.

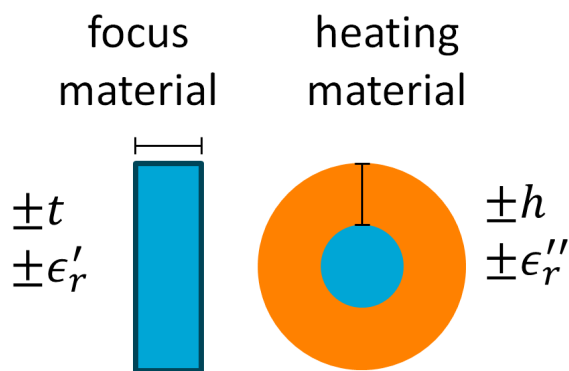


FIGURE C.1: Influence on heating distribution

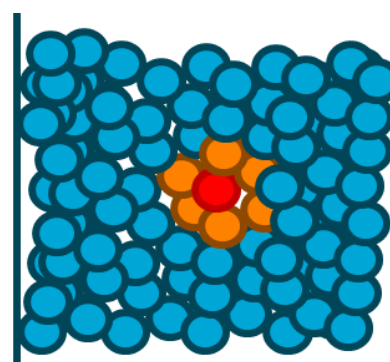


FIGURE C.2: Deactivation due to deactivation

Accelerated deactivation spots are expensive to prevent through more accurate manufacturing techniques. Thus regular regeneration could be a useful way to deal with accelerated deactivation spots. However, increased frequency of regeneration will also increase the costs. Nonetheless, lab-scale experiments can give useful information to predict these costs. Experiments in microwave reactors will deviate from each other based on accelerated deactivation spots. A normal distribution which is assumed could be fit to experiments that log selectivity in time at steady conditions. The normal distribution gives the likelihood that regeneration needs to take place after a certain time on stream. The normal distribution should be read using a volume ratio. In other words, the reactor is assumed to be constructed of many experimental volumes. The worst case scenario should give the time between regenerations. Now more accurate manufacturing technique costs could be compared to increased regeneration rate costs.

C.3 Stable heat dissipating permittivity

The stability of heat dissipating dielectric in a uniform field is similar to the stability of a stationary bubble in a downward flowing pipe. The question changed to, will a

small temperature perturbation flatten or increase the temperature perturbation? The requirements for stable dielectric heating is derived in this section.

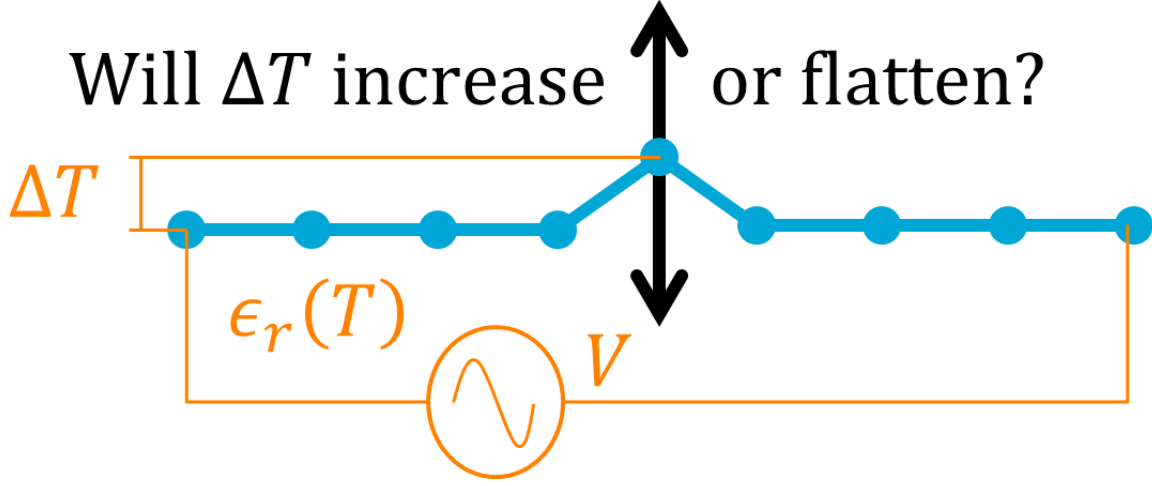


FIGURE C.3: A uniform electric field between two infinitely large plates is representable in 1 dimension. Will a small temperature perturbation flatten or increase the temperature perturbation when the material is dielectrically heated in a uniform field?

Derivation: Stable permittivity

Dielectric power loss (Equation C.1)[21] is used to define whether a small temperature perturbation will increase or flatten.

$$Q = \frac{\omega}{2} \int_V \epsilon''_{\text{eff}} |E_p|^2 dV \quad (\text{C.1})$$

Derive stability criterion

$$\text{Stable if } \frac{\partial Q}{\partial T} < 0 \implies \frac{\partial Q}{\partial T} = \frac{\partial \epsilon''_{\text{eff}} E_p^2}{\partial T} = \frac{\partial \epsilon''_{\text{eff}}}{\partial T} E_p^2 + 2\epsilon''_{\text{eff}} E_p \frac{\partial E_p}{\partial T} < 0 \quad (\text{C.2})$$

For 1D fill in Gauss' law (Equation C.3)

$$\nabla \cdot \epsilon E = 0 \implies \epsilon'_p E_p = \epsilon'_e E_e \implies E_p = \frac{\epsilon'_e E_e}{\epsilon'_p} \quad (\text{C.3})$$

$$\frac{\partial Q}{\partial T} = \frac{\partial \epsilon''_{\text{eff}}}{\partial T} E_p^2 + 2\epsilon''_{\text{eff}} E_p \epsilon'_e E_e \frac{\partial 1\epsilon'_p}{\partial T} = \frac{\partial \epsilon''_{\text{eff}}}{\partial T} + 2\epsilon''_{\text{eff}} \epsilon'_p \frac{\partial 1\epsilon'_p}{\partial T} \quad (\text{C.4})$$

The result is not surprising at all. A material becomes unstable if the dielectric loss factor increases or the dielectric constant decreases. Furthermore, there is a combination with decreasing dielectric loss factor or increasing dielectric constant that is unstable.

For 2D fill in (Equation C.5) [75]. The 2D result shows that 2D is more stable than 1D.

$$E_p = \frac{3\epsilon'_e}{\epsilon'_p + 2\epsilon'_e} \quad (\text{C.5})$$

$$\frac{\partial P}{\partial T} = \frac{\partial \epsilon''_{\text{eff}}}{\partial T} + 2\epsilon''_{\text{eff}} (\epsilon'_p + 2\epsilon_e) \frac{\partial 1(\epsilon'_p + 2\epsilon_e)}{\partial T} \quad (\text{C.6})$$

Both Equation C.4 and Equation C.6 shows (Figure C.4) that water is stable using the dielectric properties of water (Table C.1). Furthermore, the 2D result is more stable than the 1D. Thus, it is expected that water in 3D would be even more stable.

TABLE C.1: Complex relative permittivity of water for a range of temperatures at 2.45 GHz[2]

Temperature [°C]	Complex relative permittivity [-]
20	78.0 – 10.5i
30	75.0 – 8.6i
40	72.0 – 6.7i
50	69.0 – 5.1i
60	66.2 – 3.85i
70	63.9 – 3.3i
80	62.7 – 3.1i
90	62.3 – 3.0i
100	62.0 – 2.9i

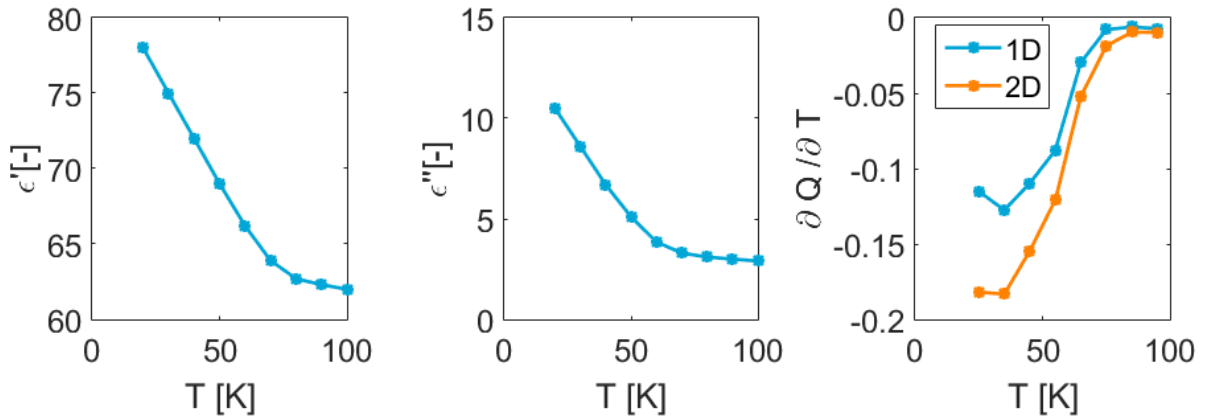


FIGURE C.4: Water is stable to heat using microwaves, because $\partial Q / \partial T < 0$

A sudden increase in temperature is unlikely. However, material deviations are common (Figure C.2). These material deviations will create fluctuating temperatures which could be seen as a sudden temperature increase. Therefore permittivity stability should be checked.

C.3.1 Diffusion temperature gradient

A temperature gradient [10] cannot exist in a continuous flow reactor unless some reactants bypass the catalyst. At least, a temperature gradient cannot exist based on diffusion,

i.e. excluding other phenomena such as thermophoresis and Ackermann correction factor (derivation C.3.1).

The following non-dimensionalisation for time, length, concentration and temperature are used in a dimensional analysis.

$$\tilde{t} = \frac{t}{\tau} \quad \tilde{y} = \frac{y}{h_h} \quad \tilde{C} = \frac{C}{\gamma} \quad \tilde{T} = \frac{T}{\theta} \quad (\text{C.7})$$

Fill in the non-dimensionalisation in heat transport and molecular transport equation.

$$\begin{aligned} \frac{\partial C}{\partial t} = D_{ij} \frac{\partial^2 C}{\partial y^2} &\implies \frac{\gamma}{\tau} \frac{\partial \tilde{C}}{\partial \tilde{t}} = D_{ij} \frac{\gamma}{h^2} \frac{\partial^2 \tilde{C}}{\partial \tilde{y}^2} \implies \frac{1}{\tau} \sim \frac{D_{ij}}{h^2} \\ \frac{\partial T}{\partial t} = \alpha \frac{\partial^2 T}{\partial y^2} &\implies \frac{\theta}{\tau} \frac{\partial \tilde{T}}{\partial \tilde{t}} = \alpha \frac{\theta}{h^2} \frac{\partial^2 \tilde{T}}{\partial \tilde{y}^2} \implies \frac{1}{\tau} \sim \frac{\alpha}{h^2} \end{aligned} \quad (\text{C.8})$$

Thus a temperature gradient without a concentration gradient could exist if

$$\frac{D_{ij}}{\alpha} > 1 \quad \text{and} \quad \tau < \frac{h^2}{\alpha} \quad (\text{C.9})$$

Which is unlikely see the rules of thumb for diffusivity (Table C.2).

TABLE C.2: Rules of thumb diffusivity

Diffusivity	Molecular	Thermal	Ratio
	D_{ij} [40, Tab 5-13]	α [76]	$D_{ij}\alpha$
Gas	10^{-5}	$10^{-4} - 10^{-5}$	< 1
Liquid	10^{-9}	$10^{-5} - 10^{-8}$	$< 10^{-1}$
Solid	$10^{-12} - 10^{-14}$	$10^{-3} - 10^{-8}$	$< 10^{-4}$

C.3.2 Shielding electromagnetic field

Kappe [17] uses the following modus tollens to proof the enhancements by non-thermal microwave effects do not exist.

TABLE C.3: Disproving Silicon carbide shielding (part 1/3)

- 1) If the enhancements are caused by the electromagnetic field, then silicon carbide phials obtain different results from Pyrex phials.
- 2) No different results are obtained.
- 3) -----
The enhancements are not caused by the electromagnetic field.

Furthermore, the following two underlying modus ponens a) and modus tollens b) need to be true.

TABLE C.4: Disproving silicon carbide shielding (part 2/3)

- 4) If a phial has a high microwave absorptivity, then it shields its contents from the electromagnetic field.
- 5a) A Pyrex phial does not have a high microwave absorptivity.
- 5b) A silicon carbide phial does have a high microwave absorptivity.
-
- 6a) A Pyrex phial does not shield its contents from the electromagnetic field.
- 6b) A silicon carbide phial does shield its contents from the electromagnetic field.

A simulation (Figure C.5) is used to show that silicon carbide phial does not shield its contents from the electromagnetic field, i.e. the simulation disproves premise 4 and thus conclusion 6b is not true. The electromagnetic field is lower at similar heating, but not gone nor significant lower.

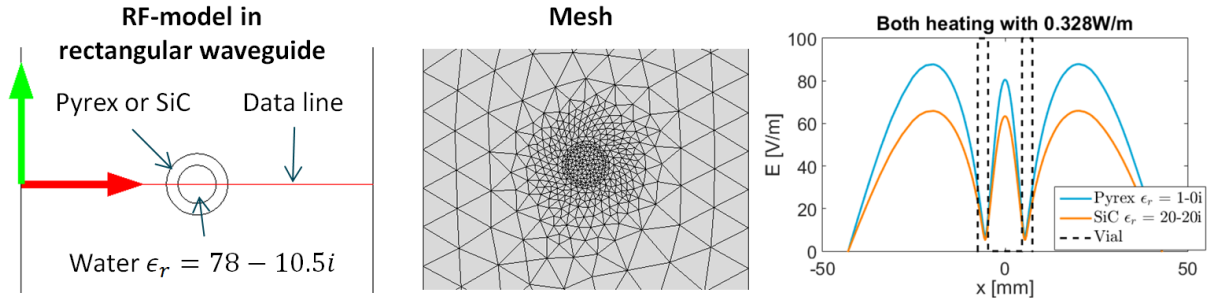


FIGURE C.5: Disproving silicon carbide (SiC) shielding (part 3/3). A simulation of a silicon carbide and Pyrex phial in a mono-mode microwave reactor with the same energy dissipation shows that a silicon carbide phial does not shield the content from an electric field.

However, questionable is whether non-thermal microwave effects would have a certain saturation, i.e. whether increasing the electromagnetic field strength beyond a certain limit will not improve the enhancements further. This simulation did not proof non-thermal microwave effects. This simulation only proofed that the current reasoning was done, is incorrect.

C.4 Limited conventional heat transfer

Derivation C.1: Temperature difference

Forced heat convection in laminar flow

$$\text{Nu}_D = 4.36 = \frac{hd}{\lambda} \quad (\text{C.10})$$

Heat consumed by reaction

$$Q = \frac{\pi d^2}{4} u_{\text{in}} C_{\text{CH}_4} X_{\text{conv}} \Delta h_f = 0.83 \text{ W} \quad (\text{C.11})$$

Temperature difference needed to supply heat to the reaction

$$T_{\text{wall}} - T_b = \Delta T = \frac{Q}{\frac{\lambda_{\text{eff}} \pi d^2}{d} 4} = 24 \text{ K} \quad (\text{C.12})$$

$$\lambda_{\text{eff}} = 4.36 (1 - \epsilon) \lambda_{\text{CH}_4} + \frac{\lambda_{\text{cat}}}{4.36} = 1.39 \text{ W}/(\text{m K}) \quad (\text{C.13})$$

$$C_{\text{CH}_4} = \frac{\rho_{\text{CH}_4}}{M_{\text{CH}_4}} = 41 \text{ mol}/\text{m}^3 \quad (\text{C.14})$$

TABLE C.5: Used values for temperature difference.

Values [77][78]		Assumed	
T	1073 K	Δh_f	5236 kJ/mol
p	1 atm	λ_{cat}	2.3 W/(m K)
u_{in}	36.8 atm	$\lambda_{\text{CH}_4} (T_{1073})$	0.15 W/(m K)
Ar/CH ₄	10/90	M_{CH_4}	16 g/mol
L	8 mm	$\rho_{\text{CH}_4} (T_{298})$	0.656 kg/m ³
d	8 mm		
ϵ	0.38		
X_{conv}	0.14		

C.5 Catalyst thickness

The maximum catalyst thickness is limited by the generalised Thiele modulus rewritten (Equation C.15)[54] which prevents under utilized catalyst.

$$\phi = h_{\text{cat}} \sqrt{\frac{\text{GHSV} \rho_{\text{cat}}}{D_{12}}} < 0.7 \implies h_{\text{cat}} \leq 0.7 \sqrt{\frac{\text{GHSV} \rho_{\text{cat}}}{D_{12}}} \quad (\text{C.15})$$

Reducing the generalised Thiele modulus below 0.7 might be necessary for microwave reactors to reduce accelerated deactivation spots, because at lower generalised Thiele modulus deviations have less influence (Equation C.16).

$$\eta = \frac{\tanh(\phi)}{\phi} \quad (\text{C.16})$$

Collect equation and manufacturing possibilities.

$$10 \mu\text{m} \leq h_{\text{cat}} = 0.7 \sqrt{\frac{\text{GHSV} \rho_{\text{cat}}}{D_{12}}} \leq 100 \mu\text{m} \quad (\text{C.17})$$

C.6 Channel width

The maximum channel width is limited by characteristic times which prevents bypassing reactant.

Characteristic time radial diffusion

$$D_{12} \frac{\partial^2 c}{\partial x^2} \implies \frac{D_{12}}{x^2} \quad (\text{C.18})$$

Characteristic time axial convection

$$u \frac{\partial c}{\partial x} \implies \frac{u}{L} \quad (\text{C.19})$$

Characteristic time axial convection needs to be bigger than characteristic time radial diffusion to prevent bypassing reactants.

$$\frac{u}{L} \geq \frac{3 D_{12}}{4 d^2} \quad (\text{C.20})$$

Average flow velocity calculated from gas-hourly space velocity.

$$u = \frac{\text{GHSV} 4dL \rho_{\text{cat}} h_{\text{cat}} \frac{T_{\text{r}}}{T_{\text{in}}}}{d^2} \quad (\text{C.21})$$

Collect equation in one and rewrite to maximum catalyst thickness.

$$d \leq \frac{1}{3} \frac{D_{12}}{\text{GHSV} \rho_{\text{cat}} h_{\text{cat}}} \frac{T_{\text{in}}}{T_{\text{r}}} \quad (\text{C.22})$$

The channel width is calculated using the maximum pressure drop and Hagen-Poiseuille equation was rewritten. The maximum pressure drop is set to be 1% of the reactor pressure.

Hagen-Poiseuille equation

$$0.01p \geq \Delta P = \frac{128 \mu L}{\pi d^4} V \quad (\text{C.23})$$

Volume flow channel

$$V = \text{GHSV} \rho_{\text{cat}} h_{\text{cat}} 4dL \quad (\text{C.24})$$

Collect both an rewrite

$$d \geq \left(\frac{100}{p} \frac{512}{\pi} \mu L^2 \text{GHSV} \rho_{\text{cat}} h_{\text{cat}} \right)^{13} \quad (\text{C.25})$$

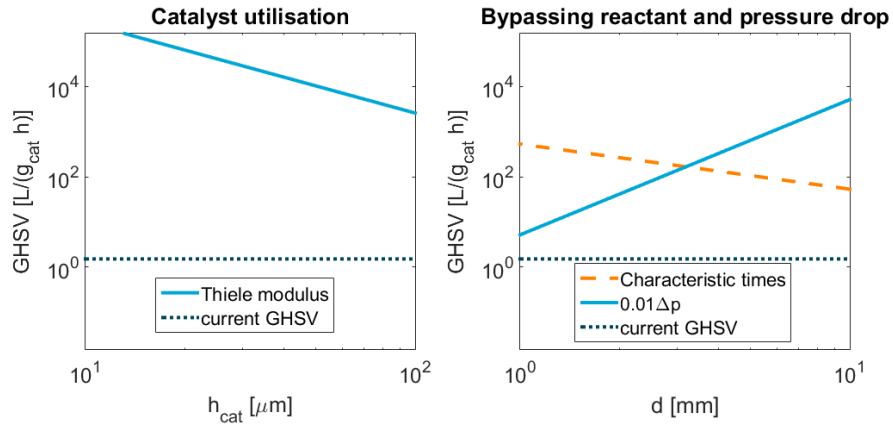


FIGURE C.6: Channel width and catalyst layer calculations for 1500 mm long asymmetric annular monolith at 1 atm.

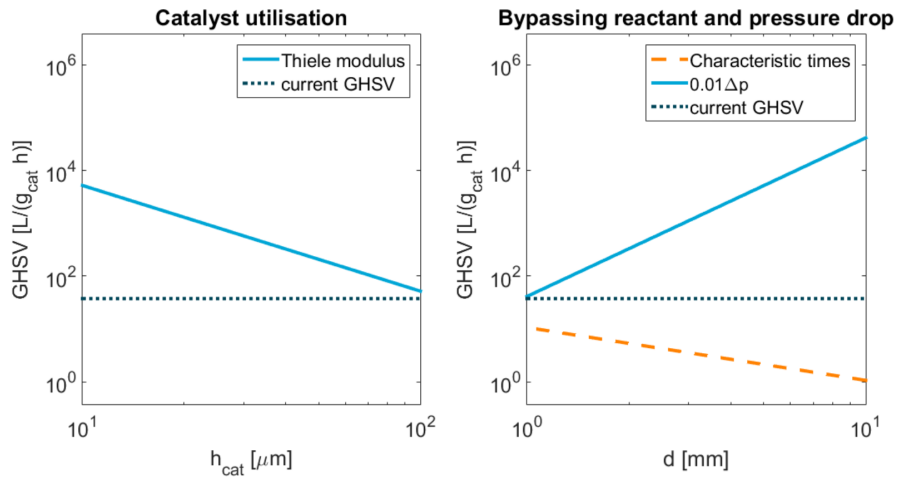


FIGURE C.7: Channel width and catalyst layer calculation for 1500 mm long asymmetric annular monolith at 50 atm. The increase of dynamic viscosity due to pressure increase was assumed to be 5. Smaller channel width is needed if h_{cat} is 100 μm . However, pressure drops prevent from making the channel width smaller.

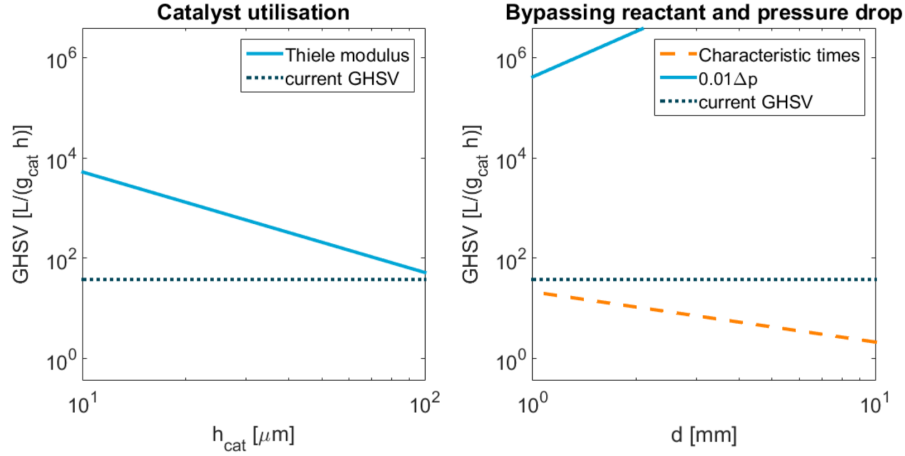


FIGURE C.8: Channel width and catalyst layer calculation for 15 mm long curved radial monolith at 50 atm. The increase of dynamic viscosity due to pressure increase was assumed to be 5. Smaller channel width is needed if h_{cat} is 100 μm .

C.7 Asymmetric annular monolith

The asymmetric annular monolith is sized using integral Gauss's law and parallel circuit theory.

$$\partial_{\Omega} \mathbf{E} \cdot d\mathbf{S} = \frac{1}{\epsilon} \Omega \rho dV \quad (\text{C.26})$$

There is no accumulation of electric charge and the electric field should stay the same.

$$\epsilon_1 E_1 r_1 = \epsilon_2 E_2 r_2 \implies \frac{E_1}{E_2} = \frac{\epsilon_2 r_2}{\epsilon_1 r_1} = 1 \implies \frac{r_2}{r_1} \epsilon_2 = \epsilon_1 \implies \epsilon_{r,\text{mon}}(r) = \frac{\epsilon_{r,\text{mon}}(r_o) r_o}{r} \quad (\text{C.27})$$

The permittivity at the outer conductor is obtained using parallel circuit theory. The parallel circuit calculates the average of the permittivity of the support, catalyst and gas.

$$\epsilon_{r,\text{mon}}(r_o) = \frac{(t_w \epsilon_{r,\text{sup}} + 2h \epsilon_{r,\text{cat}} + d \epsilon_{r,\text{gas}})}{t_w + d + 2h} \quad (\text{C.28})$$

C.8 Attenuation constant

The attenuation constant is derived from the power per unit area flowing past the point which is obtained from the Poynting vector. Halving the power of higher order modes

every 1% of the reactor length is assumed necessary.

$$P(z) = P(0) \exp(-2\alpha_f z) \implies \ln\left(\frac{P(z)}{P(0)}\right) = -\alpha_f z \implies \frac{\ln\left(\frac{P(0)}{P(z)}\right)}{z} = \alpha_f = \frac{\ln(2)}{0.01L} \quad (\text{C.29})$$

C.9 Expansion limit

The methane enters through the inner conductor. The flow speed in the inner conductor should be economical [79]. The engineering velocity limit used is for high-pressure gas transport in tubes. The speed probably needs to be lower in the travelling microwave reactor due to bends and expansion in the porous media.

$$V = \text{GHSV} V_{\text{cat}} \rho_{\text{cat}} \frac{T_r}{T_{\text{amb}}} = \pi (r_i - t_w) v_{\text{limit}} \implies r_{i,\text{in},\text{min}} = t_w + \sqrt{\frac{\text{GHSV} V_{\text{cat}} \rho_{\text{cat}}}{\pi v_{\text{limit}}} \frac{T_r}{T_{\text{amb}}}} \quad (\text{C.30})$$

$$r_{\text{exp},\text{max}} = r_i - r_{i,\text{in},\text{min}} = r_i - t_w - \sqrt{\frac{\text{GHSV} V_{\text{cat}} \rho_{\text{cat}}}{\pi v_{\text{limit}}} \frac{T_r}{T_{\text{amb}}}} \quad (\text{C.31})$$

Same goes for the exiting flow while taking the reaction expansion (mol increase) and gas expansion (temperature increase) in account through ideal gas law.

$$r_{i,\text{out},\text{min}} = t_w + \sqrt{\frac{\text{GHSV} V_{\text{cat}} \rho_{\text{cat}}}{\pi v_{\text{limit}}} \left(1 + \frac{10}{6} X_{\text{conv}}\right) \frac{T_r}{T_{\text{amb}}}} \quad (\text{C.32})$$

C.10 Dielectric loss factor

Using data from grid search

The needed reaction heat is

$$V_{\text{cat}} = (4 - h_{\text{cat}}) h_{\text{cat}} L N_C \quad (\text{C.33})$$

$$Q = \rho_{\text{cat}} V_{\text{cat}} \text{GHSV} \frac{\rho}{\text{MW}_{\text{C}_4}} X_{\text{conv}} \frac{\Delta h_f}{6} \quad (\text{C.34})$$

Minimum dielectric loss factor

The heating at the inner conductor can be calculated using dielectric power loss.

$$Q = \frac{\omega}{2} \int_V \epsilon''_{\text{eff}} |E_m|^2 dV \implies \frac{Q}{V_{\text{cat}} \pi f \epsilon_0} \left(\frac{1}{E_m^2}\right) \leq \epsilon''_{\text{r,cat}} \quad (\text{C.35})$$

The maximum electric strength in the monolith is dependent on the maximum dielectric strength possible at the inner conductor.

$$\epsilon_{i,\text{in}} E_{i,\text{in}} r_{i,\text{in}} = \epsilon_{\text{m}} E_{\text{m}} r_{\text{m}} \implies E_{\text{m}} = \frac{\epsilon_{i,\text{in}} r_{i,\text{in}}}{\epsilon_{\text{m}} r_{\text{m}}} E_{\text{i}} = \frac{\epsilon_{i,\text{in}} r_{i,\text{in}}}{\epsilon_{\text{m}} r_{\text{m}}} V_{\text{b}} \quad (\text{C.36})$$

Thus giving a limit for the minimum dielectric loss factor.

$$\frac{Q}{V_{\text{cat}} \pi f \epsilon_0} \left(\frac{\epsilon_{\text{m}} r_{\text{m}}}{\epsilon_{i,\text{in}} r_{i,\text{in}}} \frac{1}{V_{\text{b}}} \right)^2 \leq \epsilon_{\text{r,cat}}'' \quad (\text{C.37})$$

Maximum dielectric loss factor

Definition coefficient

$$c = \frac{dE^2}{dP} \implies P c_{\text{in}} = E_{\text{in}}^2 \quad (\text{C.38})$$

At the outlet, some of the power has been converted into heat.

$$(P - Q) c_{\text{out}} = E_{\text{out}}^2 \quad (\text{C.39})$$

Power converted into heat

$$Q = V_{\text{cat}} \pi f \epsilon_0 \epsilon_{\text{r,cat}}'' E^2 = V_{\text{cat}} \pi f \epsilon_0 \epsilon_{\text{r,cat}}'' P c_{\text{in}} \quad (\text{C.40})$$

To achieve uniform heating the electric field strength at inlet and outlet needs to be the same.

$$E_{\text{out}}^2 = E_{\text{in}}^2 \implies (P - Q) c_{\text{out}} = P c_{\text{in}} \implies P (c_{\text{out}} - c_{\text{in}}) = Q c_{\text{out}} = P c_{\text{in}} V_{\text{cat}} \pi f \epsilon_0 \epsilon_{\text{r,cat}}'' c_{\text{out}} \quad (\text{C.41})$$

Rewrite for a specific expansion a specific dielectric loss factor is needed.

$$\epsilon_{\text{r,cat}}'' = \frac{c_{\text{out}} - c_{\text{in}}}{c_{\text{in}} c_{\text{out}}} \frac{1}{V_{\text{cat}} \pi f \epsilon_0} \quad (\text{C.42})$$

The maximum dielectric loss factor is calculated using the coefficient of the maximum expansion.

$$\epsilon_{\text{r,cat}}'' \leq \frac{c_{\text{out}} - c_{\text{in}} (r_{\text{i}} + r_{\text{exp,max}})}{c_{\text{out}} c_{\text{in}} (r_{\text{i}} + r_{\text{exp,max}})} \frac{1}{V_{\text{cat}} \pi f \epsilon_0} \quad (\text{C.43})$$

Dielectric loss factor limits

Collect the earlier derived maximum and minimum

$$\frac{Q}{V_{\text{cat}} \pi f \epsilon_0} \left(\frac{\epsilon_{\text{m}} r_{\text{m}}}{\epsilon_{i,\text{in}} r_{i,\text{in}}} \frac{1}{V_{\text{b}}} \right)^2 \leq \epsilon_{\text{r,cat}}'' \leq \frac{c_{\text{out}} - c_{\text{in}} (r_{\text{i}} + r_{\text{exp}})}{c_{\text{in}} (r_{\text{i}} + r_{\text{exp}}) c_{\text{out}}} \frac{1}{V_{\text{cat}} \pi f \epsilon_0} \quad (\text{C.44})$$

C.11 Heating limit

Definition coefficient

$$c = \frac{dE^2}{dP} \implies P c_{\text{in}} = E_{\text{in}}^2 \implies P = \frac{E_{\text{in}}^2}{c_{\text{in}}} \quad (\text{C.45})$$

At the outlet, some of the power has been used for the reaction.

$$(P - Q) c_{\text{out}} = E_{\text{out}}^2 \quad (\text{C.46})$$

Combine

$$\left(\frac{E_{\text{in}}^2}{c_{\text{in}}} - Q \right) c_{\text{out}} = E_{\text{out}}^2 \implies \frac{E_{\text{in}}^2}{c_{\text{in}}} - \frac{E_{\text{out}}^2}{c_{\text{out}}} = Q \quad (\text{C.47})$$

The maximum electric strength in the monolith is dependent on the maximum dielectric strength possible at the inner conductor.

$$\epsilon_{i,\text{in}} E_{i,\text{in}} r_{i,\text{in}} = \epsilon_{\text{m}} E_{\text{m}} r_{\text{m}} \implies E_{\text{m}} = \frac{\epsilon_{i,\text{in}} r_{i,\text{in}}}{\epsilon_{\text{m}} r_{\text{m}}} E_i = \frac{\epsilon_{i,\text{in}} r_{i,\text{in}}}{\epsilon_{\text{m}} r_{\text{m}}} V_{\text{b}} \quad (\text{C.48})$$

Uniform heating

$$E_{\text{in}} = E_{\text{out}} = E_{\text{m}} = \frac{\epsilon_{i,\text{in}} r_{i,\text{in}}}{\epsilon_{\text{m}} r_{\text{m}}} E_i = \frac{\epsilon_{i,\text{in}} r_{i,\text{in}}}{\epsilon_{\text{m}} r_{\text{m}}} V_{\text{b}} \quad (\text{C.49})$$

Fill in expressions

$$Q_{\text{limit}} = \frac{E_{\text{m}}^2}{c_{\text{in}}} - \frac{E_{\text{m}}^2}{c_{\text{out}}} = \left(\frac{1}{c_{\text{in}}} - \frac{1}{c_{\text{out}}} \right) \left(\frac{\epsilon_{i,\text{in}} r_{i,\text{in}}}{\epsilon_{\text{m}} r_{\text{m}}} V_{\text{b}} \right)^2 \quad (\text{C.50})$$

Heating limit outside the scope of this work

The designed reactor is able to dissipate at most 20 MW. However, is the microwave generator capable of producing enough microwave power? No, microwave generators produce 6 kW at 2.45 GHz [80] and 100 kW at 915 MHz [62][63]. Thus, another 2 orders are needed without increasing the size of the generator.

C.12 Reflection porous media

A porous media might cause reflection. Therefore, the porous media was simulated using the RF-module from COMSOL. The simulation showed that reflection in the porous media is negligible if the layers are thin enough (Figure C.9).

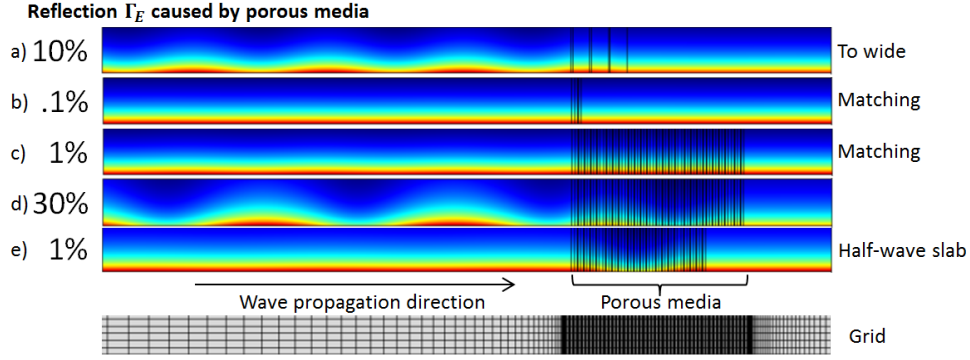


FIGURE C.9: Radial monolith or porous media reflection (Γ) simulations using a 2D-axis-symmetric with distribution mapped grid shows that width matters. a) Impedance tuned radial monolith stretched. b) Impedance tuned radial monolith few channels. c) Impedance tuned radial monolith. d) Non-matching impedance. e) Multiples of half wave length.

C.13 Reflectionless slab

The reflectionless slab was calculated by putting the cross section of the travelling microwave reactor into the RF-module of COMSOL. The mode analysis of the RF-module is used to obtain the phase constant β for the TEM-mode. The sum of the phase constant times its according length needs to be a multiple of π to obtain a half-wave slab.

$$n\pi = \beta_i x_i \quad (\text{C.51})$$

C.14 Economic potential

First the catalyst volume is obtained from the [Equation C.52](#) and the grid search [Figure 2.3](#).

$$V_{\text{cat}} = (4 - h_{\text{cat}}) h_{\text{cat}} L N_C \quad (\text{C.52})$$

Then the catalyst volume is changed to catalyst mass (catalyst loading)

$$m_{\text{cat}} = V_{\text{cat}} \rho_{\text{cat}} \quad (\text{C.53})$$

Then the catalyst mass is changed to the processable volume rate of methane

$$V_{\text{CH}_4, \text{in}} = V_{\text{cat}} \rho_{\text{cat}} \text{GHSV} (T) \quad (\text{C.54})$$

Then the processable volume rate is changed the processable mass rate of methane

$$m_{\text{CH}_4, \text{in}} = V_{\text{cat}} \rho_{\text{cat}} \text{GHSV} (T) \rho (p) \quad (\text{C.55})$$

Then mass rate is changed to the mass rate of methane converted

$$m_{\text{converted, CH}_4} = V_{\text{cat}} \rho_{\text{cat}} \text{GHSV} (T) \rho (p) X_{\text{conv}} \quad (\text{C.56})$$

Then mass rate of methane converted is changed to the mass rate of benzene produced

$$m_{C_6H_6} = V_{cat}\rho_{cat}GHSV(T)\rho(p)X_{conv}\left(\frac{MW_{C_6H_6}}{6MW_{CH_4}}\right) \quad (C.57)$$

Then the mass rate of produced benzene is changed to the mass of benzene produced in a year

$$m_{C_6H_6} = V_{cat}\rho_{cat}GHSV(T)\rho(p)X_{conv}\left(\frac{MW_{C_6H_6}}{6MW_{CH_4}}\right)\tau_{year} \quad (C.58)$$

Finally the mass of benzene produced in a year is changed to the selling price of a year of benzene production in the travelling microwave reactor using non-oxidative methane dehydroaromatization.

$$EP = V_{cat}\rho_{cat}GHSV(T)\rho(p)X_{conv}\left(\frac{MW_{C_6H_6}}{6MW_{CH_4}}\right)\tau_{year}C_{C_6H_6} \quad (C.59)$$

D | Process design

In this appendix, the process is designed using information and reasoning. The information collected is a global view on methane dehydroaromatization, possible multifunctional reactor concepts [49], information requested for separation heuristics [28] and information requested for reaction heuristics [54]. The information is first reduced based on separation, reaction and multifunctional reactor heuristics. Then all information is combined at once. In the travelling microwave reactor for methane dehydroaromatization case through reasoning about deactivation.

Process design of methane dehydroaromatization

A global overview of the methane dehydroaromatization reaction problems is given by Karakaya and Kee [24]. The methane dehydroaromatization reaction is a heat requiring reaction which is very slow [81, Fig. 2]. Therefore a catalyst is used to speed up the reaction. Further, only little conversion is possible due to thermodynamic equilibrium [35]. Therefore the products need to be separated from the exiting reactor mixture and the reactants should be recycled. Finally, the catalyst deactivates quickly.

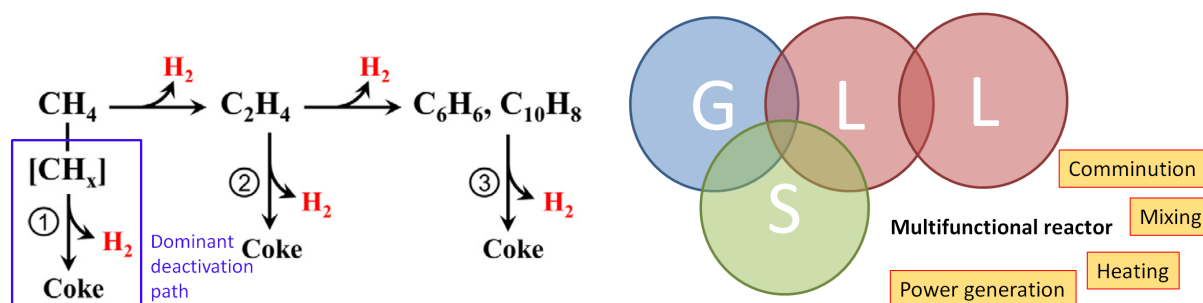


FIGURE D.1: Ethylene cracking is the main coking source [39]

FIGURE D.2: Multifunctional reactor possibilities [49]

The deactivation is dominated by ethylene cracking to coke which is reduced by hydrogen addition (Figure D.1) [38, 39]. Thus, the dominant deactivation path makes in-situ removal of hydrogen not interesting and makes removal of aromatics unnecessary for deactivation prevention. The coke can be removed using $\text{CH}_4\text{-H}_2$ swing operation [82]. Further, the components properties and reaction conditions do not make in-situ product removal interesting (Table D.1), because lower temperatures are needed to remove the aromatics from the reactor. Adding a gas turbine in the applicator will likely over-complicate the design (Figure D.2). Thus, the separation and power generation will happen after the reactor and will not be part of this design study. Some examples of possible processes are given in Figure D.3. Further, an increase in pressure will benefit the separation train, power generation and reaction rate. Therefore, an increase in pressure will be kept in mind. In short, the travelling microwave reactor for methane dehydroaromatization has to be a pressurised swinging multifunctional reactor with heating.

TABLE D.1: Relevant component data shows that membrane and simple distillation are most interesting separation methods.

Component	Component [mol%]	Molecular Weight [g/mol]	Freezing point [K]	Boiling point [K]	Kinetic diameter [Å]
Hydrogen	Med	2.016	13.95	20.38	2.89 [83]
Methane	High	16.04	90.565	111.7	3.8 [83]
Benzene	Low	78.11	278.7	353.3	5.85
Toluene	Low	92.14	178.2	383.8	
Naphthalene	Low	128.17	353.4	491.05	

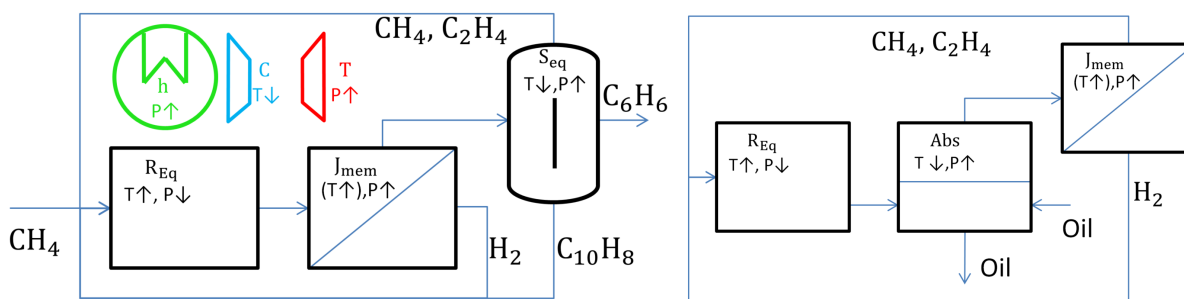


FIGURE D.3: Left) Example process with simple distillation. Right) Example process with absorption in the produced oil.

The heating in the multifunctional reactor needs to be from an alternative energy source or sources, because the experimental reaction [77][78] is already limited by heat transfer. A simple heat transfer model is used to show that the temperature difference needs to be high over a short distance to deliver the energy needed for the reaction (derivation C.1). A temperature difference between the inside wall and the bulk needs to be 24 K for a tube diameter of 8 mm at 1073 K. Thus, a different energy source is needed to gain homogeneous temperature and obtain “the same processing history for each molecule” [33]. Some examples of alternative energy sources are cavitation, microwaves, plasma and UV-light. Cavitation is not interesting, because the reactant becomes a liquid below 111.7 K. All the other energy sources can activate methane. Thus, a microwaves reactor could supply the heat for a more active catalyst. In this thesis, microwaves will be used to supply the energy for the reaction.

E | Materials

In this appendix, the materials fulfilling the constraints can be found.

Ashby's method [51] is used to select the conductor and monolith materials by using the mentioned properties in section 2.3 to filter data in CES edupack. Furthermore, some example charts used are shown in Figure E.1 and Figure E.2.

TABLE E.1: Remaining conductor materials and their properties after properties constraints.

Name	R_T	$T_{\text{creep}} [^{\circ}\text{C}]$	α	C_{vol}	ρ_e	LBB
Molybdenum, 360 grade, recrystallized	24	1011	5.1	2.7e5	5.5	both
Molybdenum, 360 grade, relieved	36	1011	5.1	2.7e5	5.5	2.45 GHz
Molybdenum, Alloy 362	40	1009	5.8	2.8e5	5.5	2.45 GHz
Molybdenum, Alloy 363	55	1011	5.1	2.8e5	5.5	2.45 GHz
Molybdenum, Alloy 366	39	1086	5.1	4.2e5	6.5	2.45 GHz
Tantalum-tungsten, Ta-10W	14	1158	5.5	5.7e6	18	both
Tantalum-tungsten, R05252	8,5	1147	6.0	5.8e6	17	both
Tantalum, T-111	14	1140	5.9	5.8e6	21	both
Tantalum, T-222	18	1153	5.8	5.8e6	19	both
Tungsten, R05200, annealed	7.5	1144	6.5	6e6	18	both
Tungsten, R05200, cold worked	21	1144	6.5	5.9e6	18	both
Titanium diboride	2.5	1026	8.5	9e4	13	none
Molybdenum disilicide	4	1345	7	2.7e5	15	none

TABLE E.2: Remaining support and container materials and their properties after properties constraints. LBB stands for the leak-before-break criterion. The often used silica quartz is added for comparability.

Name	ϵ_r'	R_T	C_{vol}	α	LBB
Boron nitride	4.3	5.5	40	8.3	yes
Magnesia	8	1.4	39.5	10.4	yes
Zirconia	10+	0.2	21	7.5	yes
Beryllia (99)	7	10.3	48	7.5	yes
Sialons	10	8.3	30	3.5	yes
Silicon nitride	9	5.8	41	3.3	yes
Silicon carbide (β)	8	10	16	3.7	yes
Alumina (85)	8.5	1.2	1.9	7	yes
Titanium dioxide	10+	0.65	28.5	10.2	yes
Chromic oxide	9	4.3	21	7.9	yes
Mullite	7.5	0.4	8.5	4.3	yes
Steatite	6.2	0.2	12.5	8.5	yes
Cordierite	5	0.25	7.5	3	yes
Silica (fused quartz)	4	1.6	7.4	0.5	no

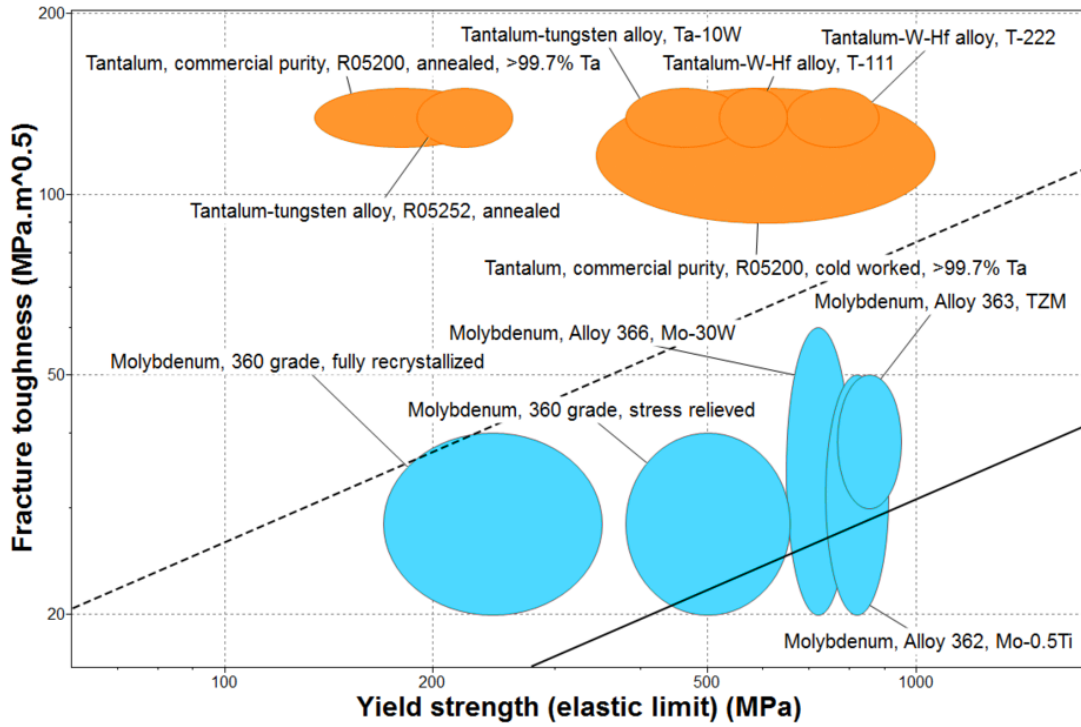


FIGURE E.1: Inside the program CES edupack, showing an example chart of leak-before-break criterion of the conductor.

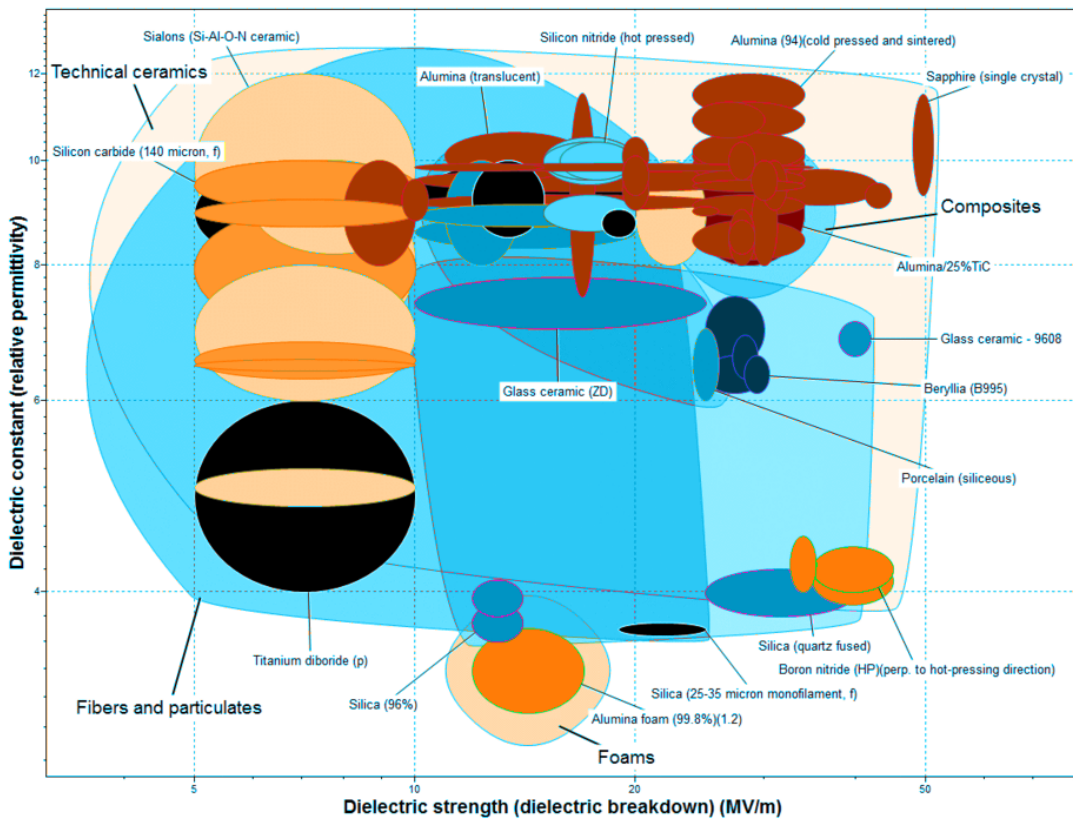


FIGURE E.2: Inside the program CES edupack, showing an example chart of dielectric constant of the monolith.

F | Pathfinder

The Pathfinder (Figure F.1) was co-developed at the start of the thesis with Guido Sturm. This reactor should have been built by March 2017. However, due to multiple hiccups, it has not been built. Furthermore, the designed reactor should be an improvement on the Pathfinder and thus was compared in Table 3.1.

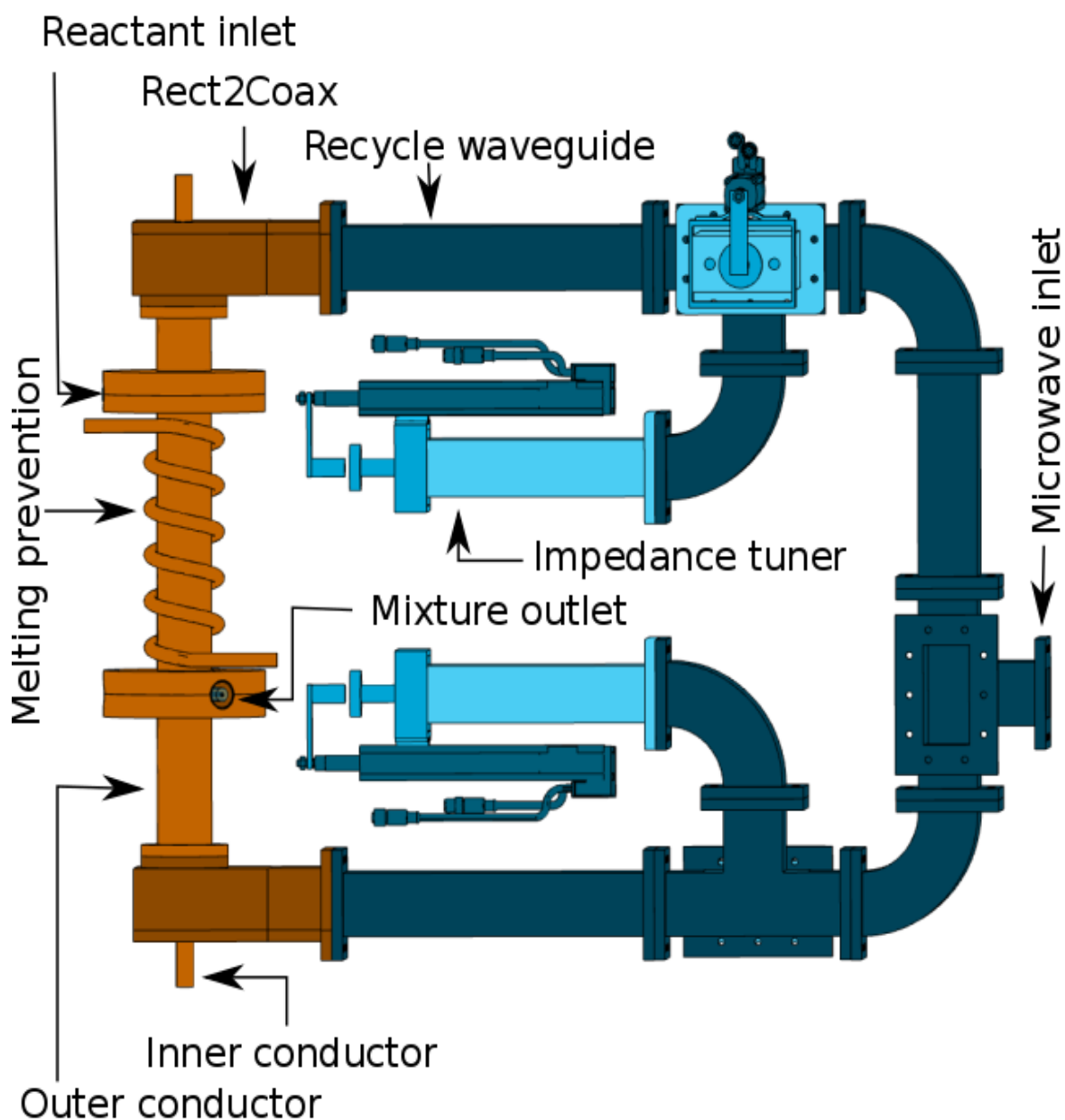


FIGURE F.1: The pathfinder reactor